NTNU

Norwegian University of
Science and Technology

Engine Controller Design and Implementation for a 255 kW Diesel Engine

Ketil Land

Marine Technology (2-year)
Submission date: June 2016
Supervisor: Eilif Pedersen, IMT
Co-supervisor: Nicolas Lefebvre, IMT

Norwegian University of Science and Technology
Department of Marine Technology

MASTER THESIS IN MARINE MACHINERY

SPRING 2016

FOR

STUD.TECHN. Ketil Land

Engine Controller Design and Implementation for a 255 kW Diesel Engine

Work description

NTNU have together with MARINTEK and ABB established the Hybrid Power Lab at MTS, consisting of multiple generator sets connected to a DC grid with two electric motors, converters, batteries and a capacitor bank. Multiple options for reduced fuel consumption arise when hybrid concepts are considered, both at the system and at the engine level. The traditional constant speed controllers are not considered optimal for use in a marine hybrid power plant like what we have in our lab now. We are therefore interested in reviewing controller design for such systems in general and to implement and test different controller concepts in our lab for reduced fuel consumption, reduced emissions and dynamic load capability at the same time. The controller shall be implemented in National Instruments LabView CompactRIO for final testing. An interest for advanced engine control systems is a prerequisite for the student selecting this assignment. The project is carried out associated with several industries and research projects linked to the Hybrid Power Lab. Research personnel and technicians will be included in this project.

Scope of work:

1. Review of necessary literature within the field of diesel engine performance and diesel engine control.
2. Identify smoke- and torque-limitations for the Perkins engine.
3. Design and install a new ECU that controls the engine speed for the Perkins engine in the Hybrid Power Lab.
4. Test the ECU with variable speed and zero generator load.

The report shall be written in English and edited as a research report including literature survey, description of mathematical models, description of control algorithms, simulation results, model test results, discussion and a conclusion including a proposal for further work. Source code should be provided on a CD with code listing enclosed in appendix. It is supposed that Department of Marine Technology, NTNU, can use the results freely in its research work, unless otherwise agreed upon, by referring to the student's work. The thesis should be submitted in two copies within June 10th.

The thesis should be submitted in three copies within 10.06 2016.

Trondheim 31.05 2016

Associate Professor Eilif Pedersen
Supervisor

Preface

This is a Master Thesis spring 5th year MSc course TMR4930 Marin Teknikk, at NTNU Marine Technology, Centre of Marine Technology.
The reader is assumed to have familiarity with diesel engine fundamentals and engine controls and National Instrument Labview software and hardware. The thesis investigates how to design and implement an engine control unit, also referred to as a ECU or governor, for a diesel engine. For testing, an engine in the Hybrid Power Lab at Centre of Marine Technology is used.

Trondheim, June 8th 2016

Ketil Land

Acknowledgment

I would like to thank my supervisor Eilif Pedersen for persuading me to choose this master thesis topic which involved a lot of practical work in the Hybrid Power Lab. A special thanks is directed to my co-supervisor Nicolas Lefebvre for many technical discussions and hours spent together testing the ECU. His Labview developed algorithms for calculating crankshaft speed and angular position provided a good starting point for developing the engine controller. Frode Gran must be thanked for creating the injector driver card and assistance with testing of the ECU and Gunnar Bremset for modifying the engine top cover to accommodate the additional injector cabling.

My dear wife Uta and our three daughters must also be thanked. Without their approval this two year Master study far from home would not have been possible.

K.L.

Abstract

A Hybrid Power Lab is established at the Marine Technology Centre by MARINTEK, ABB and NTNU. This is a DC-grid system where variable speed generators are essential to reduce fuel consumption and emissions. The traditional constant speed controller does not have the flexibility to use the full potential of this system. Therefore it would be interesting to create a platform for testing different controller concepts in the Hybrid Power Lab. In this thesis such a control platform is designed and implemented for a 255kW Perkins diesel engine in the Hybrid Power Lab. The engine offers a flexible platform for testing different controller concepts with its hydraulic/electrical controlled fuel system.

The main objective is to develop an engine controller for the Perkins engine and test it on the engine with variable speed and zero generator load.

Method used for creating the controller is a review of diesel engine performance parameters and diesel engine control. In addition a reverse-engineering method is used to collect data from the original engine controller at different speed and load levels. The behavior of the original controller is then mirrored into the developed controller for testing on the Perkins engine. The collected data include all the parameters important to engine speed control: engine speed and angular position of crankshaft, injector control oil pressure, injector current, start of injection and injection duration. The developed engine controller algorithms calculate the crankshaft speed and angular position to determine at what point fuel shall be admitted into the cylinders. The algorithms also control fuel injection pressure, injector current by a pulse width modulated signal, start of injection and injection duration.

Test runs for the engine have been done with the new controller. In running mode the engine speed is automatically controlled by the controller at a desired setpoint.

The test confirms that the developed controller is able to control the engine speed by changing the amount of fuel injected into the cylinders. A too late injection resulted in white smoke from the exhaust and by starting the injection earlier the white smoke disappeared.

Recommendations for further work are listed at the end of the document. One item that will be mentioned here is the engine coolant temperature, which has a large influence on the controlled parameters and should therefore be studied further to improve the control algorithms.

Sammendrag

På Marinteknisk Senter er det etablert en Hybrid Power Lab av MARINTEK, ABB og NTNU. Dette er et DC-grid system hvor det er viktig å ha generatorer med variabelt turtall for å redusere drivstofforbruk og utslipp. Tradisjonelle kontrollere med konstant turtall er ikke fleksible nok til å utnytte potensialet i systemet. Derfor vil det være interessant å lage en plattform for å teste ut ulike kontrollkonsepter i Hybrid Power Lab. Denne masteroppgaven ser på design og implementering av en slik plattform for en 255 kW Perkins dieselmotor i Hybrid Power Lab. Denne motoren har et hydraulisk/elektrisk styrt drivstoffsystem der en kan teste ut ulike kontrollkonsepter.

Hovedformålet med oppgaven er å utvikle en motorkontrollenhet for Perkins motoren og teste denne på motoren med variabelt turtall og null generator belastning.

Som metode for å lage kontrolleren, er det utført en gjennomgang av teori for dieselmotorens ytelses parametere og kontroll av dieselmotorer. I tillegg er det brukt en inversutviklingsmetode for å samle inn data fra den opprinnelige motorkontrolleren ved forskjellige turtall og belastningsnivåer. Virkemåten til den opprtinnelige kontrolleren gjenskapes i den nyutviklede kontrolleren for testing på Perkins motoren. De innsamlede dataene omfatter alle parametre som er viktige for turtallskontroll, dvs. motorhastighet, vinkelposisjon til veivaksel, injektor oljetrykk, injektor strøm, start av injeksjon og injeksjonens varighet. Algoritmene til den utviklede motorkontrolleren beregner veivakselens turtall og vinkelposisjon for å bestemme når drivstoff skal injiseres i sylindrene. Algoritmene kontrollerer også innsprøytingstrykk, strøm gjennom injektor ved bruk av et pulsbreddemodulert signal samt start av injeksjon og injeksjonens varighet.

Det er utført testkjøringer av motoren med den nye kontrollerenheten. I driftsmodus styres turtallet automatisk av kontrolleren for et ønsket settpunkt.

Testen bekrefter at den kontrollenheten som er utviklet, klarer å kontrollere motorturtallet ved å endre mengden av drivstoff som blir injisert i sylindrene. For sen injeksjon resulterte i hvit røyk fra eksosen.Ved å injisere drivstoffet på et tidligere tidspunkt forsvant den hvite røyken.

Anbefalinger for videre arbeid er beskrevet i slutten av masteroppgaven. Et punkt i anbefalingene er å studere kjølevannstemperaturen betydning nærmere. Denne har stor innvirkning på kontrollparametrene og kan brukes til å forbedre reguleringsalgoritmene ytterligere.

Contents

List of Figures

List of Tables

Acronyms

AC	Alternating Current
CPP	Controllable Pitch Propeller
DC	Direct Current
ECU	Engine Control Unit
FPP	Fixed Pitch Propeller
HEUI	Hydraulic Electric Unit Injector
HPL	Hybrid Power Lab
HW	Hardware
ID	Injection Duration
IDU	Injector Driver Unit
LUT	Look Up Table
MCR	Maximum Continuous Rating
PECU	Perkins Engine Control Unit
PMS	Power Management System
PWM	Pulse Width Modulation
SFOC	Specific Fuel Oil Consumption
SOI	Start of Injection
SW	Software
TDC	Top Dead Center
VI	Virtual Instrument

Nomenclature

Symbol	Definition	Units
b_e	Brake specific fuel consumption	$[g/kWh]$
D	Cylinder diameter	$[m]$
η_e	Engine overall efficiency	$[-]$
η_m	Engine mechanical efficiency	$[-]$
f_{teeth}	Teeth pulse frequency	$[Hz]$
f_{sample}	Sampling frequency	$[Hz]$
h_{LHV}	Lowe heating value for fuel	$[J/kg]$
i	Number of cylinders	$[-]$
m_f	Mass of fuel	$[kg]$
$\dot{m}_f$	Fuel mass flow	$[kg/s]$
n_{cam}	Engine camshaft speed	$[r/s]$
n	Engine crankshaft speed	$[rpm]$
n_{crank}	Engine crankshaft speed	$[r/s]$
$N_{teeth/round}$	Number of teeth on wheel	$[teeth/round]$
ω_{cam}	Camshaft angular speed	$[deg/s]$
ω_{crank}	Crankshaft angular speed	$[deg/s]$
p_{me}	Brake mean effective pressure	$[Pa]$
p_{mi}	Indicated mean effective pressure	$[Pa]$
P_e	Engine shaft power	$[W]$

Symbol	Definition	Units
$\dot{q}_f$	Fuel volume flow	$[m^3/s]$
ρ_f	Fuel density	$[kg/m^3]$
S	Piston stroke distance	$[m]$
T_e	Engine effective torque	$[Nm]$
T_{teeth}	Teeth pulse duration	$[ms]$
$T_{halftooth}$	Half tooth pulse duration	$[ms]$
$T_{toptooth}$	Top tooth pulse duration	$[ms]$
t_{ID}	Injection duration command	$[s]$
t_{inj}	Injection duration	$[s]$
t_{OD}	Opening delay	$[s]$
t_{sample}	Sample duration	$[ms]$
θ_{cam}	Camshaft angular position	$[deg]$
θ_{crank}	Crankshaft angular position	$[deg]$
θ_{360}	One rotation of camshaft equal 360deg	[deg]
θ_{720}	One rotation of camshaft equal 720deg	[deg]
V_d	Cylinder displacement	$[m^3]$
W_e	Engine effective work	$[J]$
W_i	Engine indicated work	$[J]$

Chapter 1

Introduction

This thesis gives an in-depth view of the development of an Engine Control Unit (ECU) for a diesel engine in the Hybrid Power Lab (HPL). In this chapter an introduction to the HPL is given in section 1.1. Section 1.2 and 1.3 presents the background and the objectives. Limitations are given in 1.4 and the selected approach in section 1.5. Review of literature are seen in section 1.6 and finally the structure of the thesis in section 1.7.

1.1 Introduction to the Hybrid Power Lab

The Hybrid Power Lab is established at the Marine Technology Centre by MARINTEK, ABB and NTNU. It is set up as a DC-grid system with two diesel engine driven generator sets (G1, G2) that produces AC,see figure 1.1, where G1 and G2 are variable speed controlled. Therefore the diesel engines can be operated more efficiently over its speed range and thus reduce fuel consumption and emissions. As the generators can run with variable speed, the output AC frequency from the generators can be different for the two generators. Therefore rectifiers (Rec1 and Rec2) rectifies the AC to DC before it is distributed to the consumers through the four DC buses. The four DC buses are connected together by closing the bus tie breakers (BT1, BT2 and BT3). Two inverters (Inv1, Inv2) control the speed of the electric motors (M1, M2) connected to load brakes (B1, B2) which are the consumers. Batteries are connected to DC bus 3, and capacitors are connected to DC bus 4. They can both be used as additional power sources.

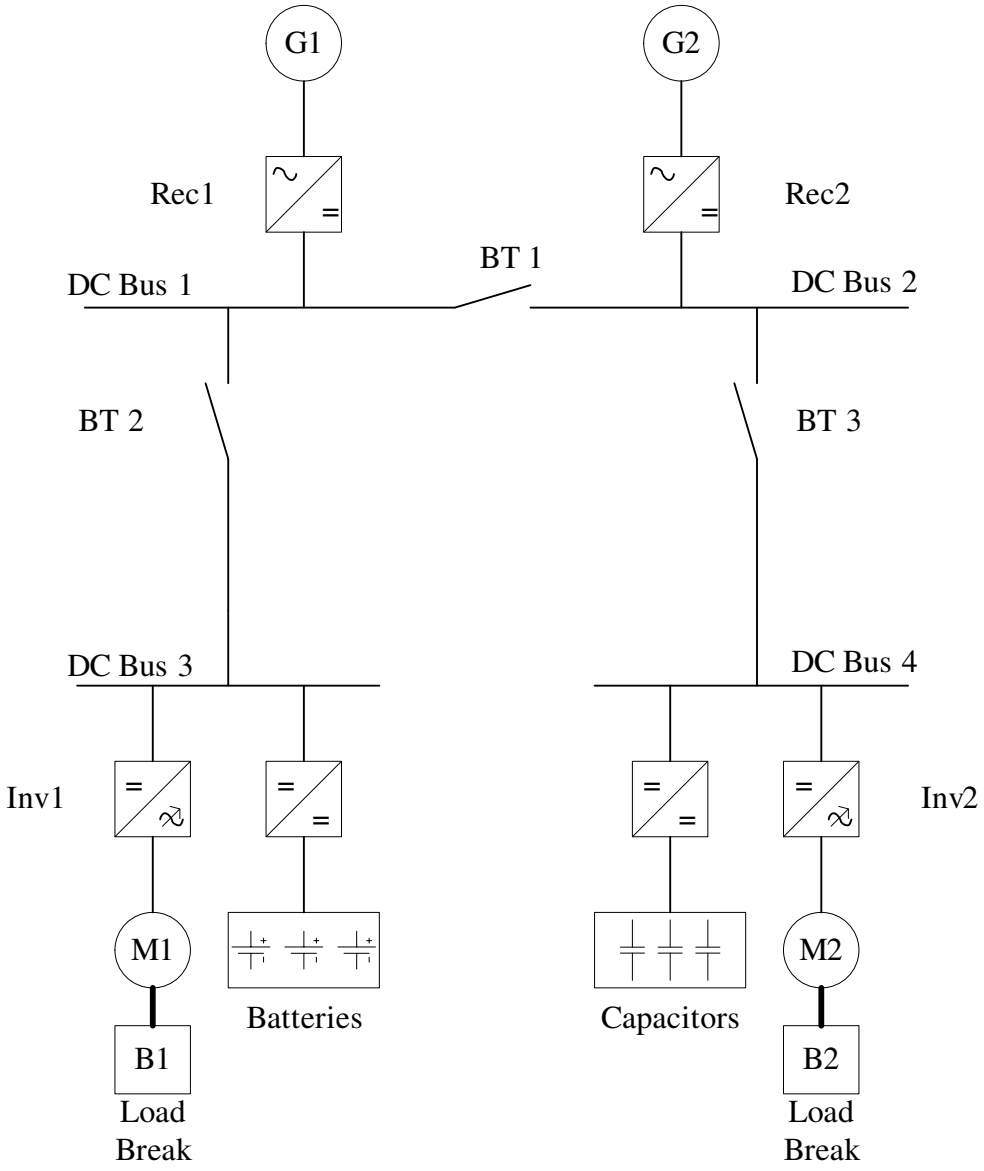

Figure 1.1: ABB DC grid at NTNU.

Four examples of diesel engine performance maps are shown in figure 1.2 to illustrate different load characteristics. Figure 1.2a, 1.2b and 1.2c show the traditional speed controller concepts. These are fixed to one operational curve which not necessarily give the optimal engine operating point. By using a DC-grid solution as shown in figure 1.2d the idea is to always find the optimal operating point in the engine performance map.

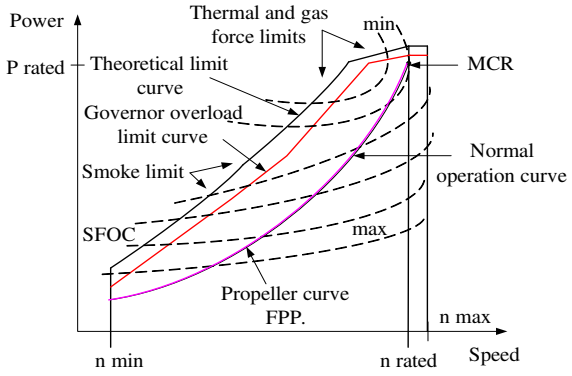

(a) Fixed Pitch Propeller (FPP)

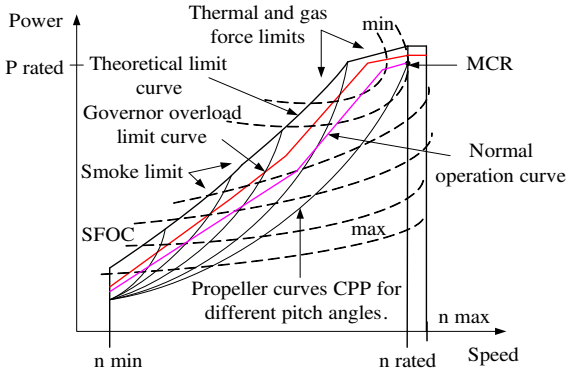

(b) Controllable Pitch Propeller (CPP)

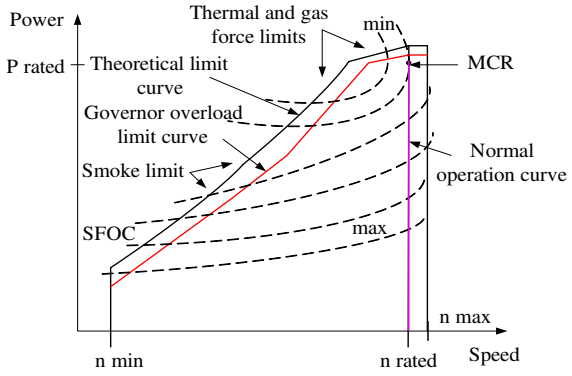

(c) Fixed speed generator

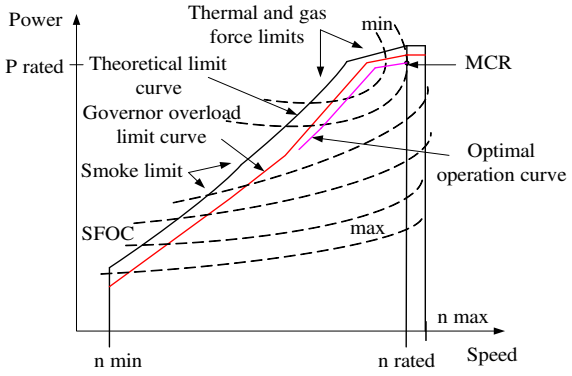

(d) Hybrid Power Lab variable speed generator.

Figure 1.2: Diesel engine performance maps.

1.2 Background

Currently, the Perkins diesel generator in the HPL does not offer sufficient power and dynamic load capability. Different tests have been carried out, especially on the fuel-feeding path, to locate the source of this limitation but without success. The reason for these limitations is assumed to be the current ECU installed on the engine, from here on referred to as Perkins ECU (PECU). Development of an in-house ECU is considered to overcome these engine limitations and to serve as a platform for testing different controller concepts. It has been decided to implement this ECU using the National Instrument Labview CompactRIO platform. Labview hardware and software are already in use at the Marine Technology Centre for control and data acquisition. Thus developing an ECU in Labview will benefit from existing knowledge. Another advantage with an in-house ECU is that control algorithms and parameters are available and

can easily be modified when required. This is a challenge with an externally made ECU where all control parameters are regarded as trade secrets by most manufacturers.

1.3 Objectives

The main objectives of this Master's Thesis are

1. Review of relevant literature within the field of diesel engine performance and diesel engine control.
2. Identify smoke and torque limitations for the Perkins engine.
3. Design and install a new ECU that controls the engine speed for the Perkins engine in the Hybrid Power Lab.
4. Test the ECU with variable speed and zero generator load.

1.4 Limitations

The thesis studies single engine operation at zero generator load and no parallel operation with the second engine in the HPL. As the engine is located inside a temperature controlled room, the inlet air temperature to the engine is assumed to be constant. This parameter will not influence engine control or performance. The main focus with the thesis is to develop an ECU that can serve as a framework or platform for testing future controller concepts. That is why the engine will be tuned for stable speed operation but not for an optimal performance.

1.5 Approach

Little or no data are available for the current PECU control parameters, hence reverse engineering is the approach to find the key parameter values for the diesel injection control. Key parameters are start of injection related to crankshaft angular position and injection duration. Engine tests with the original ECU at different speed and load conditions is done for logging of

the key parameters. The gathered data is used for mirroring the behaviour of the PECU into the new ECU.

1.6 Related Work

Engine performance calculations used for determining e.g. the required mass of fuel for a given speed and shaft power are derived from (Heywood, 1988) see section 2. Combustion parameters like start of injection, injection duration and their influence on emssions are found in (Bosch, 2006) (Baukal, 2004) (Lieuwen and Yang, 2016) (Hillier and Coombes, 2004) and are discussed in section 2.

(Bosch, 2006) provides a schematic example of the injection fuel quantity calculation process. To determine the injection quantity the response characteristics for the engine can be stored in maps for a number of engine operating points (Bosch, 2006). Inputs to the maps are throttle position and engine speed and output is start and duration of injection. It is to be noted that the injection quantity during engine start is separated from the injection quantity at engine running condition. This is because it is a function of engine cranking speed, coolant temperature and fuel composition. Injection quantity limiting factors are exhaust gas emissions, mechanical overload due to high torque or high speed, thermal limits for exhaust components and coolant system and thermal overloading of the injector coils due to excessive energizing time.

Accurate control of engine speed requires an accurate amount of fuel injected into the cylinder for every combustion cycle. Therefore opening of the fuel injectors must be precise both with regards to start of injection and duration of injection. The duration can be 1.25 ms (Bosch, 2006) which indicates a quick response time for the injector. To get this quick response time for an injector (Sybele, 2009) describes that an electronic fuel injector has three phases during opening: attack, withstand and holding phase. During the attack phase the coil will experience a rapid increase in the current to overcome the inductive current set up by the coil to counteract the changing magnetic force in the coil. After the attack phase the voltage level is reduced to keep the current at a constant level. During the withstand phase the valve piston reaches the desired position due to the magnetic force created by the coil. When the piston is in the desired position the magnetic force can be reduced. This is done by reducing the current to a lower level

and is referred to as the hold phase. A suggested tuning procedure for an injector driver is also described in (Sybele, 2009).

Pulse Width Modulation (PWM) is used to control actuators (injectors, rail oil valve) on the engine and a study of this is therefore done. PWM is a signal where the on and off period of the signal is controlled. The term duty cycle is used and it is the time the signal is on during one period. A duty cycle of 25% means the signal is on for 25% of the period duration. Signal carrier frequency is fixed (Bishop, 2008). PWM controls the power supplied to the load by switching on and off the current by changing the duty cycle value. (Bishop, 2008) also mentions induced current in the injector coils when the PWM cut the current flow. This is referred to as inductor kickback. To reduce the energy created by this induced current a diode can be placed in parallel to the actuator coils to protect the circuit components.

The Perkins diesel engine has a Hydraulic Electric Unit Injector (HEUI) system from Caterpillar Inc. A study of the system is done to understand the functionality of the involved components as well as a study of the control algorithms used. This is mentioned in more detail in section 3.4 where the engine particulars are described.

1.7 Structure of the Report

The report is organized as follows: Diesel engine theory for performance calculations are presented in chapter two. This chapter also discusses emissions and how they can be controlled. Chapter three presents the Perkins engine in the Hybrid Power Lab. Performance calculations for the Perkins engine based on available data are presented in chapter four. In chapter five reverse-engineering results are presented and discussed. Chapter six shows the architecture of the new ECU and implementation of the ECU on a Labview CompactRIO platform. Engine test runs with new ECU are presented in chapter seven. Finally, conclusion and recommendations for further work are presented in chapter eight. Appendix A provides detailed layout and component list of the Injector Driver Unit card. Appendix B shows the engine mapping tables for the developed ECU.

Chapter 2

Diesel Engine Theory

This chapter briefly presents how engine performance, section 2.1, and combustion parameters, section 2.2, are connected.

2.1 Engine Performance

Engine performance calculations can be done by using equations 2.1 to 2.8, ref. (Heywood, 1988), to find the required mass of fuel to be injected and thus the injection duration.
Cylinder displacement

$$V_d = \frac{\pi}{4} D^2 S \quad [m^3] \tag{2.1}$$

Indicated mean effective pressure

$$p_{mi} = \frac{p_{me}}{\eta_m} \quad [Pa] \tag{2.2}$$

p_{mi} is also given as

$$p_{mi} = \frac{1}{V_d} \oint_V p dV \quad [Pa] \tag{2.3}$$

Engine shaft power for a four-stroke engine

$$P_e = i V_d p_{me} \frac{n}{2} = i W_e \frac{n}{2} = T_e \omega_{crank} \quad [W] \tag{2.4}$$

Mass flow of fuel per cycle

$$\dot{m}_f = \dot{q}_f \rho_f \quad [kg/s] \tag{2.5}$$

Specific fuel consumption

$$b_e = \frac{m_f}{W_e} = \frac{\dot{m}_f}{P_e} \quad [kg/J] \quad or \quad [g/kWh] \tag{2.6}$$

Required fuel mass per cylinder cycle is then given as

$$m_f = b_e W_e \quad [kg] \tag{2.7}$$

Overall efficiency is given as

$$\eta_e = \frac{W_e}{h_{LHV} m_f} \quad [-] \tag{2.8}$$

2.2 Combustion Parameters

Both start of injection and injection duration influence the combustion and the resulting fuel consumption and emissions.

Injection Duration and Start of Injection

The injection duration t_{Inj} is determined by the required fuel mass m_f and mass flow rate of the injector.

$$t_{Inj} = \frac{m_f}{\frac{dm}{dt}} \quad [s] \tag{2.9}$$

Injection duration is defined as the injection time after the injector is opened (Bosch, 2006). Note that for electrical operated injectors the injection duration command is dependent of the time the injector needs to open and the time needed to inject the required quantity of fuel. Thus the injection duration command is a function of the opening delay of the injector and the required time to inject quantity m_f

$$t_{ID} = t_{OD} + t_{Inj} \quad [s] \tag{2.10}$$

While injection duration controls the amount injected, start of injection controls the pressure rise from the combustion. By adjusting the start of injection so that the pressure rise contin-

ues from the peak pressure of the compression, the pressure force is used to move the piston downwards to rotate the crankshaft. A too early pressure rise will create a force opposing the piston movement during compression which mean a less efficient engine. With increasing engine speed and load more fuel is injected into the cylinder by increasing the injection duration. Since the injection duration is increased and engine speed is increased, start of injection must be earlier (advanced) to get the pressure rise from combustion around peak compression pressure. Therefore an advanced injection gives a decrease in specific fuel consumption compared to late(retarded) injection, ref. (Bosch, 2006).

Nitrogen Oxides

Nitrogen Oxides (NOx) is mainly formed by thermal NOx since the air contains 78% N2. Formation of NOx is dependent on temperature and time. A higher temperature and a longer residence time of the combustion gases increases the amount of NOx and it increases exponentially with temperature (Baukal, 2004). It can be reduced by reducing the residence time at high temperatures or by reducing the maximum temperature. By advancing start of injection the temperature in the combustion chamber increases and the residence time with high temperature increases, thus the formation of NOx increases.

Carbon monoxide

Carbon monoxide (CO) is mainly due to incomplete combustion and is a product of partially oxidised carbon from the fuel. CO formation has an inverse relationship with NOx formations. While a decreasing combustion temperature increases CO and decreases NOx formation, an increasing temperature decreases CO and increases NOx formation (Lieuwen and Yang, 2016).

Hydrocarbon

Hydrocarbon (HC) formation is a result of incomplete combustion due to low flame speed, flame quenching from the cylinder walls and crevices in the combustion chamber e.g. area between liner and piston head rings and deposits in the combustion chamber. An advanced timing decreases the formation of HC and an increasingly retarded timing will increase formation

of HC (Bosch, 2006). With advancing timing the combustion temperature and time increase, while with retarded timing the combustion temperature and time decrease.

Particles and Smoke

Particles are influenced by spray formation and excess air ratio. For e.g. common rail spray formation is controlled by adjusting the high pressure fuel supplied to the injector. Excess air ratio is controlled by the amount of air delivered by the turbocharger and the injection duration. Soot emissions increase with start of injection close to TDC and with an increasing injection duration (Bosch, 2006). This is due to a lower diffusion area around TDC. Particulate emissions are also seen visually from the gasses escaping the exhaust stack and can have different colors (Hillier and Coombes, 2004). Black smoke is an indication that too much fuel is injected into the combustion chamber. Too much fuel and too little air create an imbalance in the combustion reaction and the result is large particulates of unburnt carbon in the exhaust seen as soot or black smoke. This can be controlled by reducing injection duration. White smoke is an indication that the fuel is not burnt properly and that the exhaust gases contains unburnt fuel that condenses in the atmosphere. The reason can be a too retarded timing. Thus the temperature in the combustion chamber is not high enough to burn all the fuel. This can be reduced by advancing start of injection and/or reducing injection duration. It can also be an indication of water in the fuel or a water leakage from the cooling system into the combustion chamber. Blue smoke is typically the result of an engine burning lubrication oil that is leaking into the combustion chamber due to e.g faulty piston rings, worn piston. This is not controlled by the fuel injection parameters.

Carbon Dioxide and Sulphur Oxides

Carbon dioxide (CO2) and Sulphur Oxides (SOx) are also by-products of combustion. The emission levels for these cannot be controlled by the combustion process itself since they are only dependent of the fuel composition. CO2 and SOx is created when carbon and sulphur in the fuel reacts with the oxygen in the air. SOx emissions can be reduced by changing the fuel composition or treating the exhaust gases (Baukal, 2004).

Chapter 3

Hybrid Power Lab Engine

In this chapter essential engine parameters for the small engine in the HPL are presented. The small engine is the driver in an Olympian GE250, 227 kVA generator set (Pon-Cat, 2012). It consists of a Perkins 1306C diesel engine driving an ABB generator. Note that the original generator in (Pon-Cat, 2012) is replaced by an ABB generator.

General engine and generator data are listed in section 3.1. Definition of cylinder numbering and crankshaft layout are shown in section 3.2. Sensors and actuators controlled by the PECU are listed in section 3.3. In section 3.4 the fuel system is described and finally section 3.5 present the few data that are available for the PECU.

3.1 Engine and Generator Data

Engine and generator data are shown in table 3.1 and 3.2.

Table 3.1: Perkins 1300 data.(Pon-Cat, 2012)

Model Year	2012
Model	Perkins 1306C-E87TAG4
Power	325 [bhp] @ 1800 [rpm] (60 [Hz]) 242 [kW] @ 1800 [rpm] (60 [Hz]) 300 [bhp] @ 1500 [rpm] (50 [Hz]) 224 [kW] @ 1500 [rpm] (50 [Hz])
Number of Cylinders	6
Cycle	Four stroke
Injection System	HEUI (Caterpillar)
Stroke	135.9 [mm]
Bore	116.6 [mm]
Compression ratio	16.9:1
Firing sequence	1-5-3-6-2-4
Direction of rotation	Clockwise seen from front of engine (SAE STD)

Table 3.2: ABB generator data, from nameplate on generator.

Model	AMG 0315BB04 DAE
Year	2013
Real Power	138/250 [kVA]
Voltage	3 x 450 [V]
Frequency	30 [Hz] @ 900 [rpm] 50 [Hz] @ 1500 [rpm]
Power Factor	0.9 [-]

3.2 Engine Cylinder Layout

Engine cylinder numbering and rotational direction are shown in figure 3.1.

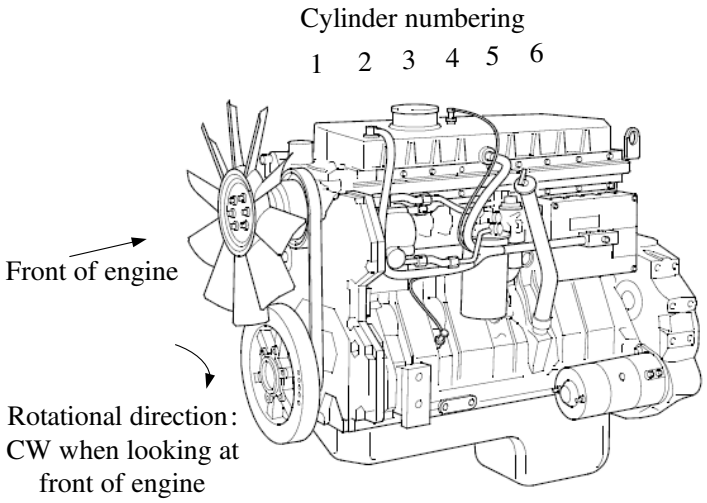

Figure 3.1: Cylinder numbering and rotational direction.

Crankshaft layout and phasor diagram is shown in figure 3.2.

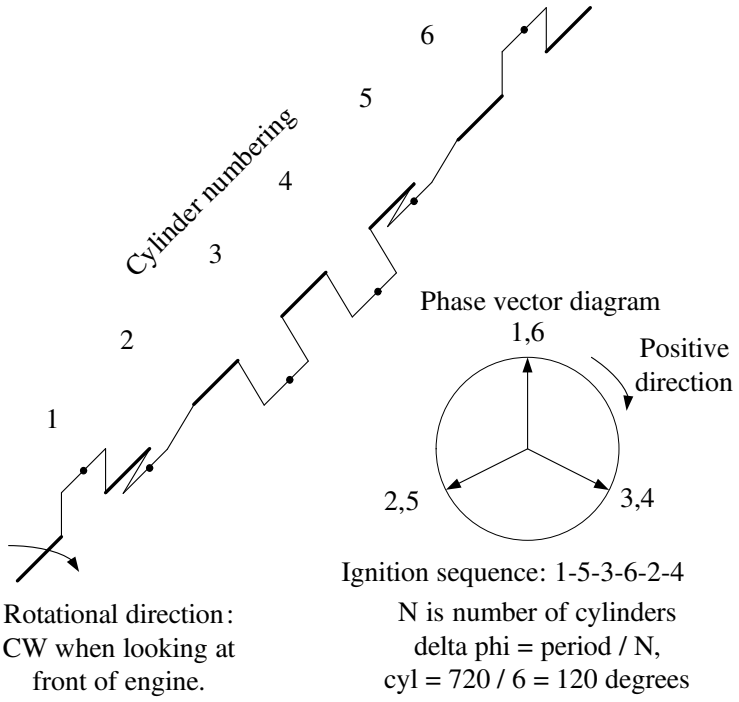

Figure 3.2: Crankshaft layout.

3.3 Sensors and Actuators

Engine sensors are shown in table 3.3 and actuators in table 3.4.

Table 3.3: Sensors.

Description	Type	Signal	Sensor Type
Rail Pressure	Analog Input	0-5V	Variable capacitance
Oil Temperature	Analog Input	0-5V	Thermistor
Oil Pressure	Analog Input	1-5V	Variable capacitance
Coolant Water Temperature	Analog Input	1-5V	Thermistor
Camshaft Encoder	Digital Input	0-5V	Hall Effect
Crankshaft Top Dead Center	Digital Input	0-5V	Hall Effect
Crankshaft Encoder	Digital Input	0-5V	Hall Effect

Table 3.4: Actuators.

Description	Type	Signal	Sensor Type
Starter Motor Engage	Digital Output	Potential free contact	Start Relay
Rail Pressure Control Valve	Digital Output	0-12V PWM	Inductive Coil
Injector Cylinder 1	Digital Output	0-110V PWM	Inductive Coil
Injector Cylinder 2	Digital Output	0-110V PWM	Inductive Coil
Injector Cylinder 3	Digital Output	0-110V PWM	Inductive Coil
Injector Cylinder 4	Digital Output	0-110V PWM	Inductive Coil
Injector Cylinder 5	Digital Output	0-110V PWM	Inductive Coil
Injector Cylinder 6	Digital Output	0-110V PWM	Inductive Coil

3.4 Fuel System

The fuel system is of HEUI type from Caterpillar (Caterpillar, 2007) as shown in figure 3.3. It consists of a low pressure fuel pump, a high pressure rail oil pump, rail oil pressure sensor, rail oil pressure regulating valve, camshaft speed pickup, PECU and one HEUI for each cylinder. The HEUI combines a high pressure injection unit and an injector nozzle in one unit and is hydraulically powered by high pressure oil supplied by a high pressure rail oil pump attached to the engine. An electrically controlled valve on the injector allows high pressure rail oil to flow into the valve chamber and stroke the valve piston. This piston is connected to a piston in the fuel chamber. Fuel is fed by a fuel supply pump to the fuel chamber. The piston area for the hydraulic oil side is larger than for the fuel side, the ratio can be 6 (Caterpillar, 2007). This gives an increase in the fuel pressure in the fuel chamber when the hydraulic oil piston strokes in accordance with Pascal's law. When the fuel pressure force is higher than the spring force the injector nozzle will open. By adjusting the hydraulic oil pressure and controlling the electric oil valve in the injector both injection time and rate can be controlled. This will be independent of engine speed (Caterpillar, 1999) since it is not camshaft operated, see figure 3.4. To determine crankshaft position and speed the PECU uses the camshaft speed pickup sensor. This is used in the injection control algorithm to determine when to open the HEUI in accordance with the cylinder firing sequence.

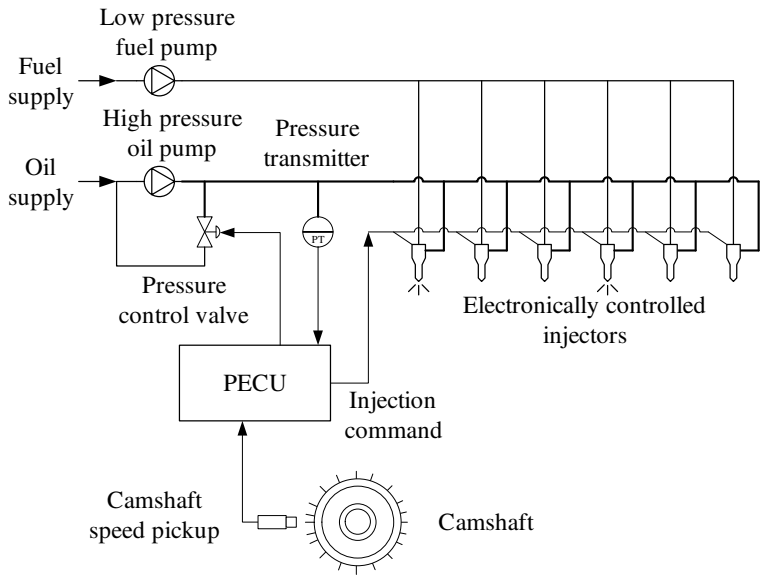

Figure 3.3: HEUI.

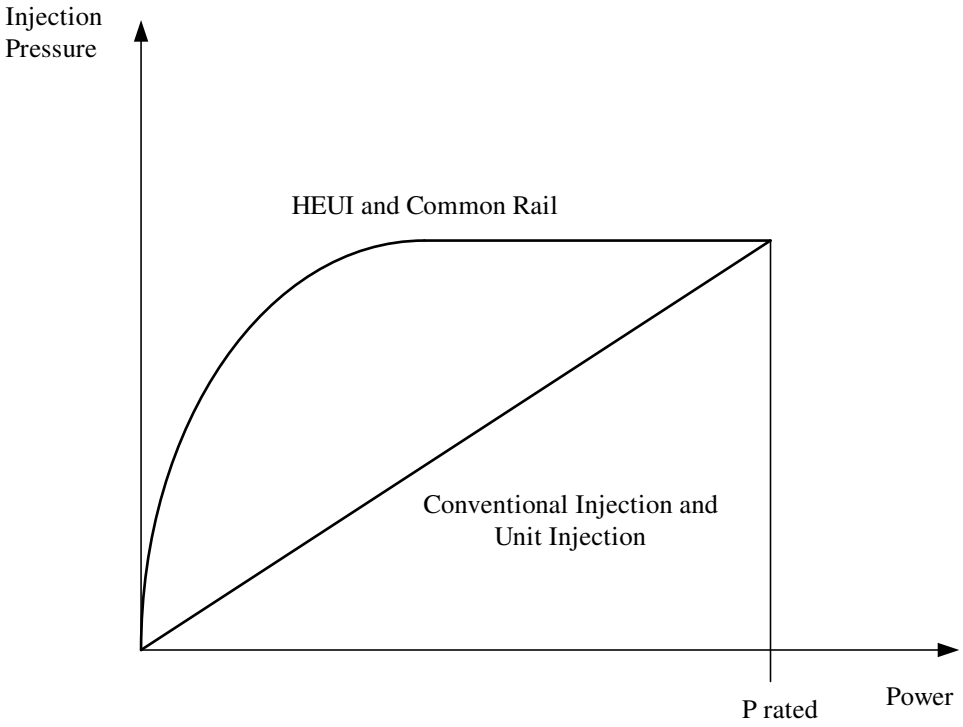

Figure 3.4: Injection pressure.

Figure 3.5 shows the top cover of the engine removed and the location of the six injectors adjacent to the air inlet and exhaust valves.

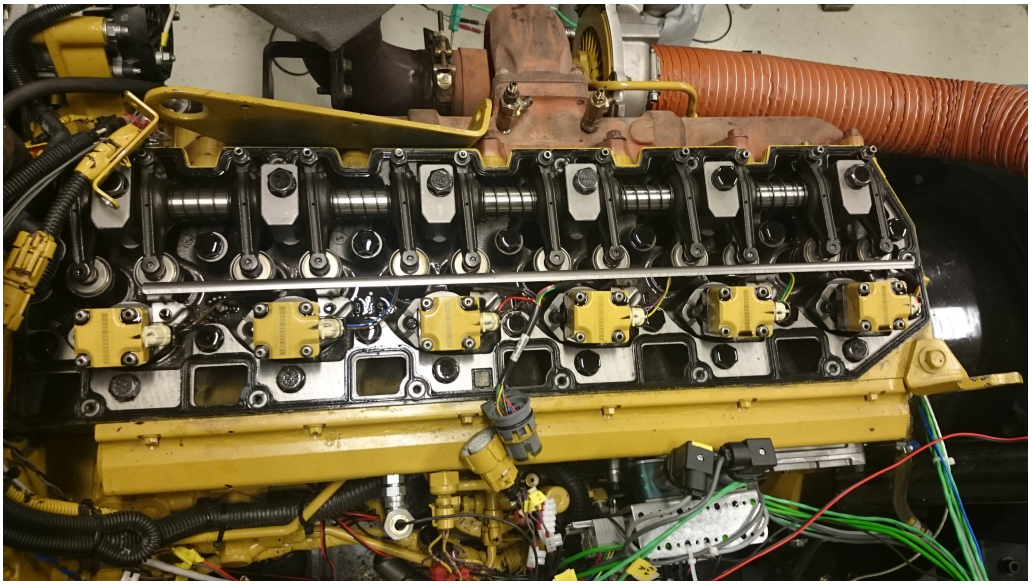

Figure 3.5: Location of injectors with electrical cabling.

3.5 Perkin Engine Control Unit

The engine is supplied with an PECU installed on the engine from the maker. No data is available for this PECU except for a brief description in the workshop manual (Perkins-Engines, 2001). The manual suggests what type of sensors that are interfaced to the ECU but does not reveal any details of the control algorithm. A chapter for fault diagnostics lists fail codes for the PECU and is mainly concerned with signal failure detection e.g short or open circuit for sensors. The manual is general for a variety of applications ranging from trucks to generator sets, thus not all items listed are valid for the Hybrid Power Lab engine.

The majority of vendors regard the ECU algorithms as proprietary information and will not share this with any 3rd party. Two patents have been found about electronic control of hydraulic actuated fuel injection systems. Patent (Barnes, 1994) provides a block diagram for a speed control loop, a block diagram for injection start control and a clock diagram for rail pressure control. In patent (Barnes, 1995) fuel injection and the relation to engine coolant temperature during engine start are described. But it is difficult to determine if or how these algorithms are implemented in the PECU.

Chapter 4

Engine Performance Calculation

This chapter presents engine performance data based on the equations given in chapter 2 and the engine data available from (Pon-Cat, 2012), see table 4.1 standby data. Standby data was selected since these give the highest maximum power for the engine. Calculations are not shown. To identify torque limitations it is assumed that the engine minimum speed is 1000rpm and the maximum is 2100rpm. Thus with the data from table 4.1 a power and torque curve is created, see figure 4.1a and 4.1b.

Discussion

From table 4.1 required fuel mass flow for a certain speed and power is found. If the injector fuel mass flow rate was known this can be used to determine the injection duration, see chapter 2. But this data is not available and therefore not possible to determine. The table also shows that with decreasing load specific fuel consumption (b_e) increases and overall efficiency (η_e) decreases. This is typical for diesel engines, see also figure 4.1c. From table 4.1 values for power, torque and mean effective pressure are given for 100% load at 1500 and 1800rpm. By drawing a line between these two 100% values the P_{emax}, T_{emax} and p_{memax} are determined, see figure 4.1a and 4.1b.

Table 4.1: Engine performance data.

P_e [%]	100	75	50	100	75	50
n [rpm]	1800	1800	1800	1500	1500	1500
n [rps]	30	30	30	25	25	25
$V_d[m^3]$	1.45E-03	1.45E-03	1.45E-03	1.45E-03	1.45E-03	1.45E-03
p_{me} [kPa]	1953	1465	977	2095	1571	1048
P_e [kW]	255	191	128	228	171	114
T_e [Nm]	1353	1015	677	1452	1089	726
$\dot{q}_f$ [l/hr]	58.9	48.9	37.8	53.9	42.1	31.5
$\dot{q}_f[m^3/s]$	1.64E-05	1.36E-05	1.05E-05	1.50E-05	1.17E-05	8.75E-06
$\rho_f[kg/m^3]$	850	850	850	850	850	850
$\dot{m}_f$ [kg/s]	1.39E-02	1.15E-02	8.95E-03	1.27E-02	9.94E-03	7.44E-03
b_e [g/kWh]	196	217	252	201	209	235
W_e [J]	2.83E+03	2.13E+03	1.42E+03	3.04E+03	2.28E+03	1.52E+03
m_f [g]	0.1545	0.1283	0.0992	0.1697	0.1325	0.0992
h_{LHV} [MJ/kg]	42.7	42.7	42.7	42.7	42.7	42.7
η_e [-]	0.43	0.39	0.33	0.42	0.40	0.36

In (Pon-Cat, 2012) BS2869 Class A2 diesel fuel is used and the fuel specific gravity is given. Lower heating value h_{LHV} for this fuel is 42.7MJ/kg (Total, 2010).

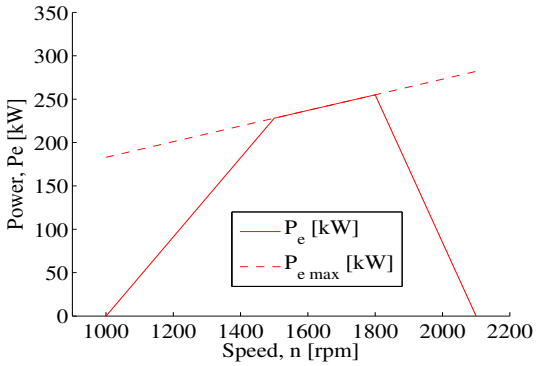

(a) Engine power vs engine speed.

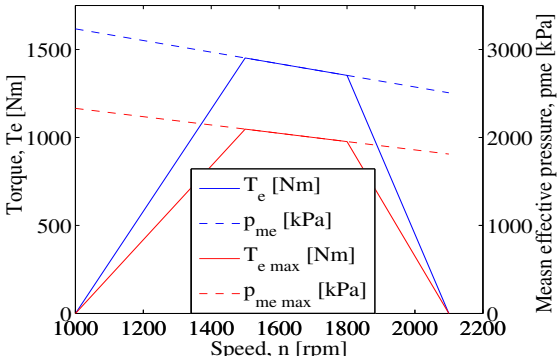

(b) Engine torque and mean effective pressure vs engine speed.

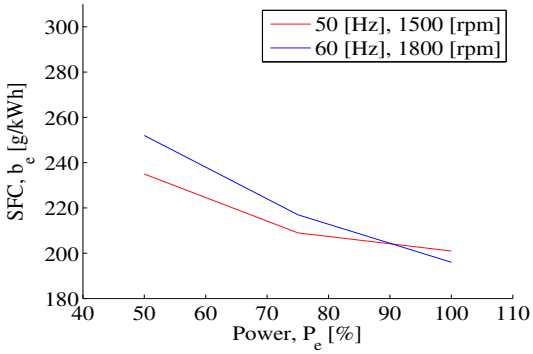

(c) Engine specific fuel consumption (SFC) vs power.

Figure 4.1: Engine performance curves.

Chapter 5

Reverse Engineering

Reverse engineering is the method chosen for the design of the new ECU, from here on referred to as ECU. A number of engine tests with the PECU is performed to collect data to mirror the PECU behavior into the ECU. This chapter presents the data gathered from these test runs. The test runs consist of one start test and 15 load tests at different engine speeds and load points. Labview DAQ "NI USB-6210"(National-Instrument, 2015) is used for data acquisition of the signals shown in table 5.1 with a sampling speed of 30000Hz. A Matlab program is created to analyze and plot the data.

First camshaft encoder, see section 5.1, and injector current characteristic, see section 5.2, are presented since these are essential both during engine start and when the engine is loaded. Start test is presented in section 5.3 and the 15 load tests in section 5.4. A discussion of the results is done at the end of each section.

Table 5.1: Signals for data acquisition.

Description	Type	Signal	Unit	Sensor Type
Rail Pressure NTNU sensor	Analog Input	0-5	[bar]	Variable capacitance
Rail Pressure sensor	Analog Input	0-5	[V]	Variable capacitance
Rail oil pressure valve control signal	Analog Input	0-5	[V]	Inductive coil
Current in injector (6)	Analog Input	0-7	[A]	Inductive coil
Current in injector (654)	Analog Input	0-7	[A]	Inductive coil
Camshaft Encoder sensor	Digital Input	0-5	[V]	Hall Effect
Cylinder 6 in cylinder pressure NTNU sensor	Analog Input	0-400	[bar]	Variable capacitance

5.1 Camshaft Encoder

The camshaft encoder registers the pulses generated by the Hall effect sensor on the engine when the camshaft teeth passes. One rotation of the camshaft consists of 24 pulses (one pulse with a short high duration and 23 with a longer high duration), see figure 5.1.To the left and right in the figure the tooth with a short high duration is seen and between these two there is 23 high pulses.

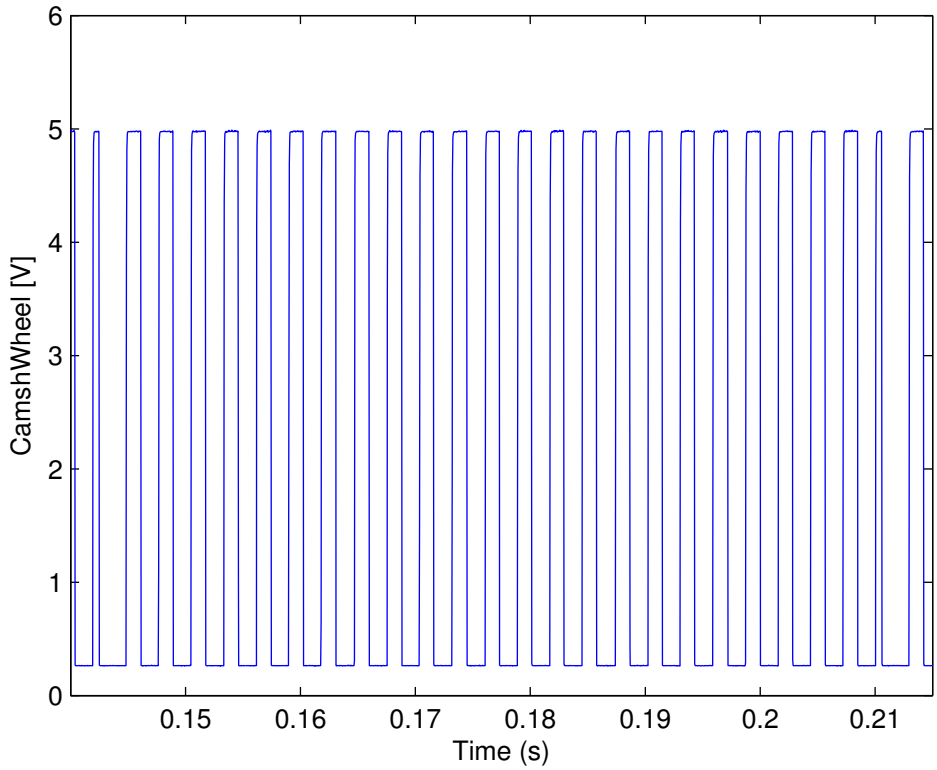

Figure 5.1: Camshaft encoder signal.

Discussion

The 24 teeth consist of 23 equal teeth and one tooth with a high period that is half the high period of the other teeth and a low period that is three quarter of the other teeth. This tooth is used for detecting one rotation of the camshaft. By counting the pulses for a given time period the camshaft speed and rotational position are determined. Since the pulse period for all 24 teeth are equal this gives

$$\frac{360deg}{24teeth} = 15deg/tooth \tag{5.1}$$

For each low and high duration this equals half the period of 15deg and gives 7.5 deg/half period for the 23 equal teeth. For the top tooth this equals 0.25 times the period for the high period and gives 3.75deg and 0.75 times the period for the low period and gives 11.25deg. Since

the camshaft speed are now known by

$$n_{cam} = \frac{N_{teeth}}{dt} \quad [r/s] \tag{5.2}$$

the crankshaft speed for a 4-stroke engine is

$$n_{crank} = 2 \cdot n_{cam} \quad [r/s] \tag{5.3}$$

the crankshaft angular speed for a 4-stroke engine is

$$\omega_{crank} = 2 \cdot \omega_{cam} \quad [deg/s] \tag{5.4}$$

and the angular position for a 4-stroke engine is

$$\theta_{crank} = 2 \cdot \theta_{cam} \quad [deg] \tag{5.5}$$

According to (Perkins-Engines, 2001) engine speed limit is 3000rpm. This gives a maximum camshaft speed of

$$n_{cam} = \frac{n_{crank}}{2} = \frac{3000rpm}{2} = 1500rpm = \frac{1500}{60} = 25r/s \tag{5.6}$$

teeth pulse frequency

$$f_{teeth} = n_{cam} \cdot N_{teeth} = 25r/s \cdot 24pulses/r = 600pulses/s = 600Hz \tag{5.7}$$

time between each tooth

$$T_{teeth} = \frac{1}{f_{teeth}} = \frac{1}{600Hz} = 1.67ms \tag{5.8}$$

and a half tooth duration of

$$T_{halftooth} = \frac{T_{teeth}}{2} = \frac{1.67ms}{2} = 0.835ms \tag{5.9}$$

for the top tooth the shortest duration is

$$T_{toptooth} = \frac{T_{halftooth}}{2} = \frac{0.835ms}{2} = 0.418ms \tag{5.10}$$

As seen from equation 5.10 the top tooth has the shortest duration. A high sampling speed is therefore required to detect it. To avoid aliasing of the signal, a conservative sampling speed of 10 times the signal is chosen. This gives a recommended sampling speed of

$$t_{sample} = \frac{T_{toptooth}}{10} = \frac{0.418ms}{10} = 0.0418ms \tag{5.11}$$

and a recommended sampling frequency of

$$f_{sample} = \frac{1}{t_{sample}} = \frac{1}{0.0418ms} = 23923Hz \tag{5.12}$$

5.2 Injector Current

In figure 5.2 the current characteristic for one injector coil is displayed. Figure 5.2a show one injection duration while figure 5.2b shows different injection durations.

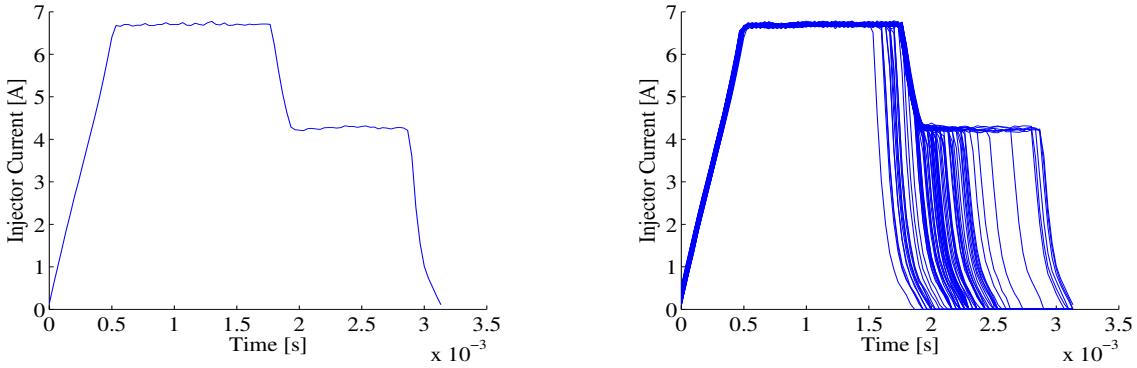

(a) One injection duration plotted.

(b) Several injection durations plotted.

Figure 5.2: Injector current curve characteristic.

Discussion

From figure 5.2a it is seen that the injector current consist of three phases, ref. also (Sybele, 2009). Phase one is a sharp increase in the current from 0 to 6.7A in 0.48ms referred to as the attack phase. This sharp increase of the current is accomplished by applying a voltage of 110V over the injector coil during phase one. For phase two and three the voltage is reduced to 55V. In phase two the current is kept at 6.7A, this is the holding phase, before the current is dropped to 4.3A in phase three, the withstand phase. Phase one and two have a fixed length of hence 0.48ms and 1.22ms. The longest injection duration observed is 3.0ms. This give a maximum time for phase three of 1.3ms. Figure 5.2b shows different current curves for varying injection durations. The shape of the injector current curve is the same for all injection durations and the only difference is the duration. It is assumed that the the current characteristic curves are equal for all six injectors. It is not possible to measure the position of the rail valve piston in the injector so it is not possible to say at what time during the injection duration the valve is in open position. Thus it is not possible to say exactly when the first fuel is injected. It is therefore assumed that recreating the curve shape will mirror the injector opening. As for the camshaft encoder the injector control signal requires high processing speed. With a signal duration for the attack period of 0.48ms and a conservative output speed of 10 times the fastest signal, this gives a recommended speed of

$$t_{output} = \frac{T_{attack}}{10} = \frac{0.48ms}{10} = 0.048ms \tag{5.13}$$

and a recommended output frequency of

$$f_{sample} = \frac{1}{t_{sample}} = \frac{1}{0.048ms} = 20833Hz \tag{5.14}$$

(Sybele, 2009) mentions PWM with half period duration in microsecond for control of injector current in the holding and withstand phase. From the gathered data it is not possible to see the duration of these assumed PWM signals.

5.3 Start Test

Figure 5.3 shows the engine speed change during start from standstill, 0rpm, to idle speed, 1000rpm. A test is also performed to see the highest speed reached when the engine is only rotated by the starter motor, also referred to as cranking (Bosch, 2006). This is a cranking speed of 240rpm with a cylinder pressure of 38bar.

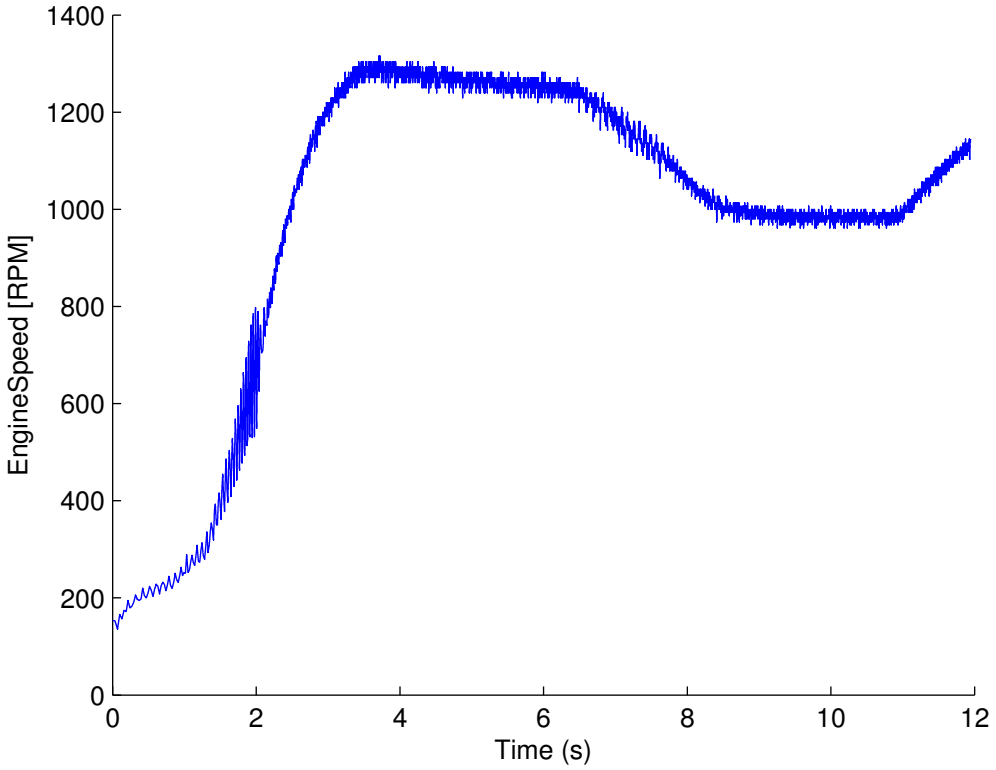

Figure 5.3: Engine speed change during starting.

Discussion

With a cranking speed of 240rpm it is assumed from figure 5.3 that fuel is injected into the cylinders to enable the acceleration from 240rpm to the maximum starting speed of approximately 1280rpm. From 200-800rpm the speed signal changes with an increasing varying speed magnitude with a maximum of +/- 150 at 650rpm. The rail oil pressure also has varying magnitude with a maximum of +/- 5bar at 121bar during this period. This suggests that the engine speed is uneven during the initial firing. At approximately 800rpm the engine speed stabilises with a

smaller varying speed magnitude of +/- 12 suggesting that a more stable ignition occurs as the engine accelerates to 1280rpm. The engine runs at 1280rpm for three seconds at 1280-1240rpm before it drops to the idle speed of 1000rpm. After twelve seconds the engine speed set point is manually changed and the engine speed starts to ramp up.

5.3.1 Rail Pressure During Start

The rail pressure as shown in figure 5.4 is controlled with the current applied to the coil of the rail oil pressure control valve shown in figure 5.5.

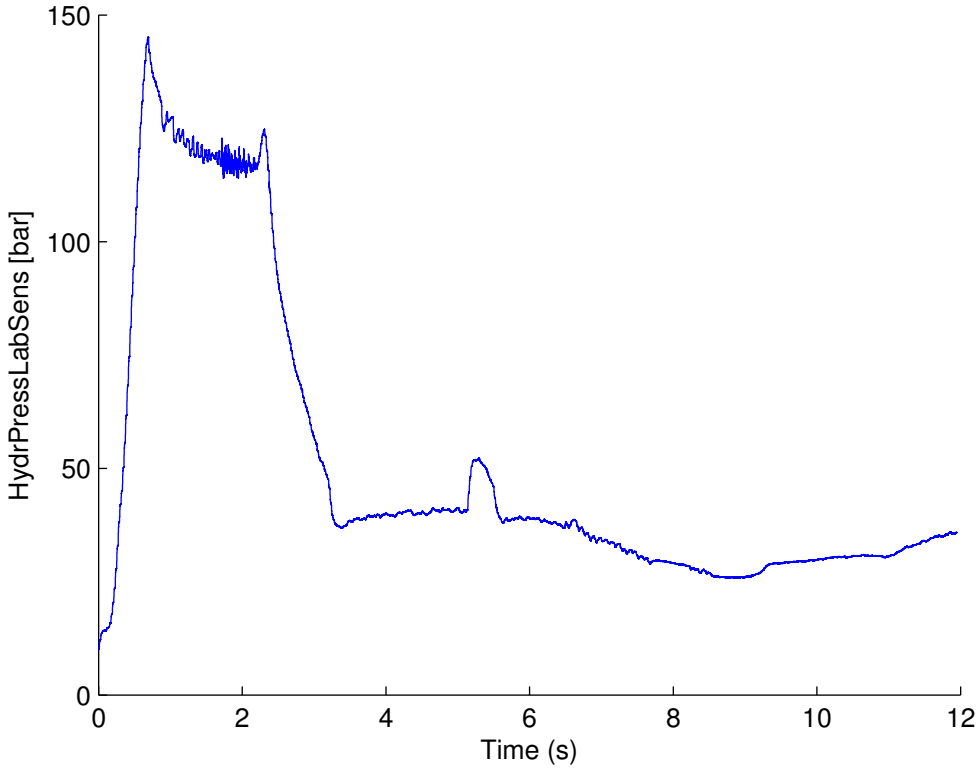

Figure 5.4: Rail oil pressure NTNU sensor.

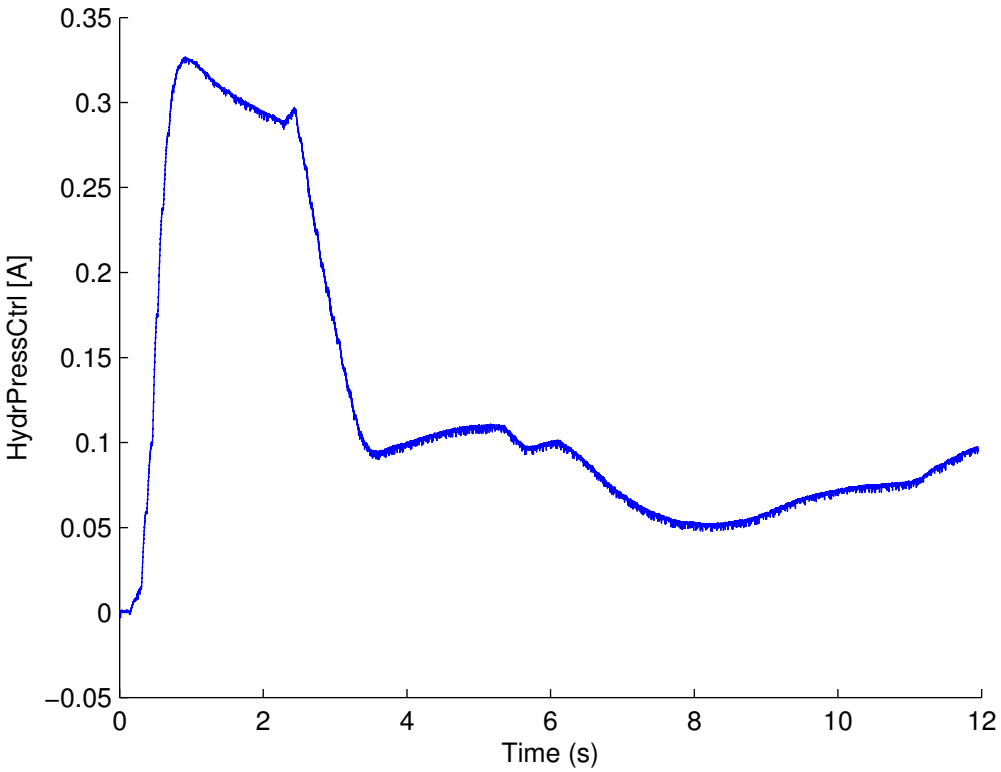

Figure 5.5: Rail oil pressure control valve current.

Discussion

During start, the rail valve is closed to increase rail oil pressure for the first injections. A high rail pressure gives a diesel spray with small droplets into the cylinders for the initial ignitions. As the engine accelerates the rail pressure is reduced to reduce the rate of fuel injected into the cylinder.

5.3.2 Injector Timing During Start

Figure 5.6 shows the variation in the current signal sent to the injector coil during start.

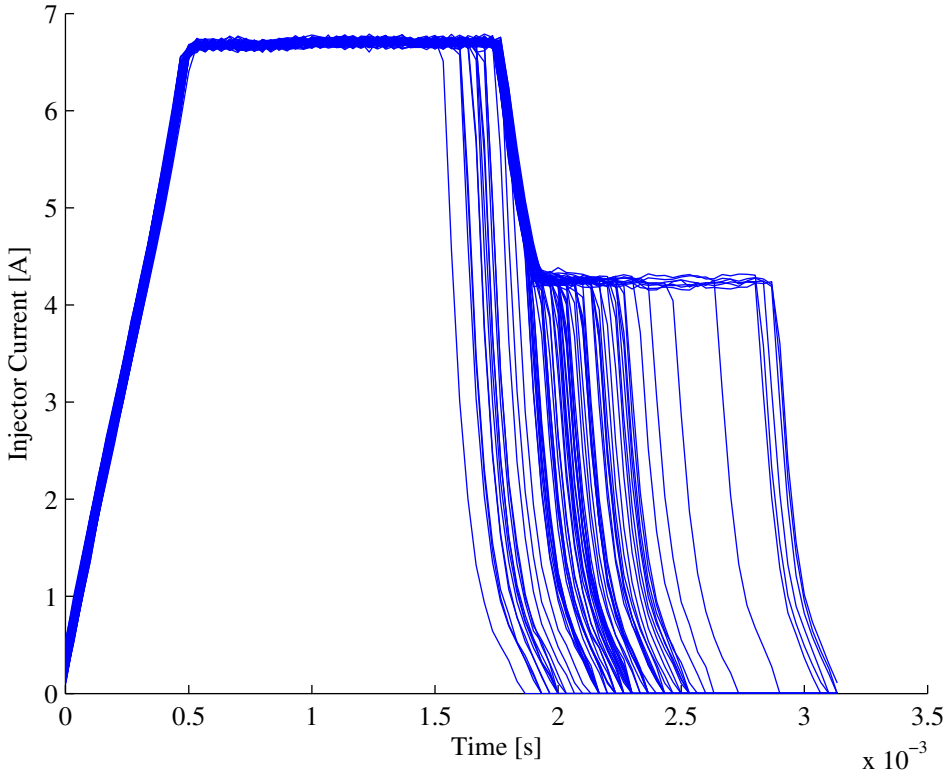

Figure 5.6: Injector current during start.

Discussion

The initial injection period is 2.7ms and increases with increasing speed and decreasing rail pressure during the engine speed acceleration from 240-850rpm. The reason for a high pressure is to increase the energy released during combustion to increase the angular acceleration of the crankshaft. As the engine speed increases, the angular acceleration is decreased, thus the torque is decreased by decreasing the energy released from the combustion. Therefore from 850rpm the injection duration and rail pressure is reduced to an injection duration of 2.1ms and a rail pressure of 39bar to limit the engine speed to 1280rpm.

5.3.3 Cylinder Pressure During Start

Cylinder pressure variations during start is shown in figure 5.7. Figure 5.8 shows zoomed in versions of the pressure variation in figure 5.7.

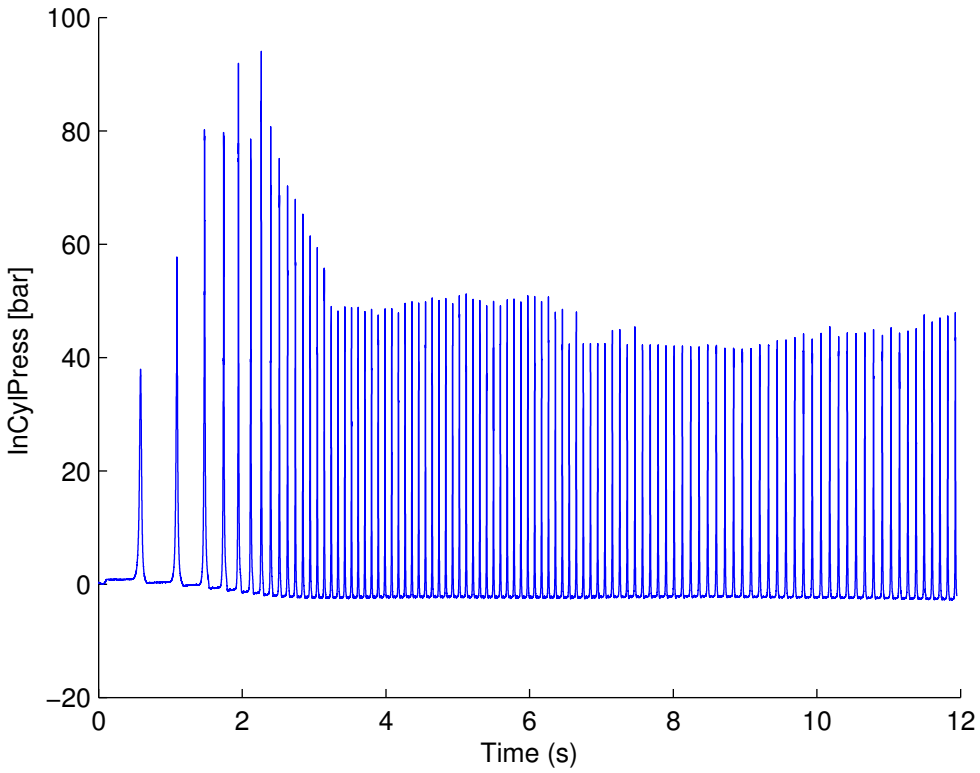

Figure 5.7: Cylinder pressure during start.

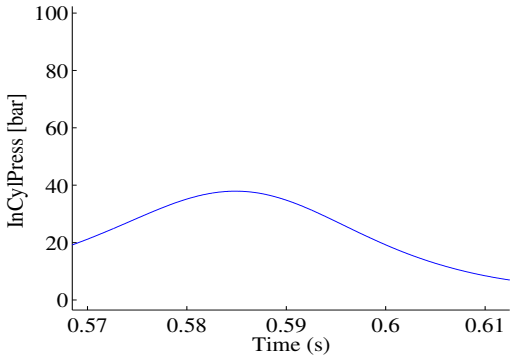

(a) Cylinder pressure at cranking speed.

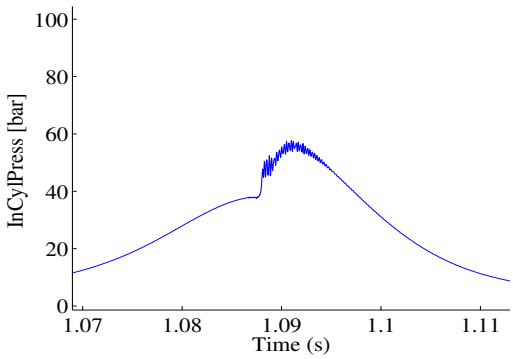

(b) Cylinder pressure at first ignition.

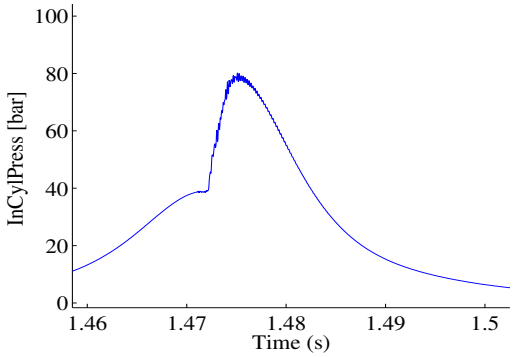

(c) Cylinder pressure at second ignition.

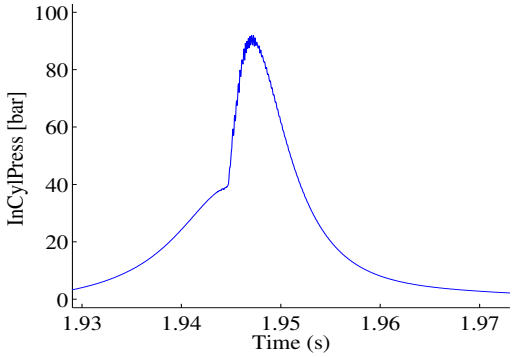

(d) Cylinder pressure at fourth ignition.

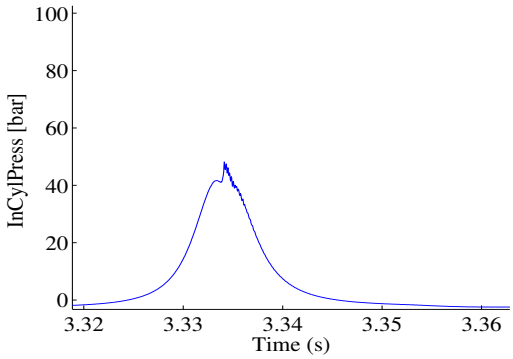

(e) Cylinder Pressure at 1240rpm.

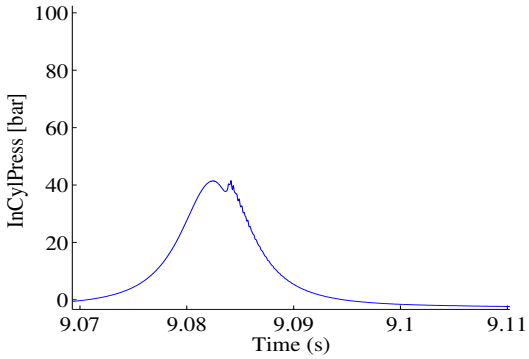

(f) Cylinder Pressure at 1000rpm.

Figure 5.8: Cylinder pressure during start.

Discussion

The cylinder pressure is approximately 38bar during cranking speed. It increases to approximately 94bar during initial firing due to the high rail oil pressure. As the speed increases and the rail oil pressure decreases, the cylinder pressure decreases to approximately 50bar when the engine is at 1250rpm. At the end of the start the engine speed drops to 1000rpm and the cylinder

pressure decreases to approximately 40bar.

5.4 Load Test

To see how the engine parameters change with load and speed, 15 operating or load points are tested , see figure 5.9. Each point is defined by an engine speed value and a generator load value. Engine speed is adjusted by changing the engine speed set-point sent to the PECU and then the engine actual speed feedback is visually identified from the engine monitoring display. Generator load is adjusted by changing the torque set point for the load brake and the generator load value is visually identified from the ABB Power Management display. For each load point there is a maximum power value, when this value is exceeded the engine stops.

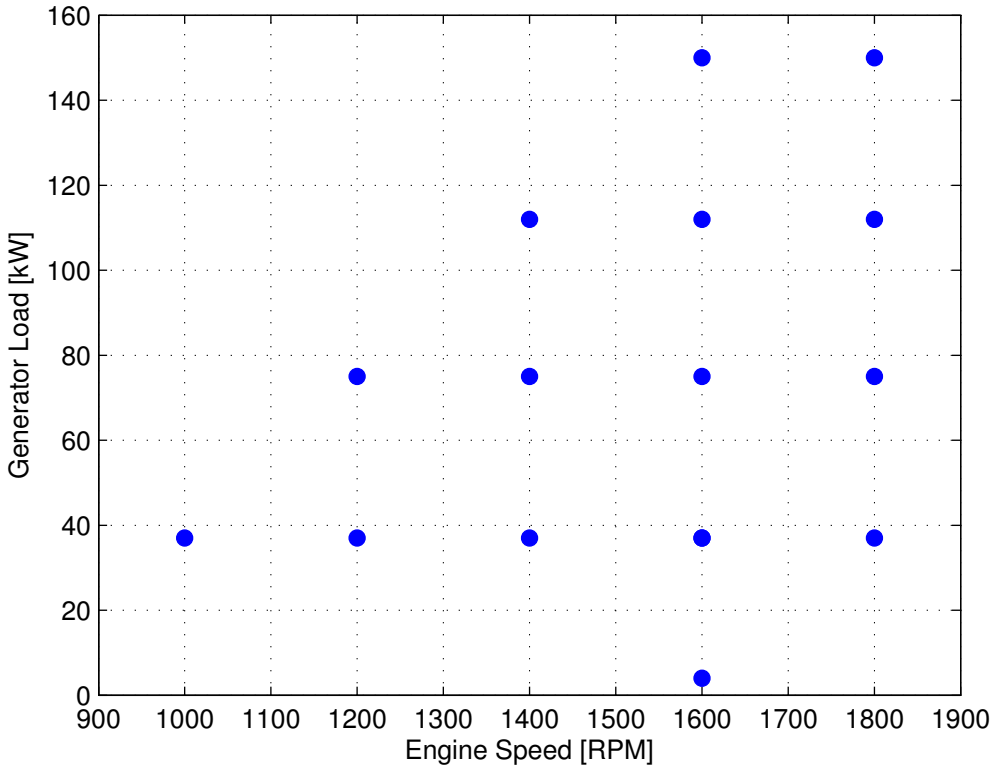

Figure 5.9: Engine load test points.

Discussion

Note that power shown is for generator power, not engine power. A generator will have mechanical losses, thus the engine shaft power is higher than what is indicated in figure 5.9. However, with a typical efficiency of 0.96 (Sørensen, 2013) for the read power value in the ABB PMS this is deemed accurate enough since generator power and engine speed are visually identified.

Between the maximum power points for each speed in figure 5.9 a maximum power or limit line for the engine can be drawn. As is shown in figure 1.2 one part of this limit line is the smoke limit and the second part is the torque limit. From figure 5.9 the maximum power increases from 1000rpm to 1600rpm. This suggests that the smoke limit is in this range. At 1600 to 1800rpm the engine's maximum power is constant, which implies that the torque limit is in this range. Assuming that the smoke limits are the same for a prime and standby generator(Pon-Cat, 2012) power and torque curves from figures 4.1 and 5.9 can be combined in figure 5.10. Thus the smoke and torque limitations for the engine are identified.

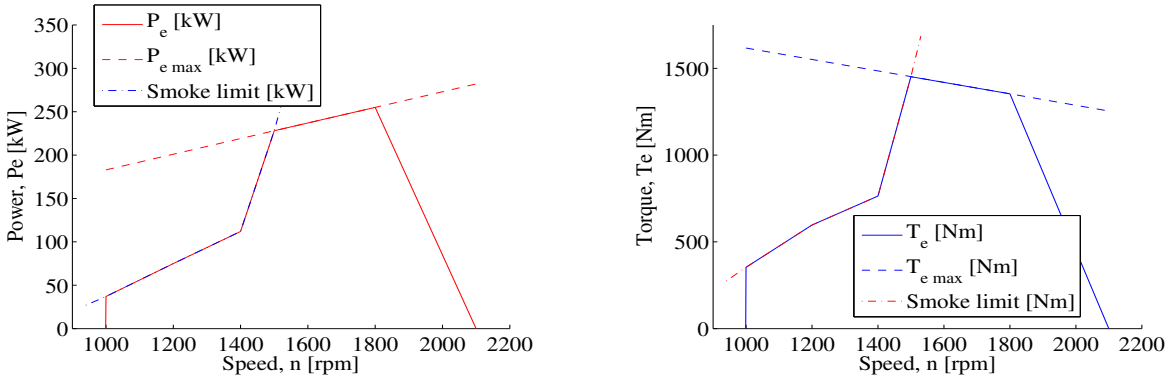

(a) Engine power vs engine speed.

(b) Engine torque vs engine speed.

Figure 5.10: Engine performance curves.

5.4.1 Rail Oil Pressure

Rail oil pressure as a function of engine speed and generator load is shown in figure 5.11b.

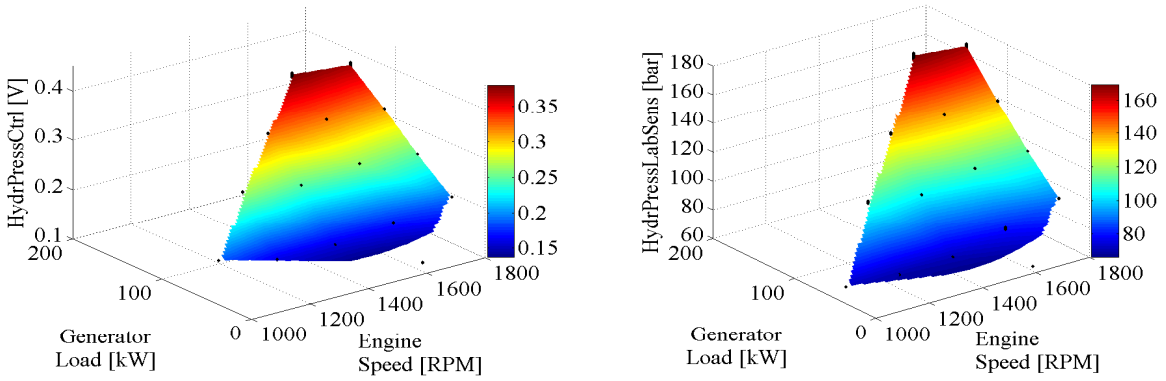

(a) Rail oil control valve current.

(b) Rail oil pressure NTNU sensor

Figure 5.11: Rail oil pressure control.

Discussion

As mentioned above the rail oil pressure is a function of engine power and engine speed. An increase in rail pressure will give an increase in the rate of fuel that can be injected since a higher rail pressure gives a higher fuel pressure in the injector to overcome the spring force that closes the injector needle. In figure 5.11a it is shown that the current to the rail control valve increases with increasing load. To increase the pressure, see figure 5.11b, an increase of the current through the coil is needed to keep the valve closed for a longer time.

5.4.2 Injector Timing

Injection start and duration for different speed and load points are shown in figure 5.12.

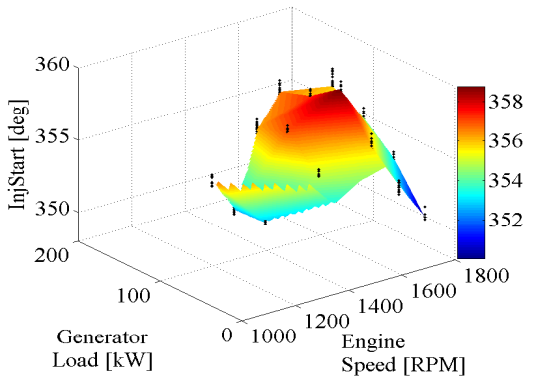

(a) Injection start [deg].

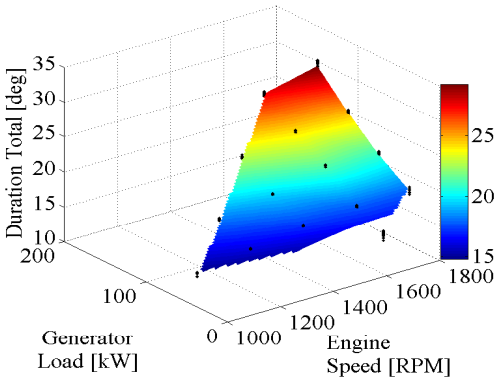

(b) Injection duration [deg].

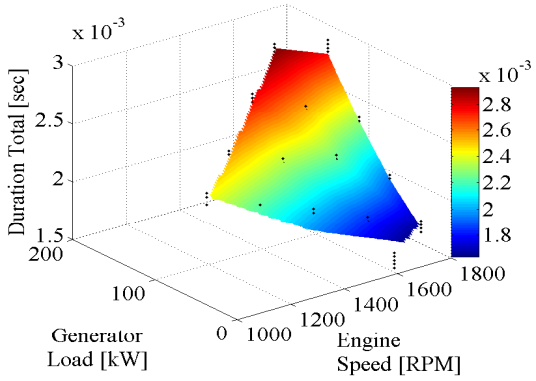

(c) Injection duration [s].

Figure 5.12: Injection start and duration.

Discussion

Figure 5.12 indicates that the injection duration increases with increasing load which is reasonable since more fuel is needed. Injection duration is also a function of the rail oil pressure since this controls the rate of fuel that is injected. Increase in rail pressure increases amount of fuel that is injected for the same injection duration since the fuel pressure force increases with increasing rail pressure in the injector. Start of injection is advanced for increasing speed and low load and is retarded for increasing load around 1500rpm, see figure 5.12a. Advance here means early injection before Top Dead Center (TDC) and retarded means injection close to or after TDC. With no data available for the injectors it is not possible to establish the amount of fuel injected.

5.4.3 Cylinder Pressure

Cylinder pressure variations when running with load are shown in figure 5.13.

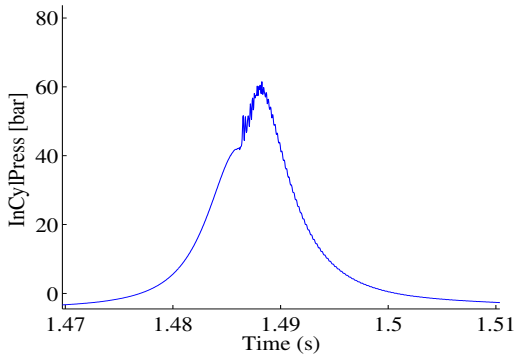

(a) Cylinder pressure at 1000rpm and 37kW.

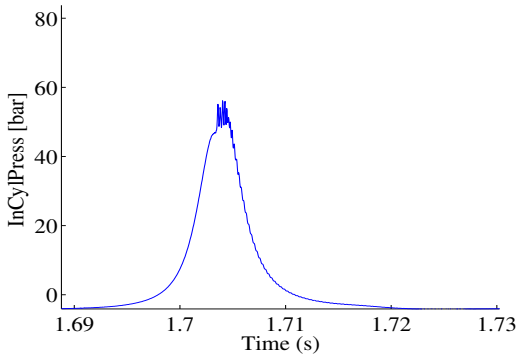

(b) Cylinder pressure at 1800rpm and 37kW.

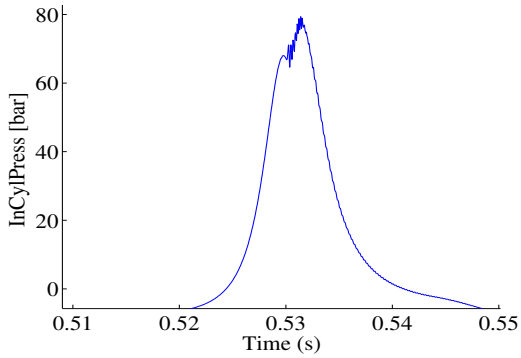

(c) Cylinder pressure at 1600rpm and 150kW.

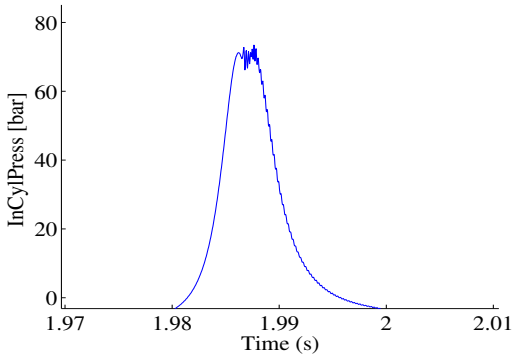

(d) Cylinder pressure at 1800rpm and 150kW.

Figure 5.13: Cylinder pressure during load test.

Discussion

Figure 5.13 shows that an increase in engine speed at constant load decreases the cylinder pressure. This is seen by comparing figure 5.13c and 5.13d where the pressure decreases from around 80bar to around 70bar. Since the engine shaft power (P_e) is constant, the brake mean effective pressure (p_{me}) must decrease with increasing speed (n). This is in accordance with equation 5.15 for a four stroke engine.

$$p_{me} = \frac{2 \cdot P_e}{i \cdot V_d \cdot n} = \frac{2 \cdot P_e}{i \cdot V_d} \cdot \frac{1}{n} = const \cdot \frac{1}{n} \tag{5.15}$$

Where i is number of cylinders and V_d is cylinder displacement. A decrease of p_{me} gives a decrease in mean indicated pressure (p_{mi}) assuming a constant mechanical efficiency (η_m), equation 5.16

$$p_{mi} = \frac{p_{me}}{\eta_m} = \frac{1}{\eta_m} \cdot const \cdot \frac{1}{n} = const \cdot \frac{1}{n} \tag{5.16}$$

p_{mi} is also given as in equation 5.17

$$p_{mi} = \frac{1}{V_d} \oint_V p dV \tag{5.17}$$

and it follows that the only way to reduce p_{mi} is by reducing the cylinder pressure p since V_d is constant.

5.4.4 Summary and Conclusion

It is apparent that the camshaft speed encoder requires a high processing speed with a minimum sampling speed of 0.0418ms which equals a frequency of 23923Hz, see section 5.1. Also for the injector current control there is a requirement for a high processing with a minimum speed of 0.048ms which equals a frequency of 20833Hz, see section 5.2. To satisfy both requirements, the higher of the two frequencies must be chosen. Therefore the required sampling speed is set to a minimum of 0.0418ms.

From the gathered data for starting a start table is created to see the development of injection parameters during start, see table 5.2. Note that throttle position is ignored during start since it is assumed that the engine is only using table values during start.

Injection parameters for a running engine are gathered from the load tests performed, see table 5.3. The load test point identification values are generator load and engine speed in the two left columns. The maximum assumed engine speed with load is 2100rpm but only load tests up 1800rpm are performed. For zero generator load only one test is performed for 1600rpm and data for 1000 and 1200rpm are taken from the gathered start data. Thus for an engine speed of 900, 1400 and 1800rpm no data are available and the data is only assumed. The assumed data is created with curve fitting to the available data. When the engine is up and running the engine speed is assumed controlled by a throttle position controller, like a gas pedal in a car. Thus a

throttle position value from 0-100% is used. To increase engine speed or compensating for increasing engine load the throttle position is increased and vice verse to decrease. Therefore an increasing throttle position value is used for increasing speed and load. Assumed idle speed for the engine is 1000rpm at zero engine load. However, to have some operational area for the throttle controller a minimum engine speed limit of 900rpm is needed. For this speed a minimum throttle position of 8% is recommended.

Engine smoke and torque limits were identified in figure 5.10. From the figure it is clear that engine maximum power is higher than the current engine configuration. Note also that the ABB generator is rated for a power of 182kW, ref. table 3.2, while the engine rated power is 255kW in standby(Pon-Cat, 2012).

Table 5.2: Engine start data summary.

Generator Load [kW]	**Engine Speed [rpm]**	**Rail Press Ctrl [A]**	**Rail Press Lab Sensor [bar]**	**Injection Start TDC [deg]**	**Injection Duration [deg]**	**Inj Duration [ms]**	**Throttle Position [%]**
0	261	0.31	129.41	3.1	4.2	2.700	-
0	861	0.29	120.57	-5.0	14.0	2.711	-
0	1019	0.28	88.75	-7.2	13.6	2.233	-
0	1213	0.16	53.77	-11.2	16.0	2.200	-
0	1286	0.09	38.55	-7.2	16.1	2.089	-
0	1242	0.10	37.90	-6.3	12.4	1.667	-
0	1002	0.05	25.95	-2.5	11.0	1.833	-

Table 5.3: Engine load test data summary.

Generator Load [kW]	**Engine Speed [rpm]**	**Rail Press Ctrl [A]**	**Rail Press Lab Sensor [bar]**	**Injection Start TDC [deg]**	**Injection Duration [deg]**	**Inj Duration [ms]**	**Throttle Position [%]**
0	900	-	29	0.0	14.6	2.7	8
0	1000	0.08	31.41	-2.2	15.4	2.57	10
0	1200	0.1	37	-6.0	14.7	2.04	13
0	1400	-	45	-6.8	15.5	1.85	16
4	1600	0.17	63.16	-6.0	15.5	1.614	18
0	1800	-	86	-5.0	16.2	1.5	20
37	1000	0.19	71.57	-3.3	14.6	2.430	25
37	1200	0.16	69.39	-7.3	16.0	2.219	30
37	1400	0.16	70.98	-5.1	17.0	2.028	35
37	1600	0.17	77.50	-4.1	17.7	1.842	40
37	1800	0.19	90.94	-10.0	17.8	1.645	45
75	1200	0.27	109.83	-7.4	18.4	2.554	50
75	1400	0.25	103.81	-3.0	19.7	2.346	55
75	1600	0.26	111.62	-1.2	21.5	2.240	60
75	1800	0.25	112.87	-7.0	20.8	1.930	65
112	1400	0.32	136.02	-3.8	23.1	2.753	70
112	1600	0.32	138.26	-2.7	24.4	2.544	75
112	1800	0.31	137.58	-5.2	24.8	2.299	80
150	1600	0.38	169.37	-3.4	28.1	2.928	85
150	1800	0.37	165.40	-4.1	29.7	2.748	90
183	2000						95
183	2100						100

Chapter 6

Engine Control Unit Development

This chapter gives a description of the ECU developed. The architecture for the ECU is depicted in figure 6.1 and is explained in detail in the following sections. It is decided to use a National Instrument Labview CompactRIO SW/HW platform because of an already existing knowledge base at NTNU. The CompactRIO has two controllers, one Realtime (RT) controller and one Field Programmable Gate Array (FPGA) controller that communicate through a PCI bus. Due to the high processing speed required for the engine speed and camshaft position processing and the firing synchronization, the ECU software is divided into two separate parts, one RT part and a FPGA part. The ECU is controlled by the RT program, which contains several algorithms. The algorithms consist of several Labview subVIs in the RT controller and a main FPGA program that runs on the FPGA controller. The FGPA program also consists of several subVIs as well as handling the interface to the I/O cards. This is also seen from figure 6.1 where there is a RT part that represents the main RT program with several blocks for "Analog conversion" etc. This block represents a subVI. It is to be noted that one subVI can consist of multiple other subVIs. The same is the case for the FPGA controller where the main FPGA program consists of several subVIs.

Five main parts make up the ECU; Labview CompactRIO hardware and software platform, section 6.1 , RT controller, section 6.2. , FPGA controller, section 6.3. , Hardware, section 6.4. and Engine interface, section 6.5.

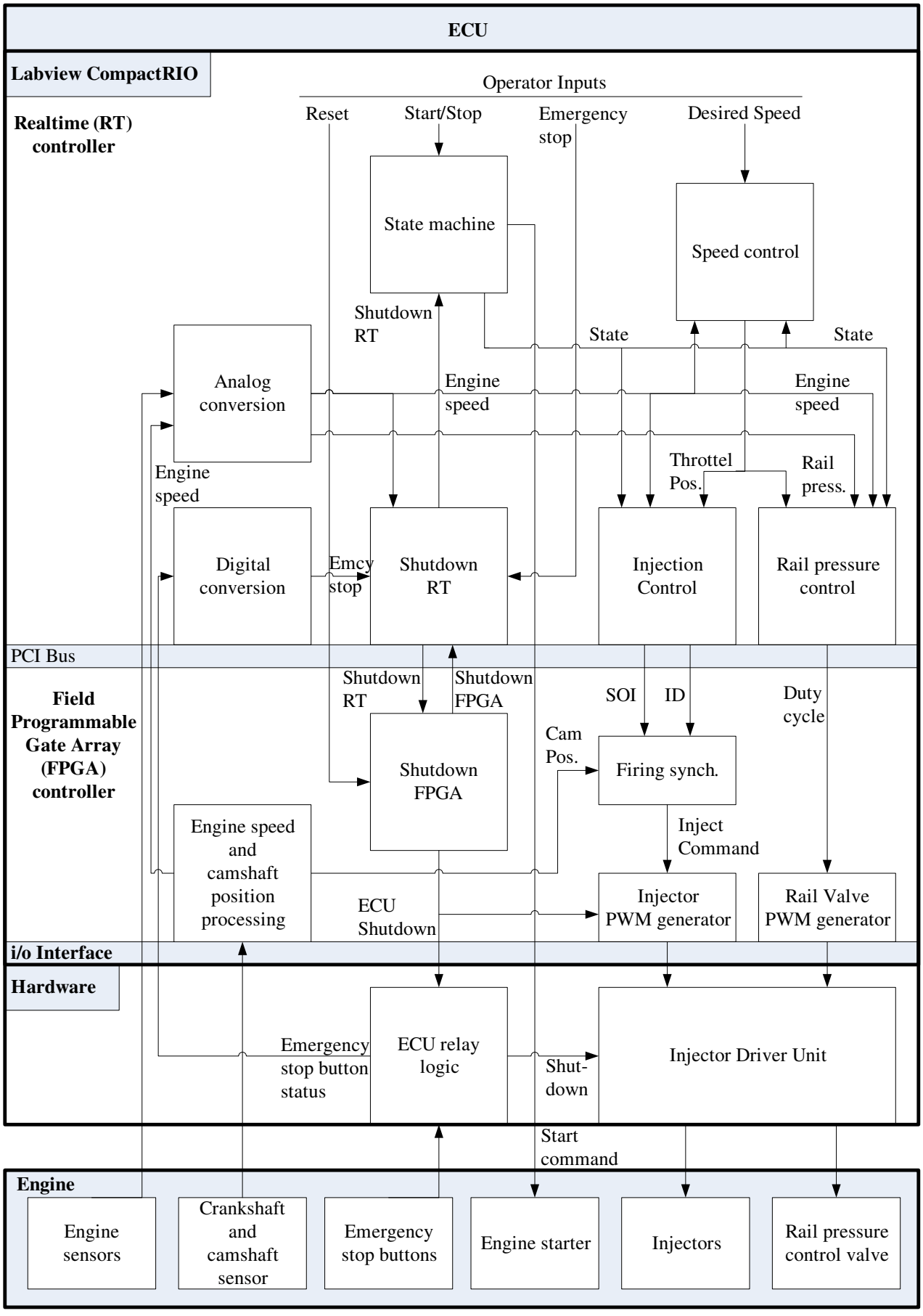

Figure 6.1: ECU architecture.

6.1 ECU Hardware and Software Platform

A Labview Field Programmable Gate Array (FPGA) and Realtime (RT) controller, named "CompactRIO", is used as a platform for the new ECU. The main reason for choosing the CompactRIO is that it is used at the NTNU Marine department for educational and research purposes. National Instruments Labview software and hardware package is widely used by educational and research institutions as well as in the industry. It is a powerful tool for data acquisition and control and can be run on a standard computer or dedicated Labview hardware platform or a combination of both.

6.1.1 Hardware Platform

The CompactRIO module contains a RT controller, a FPGA controller and a number of I/O module slots depending on the type chosen. The basic backplane hardware module is available with different numbers of I/O slots and customized with I/O modules for analog-input/-output, digital-input/-output, thermocouple etc. A CompactRIO module with four I/O slots is shown in figure 6.2. If required the backplane can be extended with additional I/O slots.

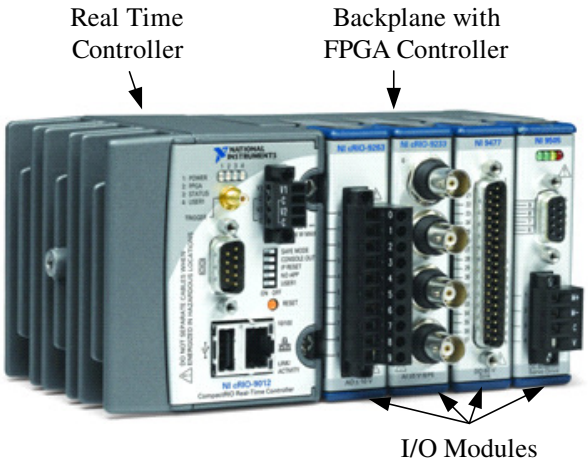

Figure 6.2: CompactRIO module with 4 i/o module slots (Source: National Instrument).

The I/O modules are interfaced to the FPGA controller and signals can be distributed from the FPGA to the RT controller through a PCI bus integrated in the backplane. From the RT controller the signals can be distributed to a standard PC for display purposes, see figure 6.3.

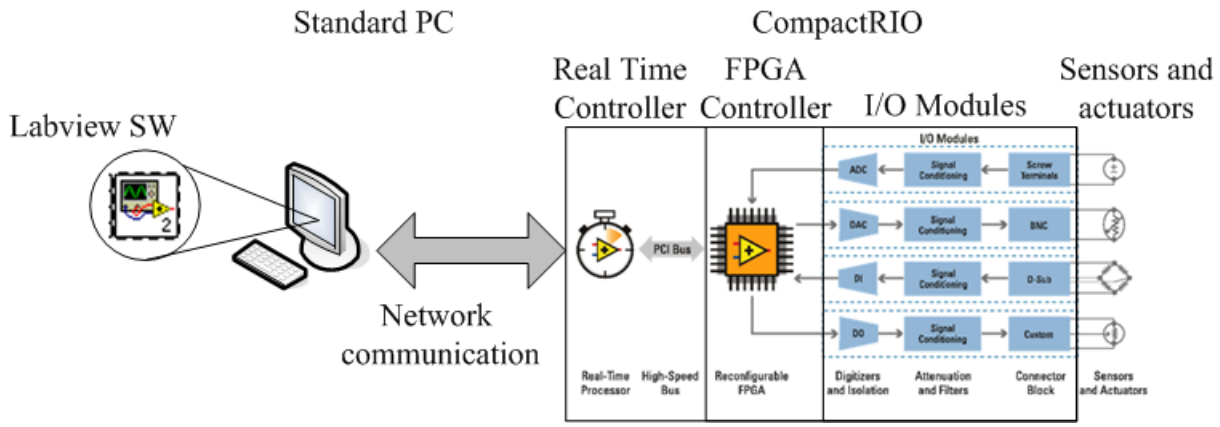

Figure 6.3: Architecture of a CompactRIO system (Source: National Instrument).

Labview HW modules in the project are shown in table 6.1.

Table 6.1: Labview HW.

Version:	CompactRIO	
IO Type	**Slot**	**Module Type**
Analog Input	1	NI 9205
Digital Input/Output	2	NI 9401
Digital Input/Output	3	NI 9401

6.1.2 Software Platform

The Labview software is built up of what is called Virtual Instrument (VI) that provides a graphical user interface. Each VI contains a block diagram window and one front panel window. The block diagram contains the logic blocks that control the process while the front panel displays the process values and buttons for operator interaction. Depending on the requirement, the VI's can be set to run either on a standard PC, RT controller or FPGA controller. The requirement will typically be process speed of the VI needed for processing the data and the criticality of the VI. A critical VI should run on the FPGA since it controls the I/O and has the highest process speed and stricter configuration requirements than the standard PC and RT controller.

Application development of the VI is done by accessing a graphical library that contains indi-

cators and logical blocks. By wiring the graphical blocks together the application shall perform as decided by the developer.

Best practises for development of Labview for CompactRIO can be found in (National-Instrument, 2009). Since the FPGA will run the most critical part of the process the following best practices are important to follow when developing the VI's. These should also be taken into account when developing VI's for the RT controller and a standard PC.

Best practice requirements for FPGA VI implementations to ensure modularity and readability in this project are:

- Use one unique main loop.
- Use one subVI for each elementary function.
- Avoid using delay timers and wait functions.
- Avoid using i/o nodes in subVI.
- Use cluster for inputs and outputs of each subVI.

It is recommended to avoid developing on the FPGA if possible. The FPGA has a limited number of gates thus complex logic, especially arrays, will quickly use all available space of the FPGA. Compilation of the FPGA also takes considerably longer time than compilation of the RT, up to 25 minutes for complex VIs compared to 30 seconds for a RT VI. Another challenge is that there is no dynamic update of the front panel for subVIs used by the main FPGA VI and the measuring tool for measuring wire values are not working when running against the controller. This makes debugging a challenge. None of these challenges exist for RT VIs.

Labview SW version in the project is shown in table 6.2.

Table 6.2: Labview SW.

Version:	Labview 2014

6.2 RT Controller

This section gives a detailed description of the RT controller SW. The main RT VI is the main SW for the ECU and the main engine process control is performed by the VI. It acts as the user interface for the operator inputs as shown in figure 6.1.
The main RT VI is:

- V0_ECUControl.vi

and it contains the following subVI's:

- AnalogConversion.vi
- DigitalConversion.vi
- Shutdown_RT.vi
- SpeedControl.vi
- RailPressControl.vi
- InjectionControl.vi

6.2.1 Main RT VI

The main RT VI consists of one main timed loop VI, "V0_ECUControl.vi", with several subVIs and operates with a frequency of 1kHz and a sampling rate of 10 which gives an update rate of 10ms for the main VI and its subVIs. It reads and writes data to the FPGA main VI through a PCI bus. To monitor if the RT controller is running a watchdog is configured in the VI and interfaced to the FPGA. When the main RT VI is started it calls and starts the main FPGA VI "FPGA_main_running.vi" and its subVIs and enables the I/O interface. The main RT VI also has a textfile link that reads and writes ECU configuration to/from the RT controller memory. This configuration file contains e.g PID controller settings and different engine maps.

Operator Inputs

The main operator inputs are shown in figure 6.4. Buttons for remote start/stop and speed set-point are also implemented but is not interfaced to any external equipment.

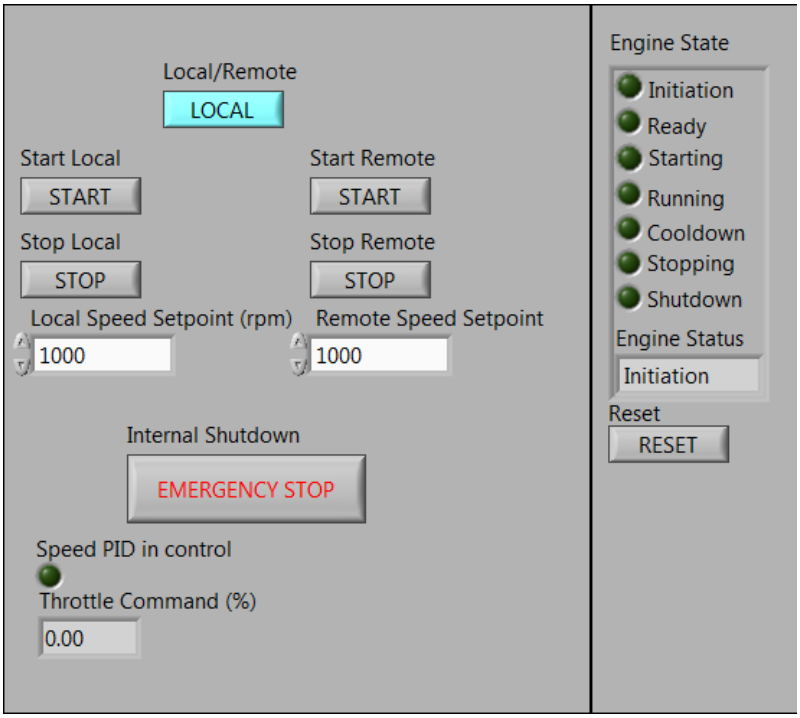

Figure 6.4: Buttons for local, remote, start, stop etc.

6.2.2 State Machine

The ECU operates with the engine in different predefined states, see figure 6.5. Transition conditions between the states are shown in the figure and only one state can be activate at a time. Depending on the active state an interface to the injection control architecture enables or disables the speed and injection control. The "Starting" state performs a start sequence that brings the engine from state "Ready" to "Running", this is also the case for the "Stopping" state. It performs a stop sequence that brings the engine from state "Running" to "Ready". The state machine is implemented as part of the main RT VI "V0_ECUControl.vi" and not as a subVI.

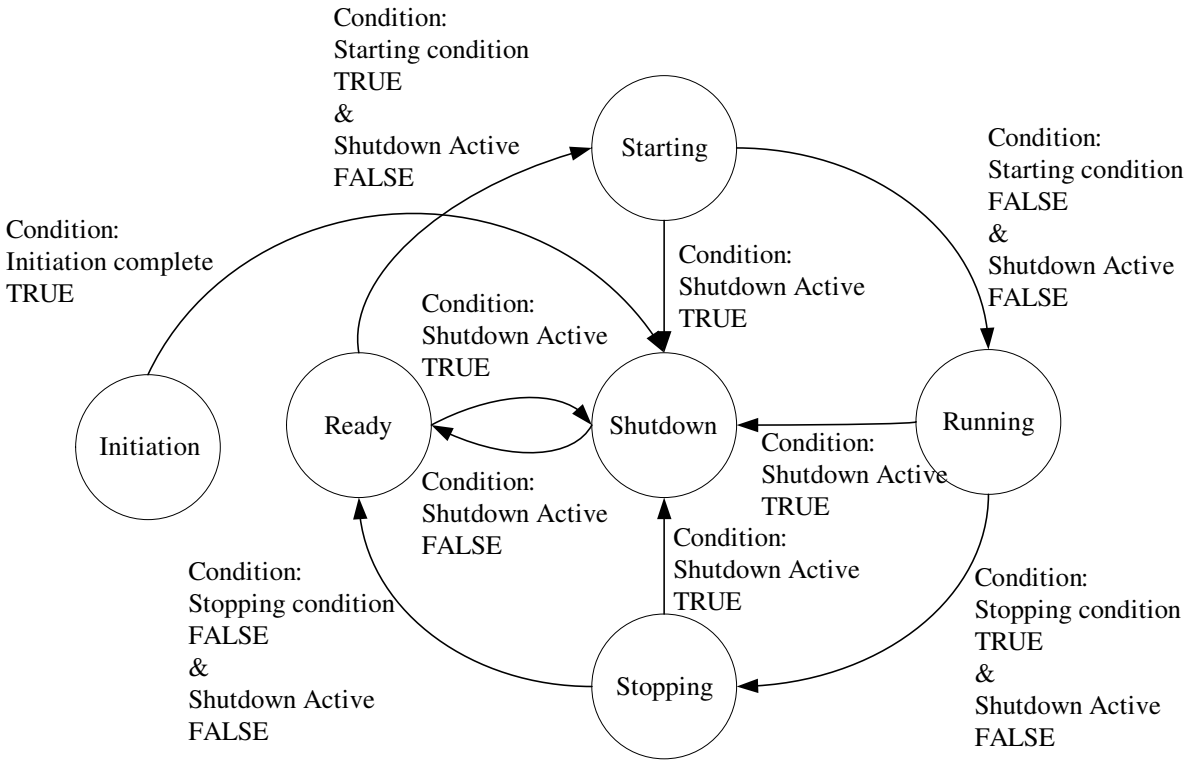

Figure 6.5: State machine.

For a description of the different states see table 6.3.

Table 6.3: State machine states.

State	Description
Initiation	Initial state where the ECU uploads and sets all setable parameters to predetermined initial values.
Ready	When the engine is ready for start it will be in this state. Initiation state must be completed and the engine shutdown state must be reset.
Starting	In this state the the engine is started from standstill by the starting sequence. The engine will remain in this state until the sequence is complete.
Running	This is the state where the speed control is controlling the engine. This is the operating state for the engine and both engine speed and power output from the engine can be changed as required.
Stopping	This is the normal stopping state for the ECU and is controlled by the stop sequence. It gives a more gentle stop of the engine since the engine speed is ramped down to idle speed before fuel injection is stopped.
Shutdown	All the other states will go to this state if there are any critical failures in the state that is active. Initiation state will by default go to shutdown state as a safety measure.

6.2.3 Analog Conversion

The analog monitoring function consists of one analog-conversion module in the RT that reads analog values from the FPGA, see figure 6.6. Scaling of analog signal is done in the analog conversion module in accordance with the signal range, e.g 0-5V equals 10-35bar. The modules also pack the signals into a cluster to make it easier to distribute the signals for use in other parts of the logic where the signal requested must be unpacked. After scaling and packing the signals are used for display purposes, shutdown logic or process control logic e.g PID controller process value input.

The Labview logic for the analog conversion modules is located in subVI "AnalogConversion.vi".

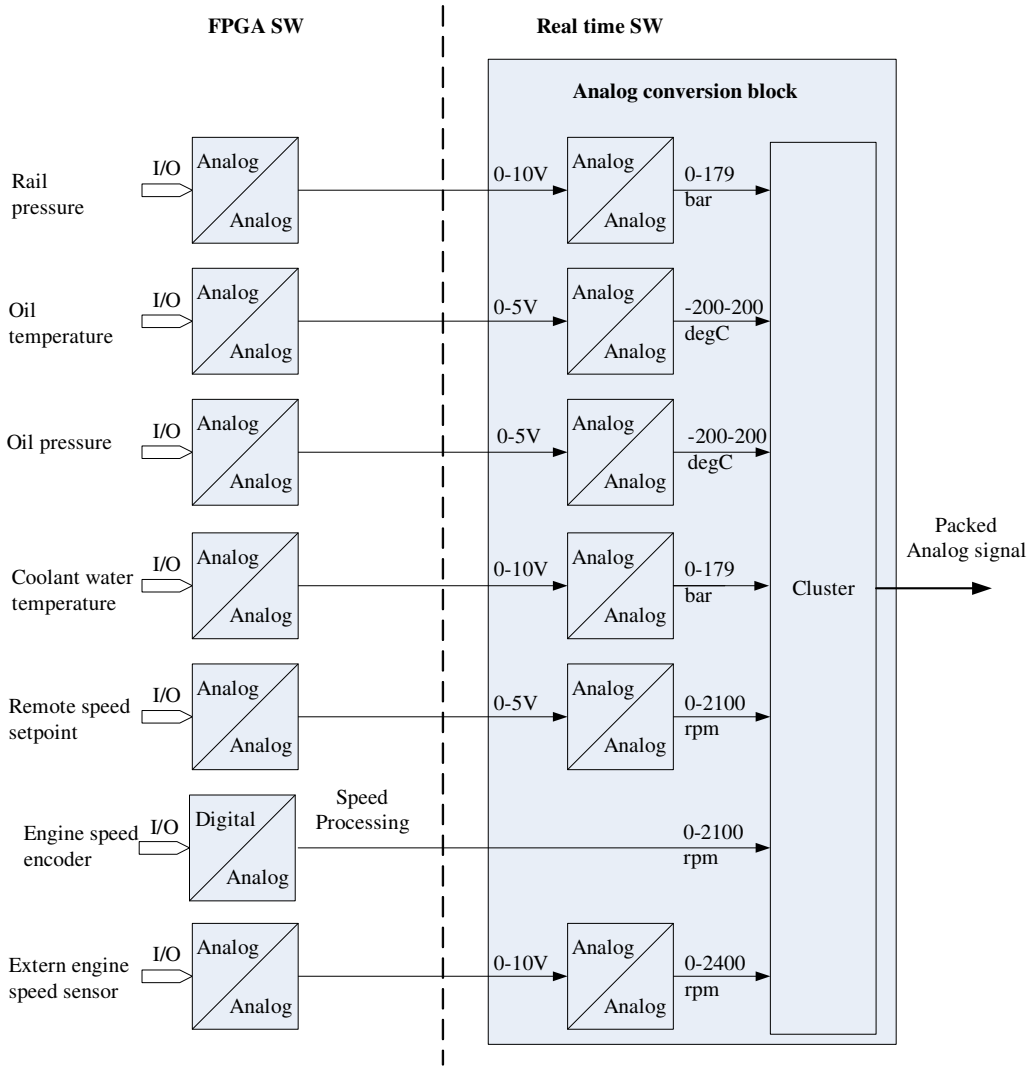

Figure 6.6: Analog conversion.

6.2.4 Digital Conversion

The digital monitoring function consists of one digital-conversion module in the RT that reads digital values from the FPGA, see figure 6.7. The modules also pack the signals into a cluster to make it easier to distribute the signals for use in other parts of the logic where the signal requested must be unpacked.

The Labview logic for the digital conversion modules is located in subVI "DigitalConversion.vi".

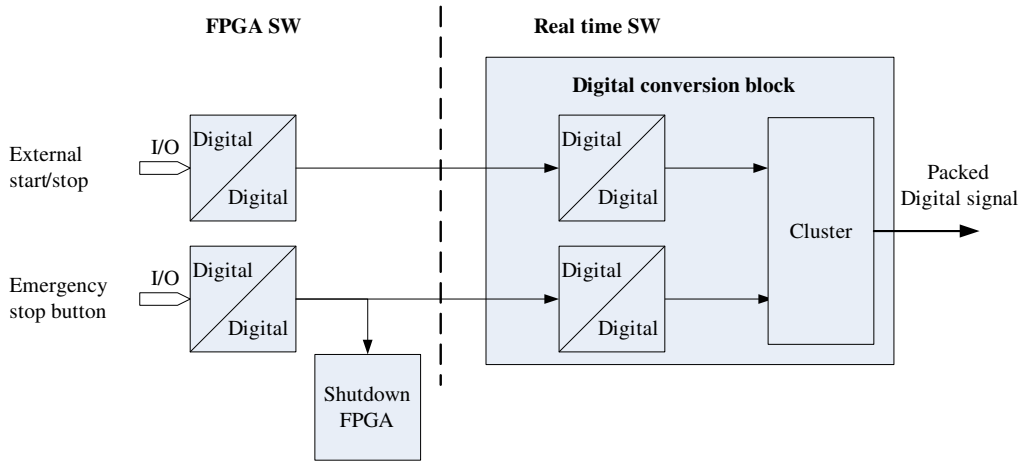

Figure 6.7: Digital conversion.

6.2.5 Shutdown RT

The logic for generating a shutdown in the RT controller is shown in figure 6.8 and is an OR gate with multiple inputs. When one or more of these inputs are true the shutdown output of the OR gate is set true. The Shutdown RT output status is linked to the Shutdown FPGA logic.

The Labview logic for the RT shutdown function is located in subVI "Shutdown_RT.vi".

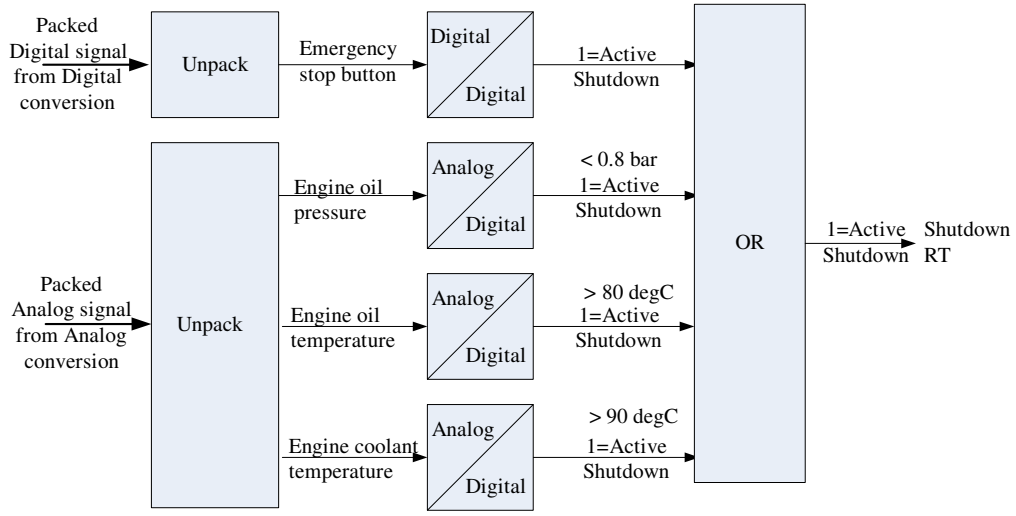

Figure 6.8: Shutdown RT logic.

6.2.6 Engine Speed Control

The main control parameter is the engine speed. To keep the actual speed at the desired reference speed the engine throttle is adjusted with a PID controller, see figure 6.9. The output from the controller is the throttle command and this is used in the rail pressure controller and injection controller to adjust the settings for rail pressure, start of injection and injection duration. When the engine is in state "Ready" and "Shutdown" the throttle is set to 0%. The throttle is also set to 0% in the "Stopping" state when stop fuel injection is activated. During state "Starting" the PID controller is in a tracking mode where it tracks the actual engine speed as its setpoint. This keeps the controller output at its minimum value since the error between setpoint and measured value is zero. When the engine transits to the state "Running" the setpoint is switched to desired speed setpoint and depending on the error value the controller changes the output value. The speed controller is only active when the engine is in state "Running" and initially in state "Stopping" to reduce the speed below 1100rpm before fuel is cut to stop the engine.

The Labview logic for the engine speed control is located in subVI "SpeedControl.vi".

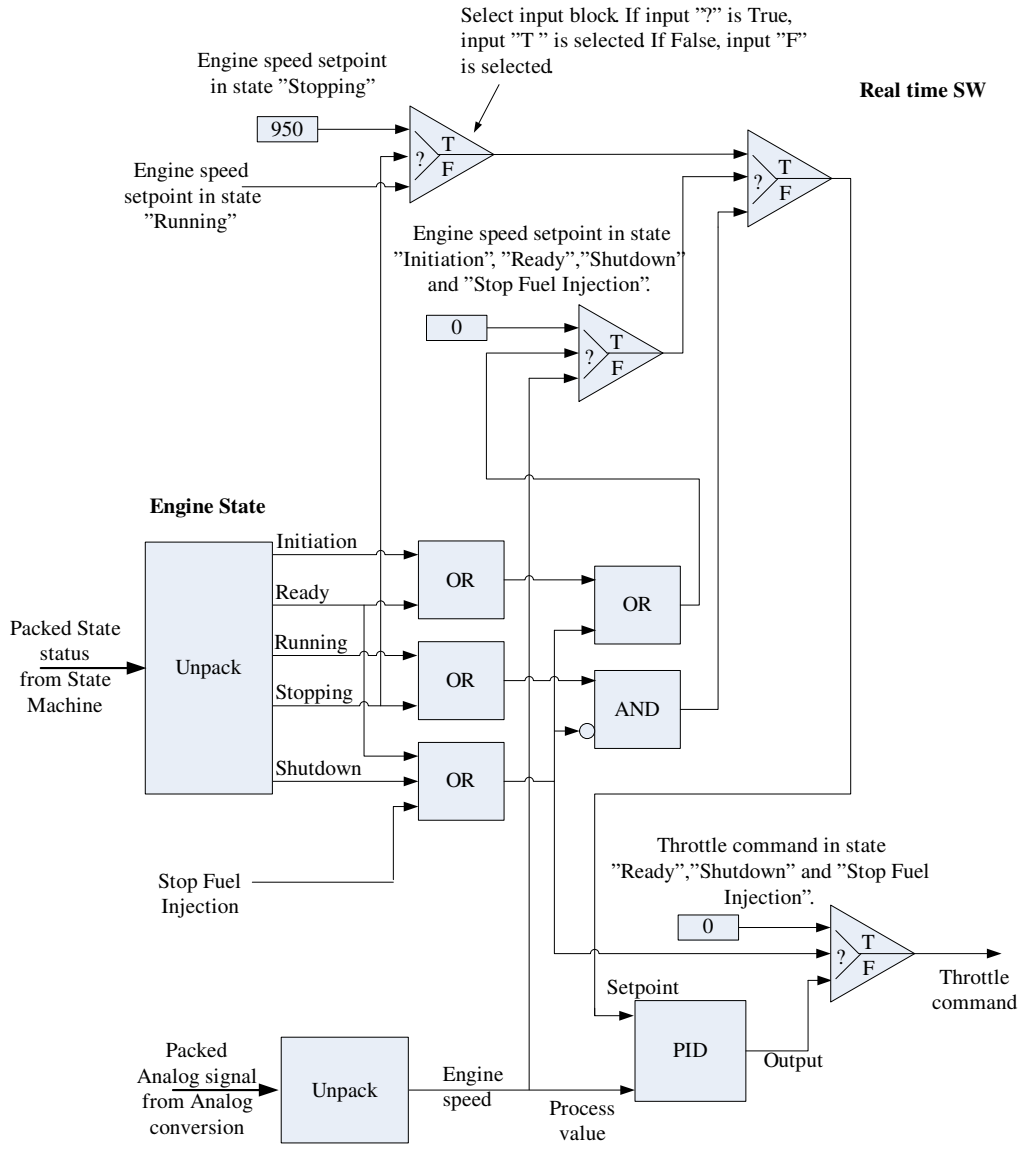

Figure 6.9: Speed controller.

6.2.7 Rail Pressure Control

The rail oil pressure is essential for controlling the rate of fuel injected and thus it is an important parameter for controlling the engine speed. To control the pressure the duty cycle for the rail control valve is adjusted, see figure 6.10. When the engine is in state "Ready" and "Shutdown" the duty cycle is set to 0%. The duty cycle is also set to 0% in the "Stopping" state when stop fuel injection is activated. During state "Starting" the duty cycle is a function of engine speed and is defined in the 1-dimensional table "LUT Rail valve Duty cycle Start". The main purpose

of having a start table is to get a high rail pressure of approximately 129bar to produce a fuel spray into the cylinder with small droplets for the initial ignition and to assure that enough fuel is injected at low speed. As the engine ramps up in speed after the initial ignition the table will reduce the duty cycle value since less fuel is needed as the rotational inertia of the engine increases. When the engine transit to the state "Running" the PID controller is in control. The controller receives a pressure setpoint from the 2-dimensional table "LUT Rail Pressure" which is a function of throttle command and engine speed. This setpoint is then compared with actual rail pressure value and the PID output is adjusted accordingly. The output from the rail pressure controller is a duty cycle value which is sent to the PWM signal generator which produces a PWM signal to drive the rail control valve.

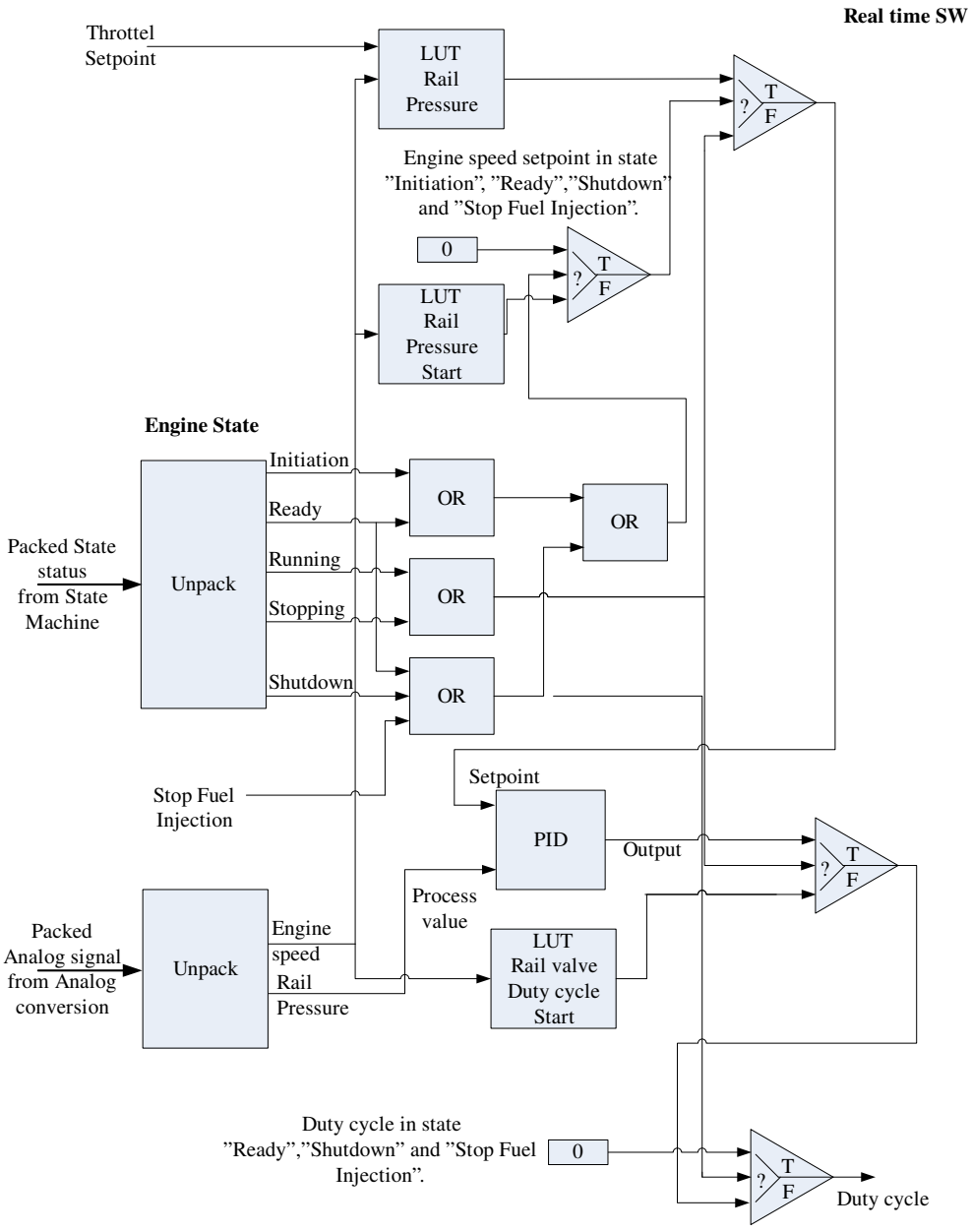

Figure 6.10: Rail pressure controller.

The Labview logic for the rail pressure control is located in subVI "RailPressControl.vi".

6.2.8 Injection Control

Start Of Injection (SOI) and Injection Duration (ID) are controlled by the injection control, see figure 6.11. ID is related to the rail oil pressure and these two together determine the quantity of fuel that is injected into the cylinder. When the engine is in state "Shutdown" the SOI is 0deg

and ID is 0ms. During state "Starting" the SOI and ID are a function of engine speed and are defined in the 1-dimensional tables "LUT Injection Start Starting" and "LUT Injection Duration Starting". As for the rail pressure control the ID must allow enough fuel to be injected for the initial ignition. Thus the ID is long, up to 2.2ms, for the initial injection and is reduced as the engine speed ramps up after the initial ignition. The SOI during start is close to the TDC for the initial injection since this is where the highest temperatures are experienced and this improves the fuel auto ignition. When the engine transit to the state "Running" the SOI and ID are determined by the 2-dimensional tables "LUT Injection Start Running" and "LUT Injection Duration Running". The input to these two tables is throttle command from the speed controller and engine speed. The output from respective tables is SOI in degrees and ID in milliseconds.

The injection control has a fuel limiter function to prevent that a too high quantity of fuel is injected. To much fuel injected can lead to high thermal stresses and mechanical loading of components and must therefore be avoided. The ID limit is always active and is determined from the 2-dimensional table "LUT Injection Duration Limit" which has rail pressure and engine speed as input and ID limit as output. A minimum function is used to find the lowest value of desired ID and the ID limit. The lowest value of the two is used. An indicator on the main RT VI displays if the limitation mode is active which is the case if desired ID > ID limit. The Labview logic for the injection control is located in subVI "InjectionControl.vi".

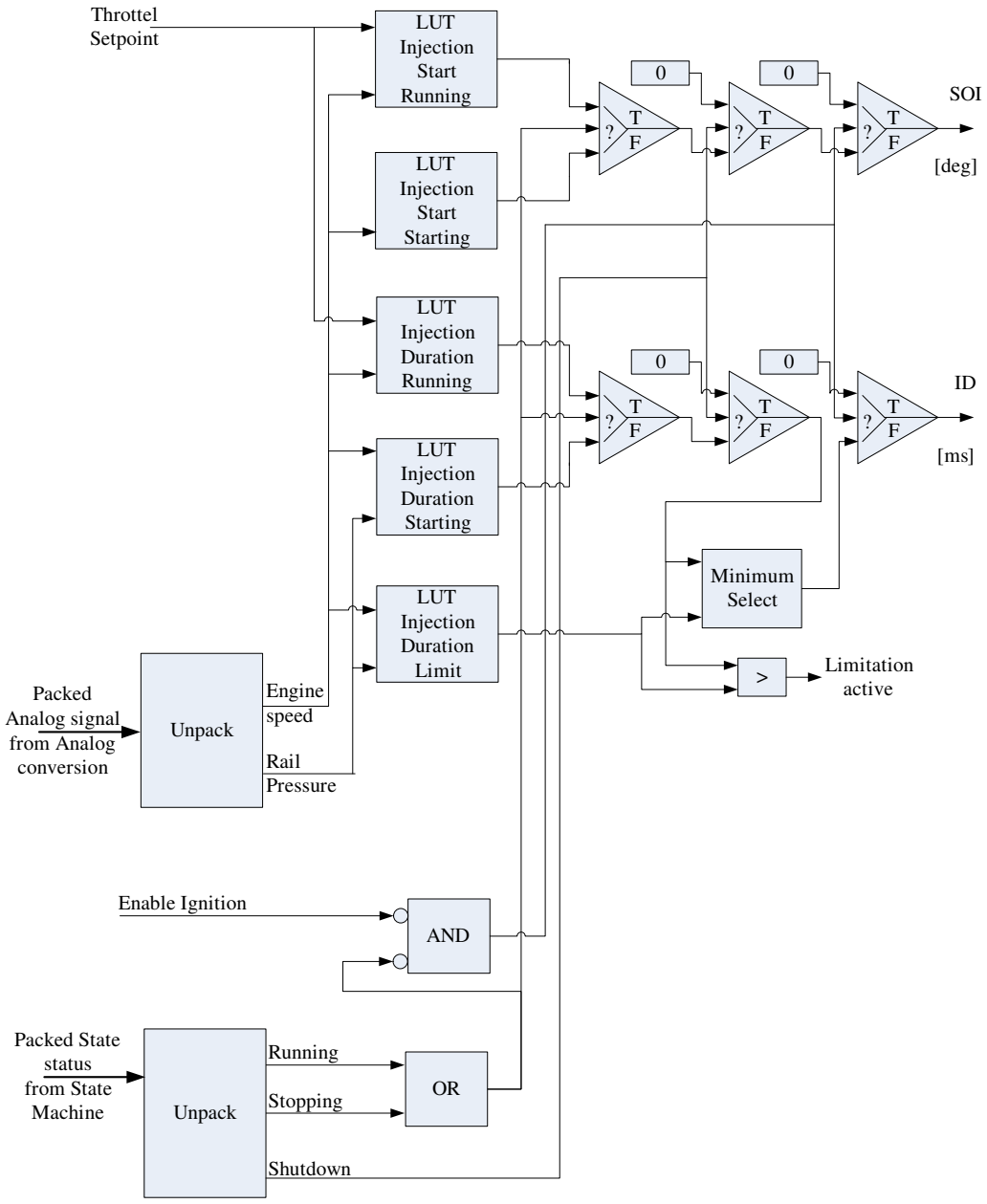

Figure 6.11: Injection control.

6.3 FPGA Controller

This section gives a detailed description of the FPGA controller SW. The main task of the FPGA is i/o card control, shutdown, processing of engine speed and camshaft position and injector control. It is a subalgorithm to the main RT VI and it runs on a different controller, the FPGA controller. Communication with the main RT controller is through a PCI bus. The main FPGA

VI is:

- FPGA_main_running.vi

and it contains the following subVI's:

- ProcCamshaftSignal.vi
- AngularPosEstimate.vi
- MonitorPosCamCrank.vi
- InjectorCommandsX6.vi
- InectorInterfacex6_2mod.vi
- Shutdown_FPGA.vi
- TeethDetection.vi

6.3.1 Main FPGA VI

The main FPGA VI, "FPGA_main_running.vi", is configured as an endless loop (while loop) that always runs when called from the main RT VI, see section 6.2.1. It contains several subVI's and operates with a clock frequency of 40MHz for the main VI and its subVI's. The main tasks are i/o card control, shutdown, processing of engine speed and camshaft position and injector control.

6.3.2 Engine Speed and Camshaft Position Processing

Engine speed and camshaft position are essential parameters for diesel engine control because these are used as input parameters to the speed control, section 6.2.6, and the firing synchronization, section 6.3.3. First the measured position for the camshaft is calculated in crankshaft ignition cycle degrees. For a 4-stroke engine the crankshaft makes two rounds of 360deg rotation between each ignition for a given cylinder. This equals 720deg of rotation for the crankshaft. Two rounds of rotation for the crankshaft equal one round of rotation for the camshaft between each ignition cycle. Therefore by defining one rotation of the camshaft as 0 to 720deg

the camshaft angular position is used directly to determine start of injection. It also needs an angular offset between the cylinders in accordance with the firing sequence. It consist of three subVI's:

- TeethDetection.vi
- ProcCamshaftSignal.vi
- AngularPosEstimate.vi

TeethDetection.vi

The "TeethDetection.vi" reads the digital camshaft encoder input from the i/o card, see figure 6.12. This signal switches between a low, 0V, and high, 5V, value as the teeth on the camshaft wheel rotate and pass the encoder. The subVI logic detects rising/falling edge of the signal i.e if it transitions from low-to-high or high-to-low and classifies it as a "Top end" or "Down end" event type ("Top end" is the end of a high period while "Down end" is the end of a low period). Thus the logic detects both the low and high period for the 24 teeth. The first detection must be high to low. The task is to measure the time in low and high periods, i.e. half tooth duration. This is done by a timer which is stopped when transition between low and high occurs. The stopped timer value is measured and the timer restarted. Measured time and event type are then forwarded to "ProcCamshaftSignal.vi" for processing of the camshaft signal to angular position in deg, angular speed in deg/s and rotational speed in r/s.

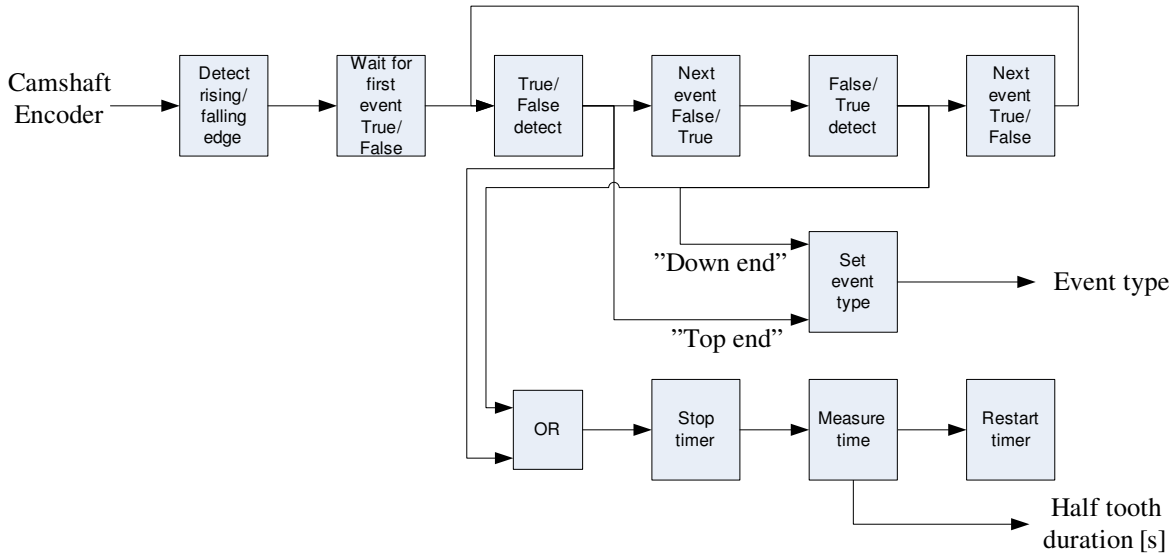

Figure 6.12: Half tooth duration logic.

ProcCamshaftSignal.vi

Angular position and speed are determined in the subVI "ProcCamshaftSignal.vi". This sbVI receives event type and the duration for a half tooth in low or high position. As mentioned in section 5.1 the camshaft consists of 24 teeth where 23 are equal and one unique top tooth for detecting one round of rotation. This gives 7.5 degrees/half period for the 23 equal teeth. For the unique one round detection tooth, 3.75deg for the high period and 11.25deg for the low period. Note that these values are valid when camshaft reference of 360deg/r is used. Since the used camshaft reference is 720deg/r which are the double of 360deg/r, the half tooth angular length must be doubled, see table 6.4.

Table 6.4: Half tooth degrees.

		Camshaft half tooth size	
		Camshaft reference 360 [deg/r]	Camshaft reference 720 [deg/r]
Tooth number	Signal Period	θ_{360}[deg]	θ_{720}[deg]
1-23	High	7.5	15
1-23	Low	7.5	15
24	High	3.75	7.5
24	Low	11.25	22.5

The event type received is "down end" or "top end". When an event type is received a half tooth size value is added to the current angular position. Thus the new angular position is an increment of the half tooth size from table 6.4, ref. equation 6.1

$$\theta_{cam}(k) = \theta_{cam}(k-1) + \theta_{720} \quad [deg] \tag{6.1}$$

For the 23 equal teeth this addition is done for all high and low periods and gives 690deg see equations 6.2

$$\theta_{Teeth1-23} = N_{Teeth} \cdot 2 \cdot \theta_{720} = 23 \cdot 2 \cdot 15 = 690deg \tag{6.2}$$

The last 30deg are the top tooth, tooth 24, where a "top end" adds 7.5deg and "down end" adds 22.5deg, ref. equation 6.3

$$\theta_{Tooth24} = \theta_{720high} + \theta_{720low} = 7.5 + 22.5 = 30deg \tag{6.3}$$

Thus 720deg are accomplished for one round of camshaft rotation as shown in equation 6.4

$$\theta_{cam} = \theta_{Teeth1-23} + \theta_{Tooth24} = 690 + 30 = 720deg \tag{6.4}$$

The top tooth of the camshaft is offset -90deg from the TDC of cylinder 1 (Perkins-Engines, 2001). This means that when cylinder 1 is in its TDC position the top tooth position of the

camshaft is given by equation 6.5

$$\theta_{camTDC} = \theta_{cam} + \theta_{offset} = 720 - 90 = 630deg \tag{6.5}$$

Top tooth detection for the camshaft is important to determine TDC of the crankshaft. When top tooth is detected it resets camshaft position at the next high to low transition to an offset position of 637.5deg. For the next transition low to high it adds top tooth low period incremental values θ_{720}, see table 6.4. Thus it influences both camshaft angular position and the TDC position which is essential for determining the start of injection. The first time the top tooth is detected, "synchronization OK" is set to verify detection of top tooth. To detect the top tooth a sub algorithm "FirstToothDetection.vi" is used. It samples the last three durations for the high period tooth duration and compares them. Figure 6.13 shows a pulse train of the last three pulses where t_c represents the top tooth. Pulse durations t_a, t_b and t_c are stored in an array and then compared in the top tooth detection logic shown in figure 6.14. When t_c, which is the last sampled value, is within the limits defined by t_a and t_b in the logic top tooth is detected. The limits are that 2*t_c must be within +/- 25% of both t_a and t_b.

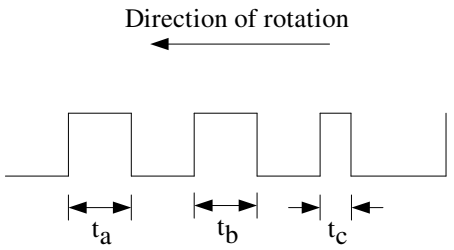

Figure 6.13: Pulse train for camshaft encoder.

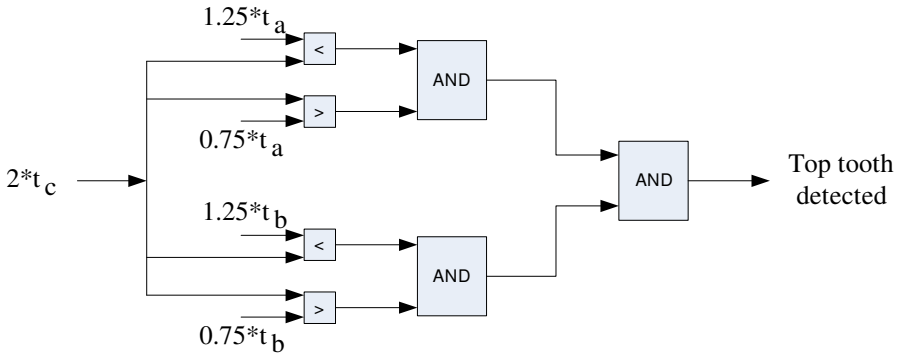

Figure 6.14: Logic for detecting top tooth.

For calculation of engine speed the added angular position increment value, θ_{720}, is divided by the duration received for a half tooth (Note: quarter and three quarter tooth for the top tooth). This gives engine speed in deg/s which divided by 360deg/r gives r/s. An average filter is added to filter the resulting engine speed. The filter samples every time a position increment occurs and takes the average of the 48 last samples. These 48 samples represents two rotations of the camshaft, i.e four rotations of the crankshaft.

Output from the VI is camshaft position in deg, camshaft speed in deg/s, filtered crankshaft speed in r/s, filtered crankshaft speed in rpm and synchronization OK.

AngularPosEstimate.vi

The angular position estimate sub algorithm receives camshaft position in deg, camshaft speed in deg/s and synchronization status from the sub algorithm that processes the camshaft signal. If synchronization is OK, it compares its calculated measured position with the camshaft position received. If these differ, the assessed and calculated measured positions are reset to the received camshaft position. When the calculated measured and input camshaft positions are equal, the assessed position is determined.

To determine the assessed position the calculated measured position is first determined:

$$\theta_{meas}(k) \quad [deg] = \theta_{meas}(k-1) \quad [deg] \quad + \quad \omega_{cam} \quad [deg/s] \quad \cdot \quad t \quad [s] \tag{6.6}$$

The calculated measured position is then compared with current assessed position and a new assessed position is determined:

- If calculated measured position > assessed position or position is between 690 and 30deg -> Use calculated measured position.
- If calculated measured position < assessed position or position is between 30 and 690deg -> Use assessed position.

This new assessed position is forwarded to the injector command sub algorithm. The reason for having limit values of 690 and 30deg is that this is around the top dead center area where fuel is injected.

6.3.3 Firing Synchronization

Firing synchronization is done by the injector command algorithm in subVI "InjectorCommandX6.vi". It receives assessed position from subVI "AngularPosEstimate.vi" and injection start and duration from the RT injection control logic, see figure 6.15. Start Of Injection (SOI) is given in camshaft 720deg/r and is added to the cylinder angular offset, called reference. Then a limit check is performed to check if the assessed position is within +/- 0.1deg of the cylinder SOI. If it is within the limits, the injection timer is started. As long as the timer value is smaller than the received injection duration (ID) an inject command is sent to the injector.

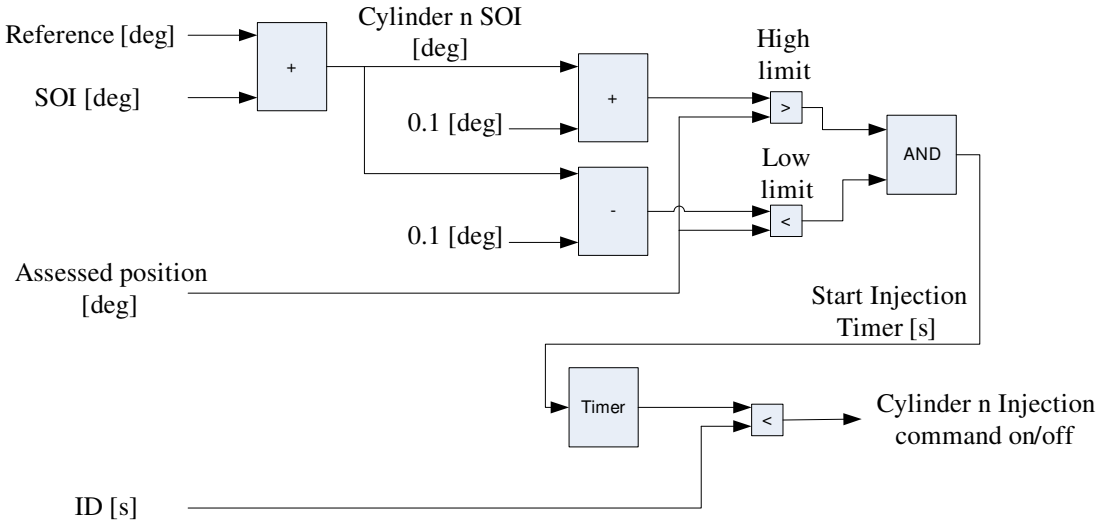

Figure 6.15: Logic for injection command.

All cylinders are set to fire in accordance with the firing sequence 1-5-3-6-2-4, ref. table 3.1. This gives a firing offset or reference angle for each cylinder as shown in table 6.5. Note that the camshaft is given in 720deg/r.

Table 6.5: Cylinder firing offset.

Cylinder number	Reference [deg]
1	0
5	120
3	240
6	360
2	480
4	600

6.3.4 Injector PWM Generator

Injector PWM generator main task is to create a current characteristic for the injectors coil as shown in section 5.2 and in (Sybele, 2009). The control solution made is modelled with inputs from the Skynam document (Sybele, 2009).

The injector interface VI "InjectorInterfacex6_2mod.vi" receives an injection command for the cylinder to inject fuel, see section 6.3.3. This inject command switches on a PWM generator for the injector which will generate a 0-5V pulse train which is sent to the Injector Driver Unit (IDU), see section 6.4.2. The IDU will then set up a 0-110V pulse train to the injector to open it. To control the injector current in the three phases; attack, holding and withstand, a PWM generator is used. For the attack part the high command and the inject command are switched on so that a rapid increase of current occurs. The on duration is made as a timer with a value of 480us. When the timer times out the high- and inject-command is switched off. The duration of this timer shall last so long that the injector current reaches its holding level of 6.7A. For the holding and withstand phases the aim is to keep the current at a certain constant level, 6.7A for holding and 4.3A for withstand. To tune these current levels a total of 16 passive and active pulse durations in microseconds are available for PWM, see figure 6.16. The sum of all the timers in the three phases determines the maximum injection time for the injector. To extend the max injection time pulse duration 16 is repeated to get the required maximum time.

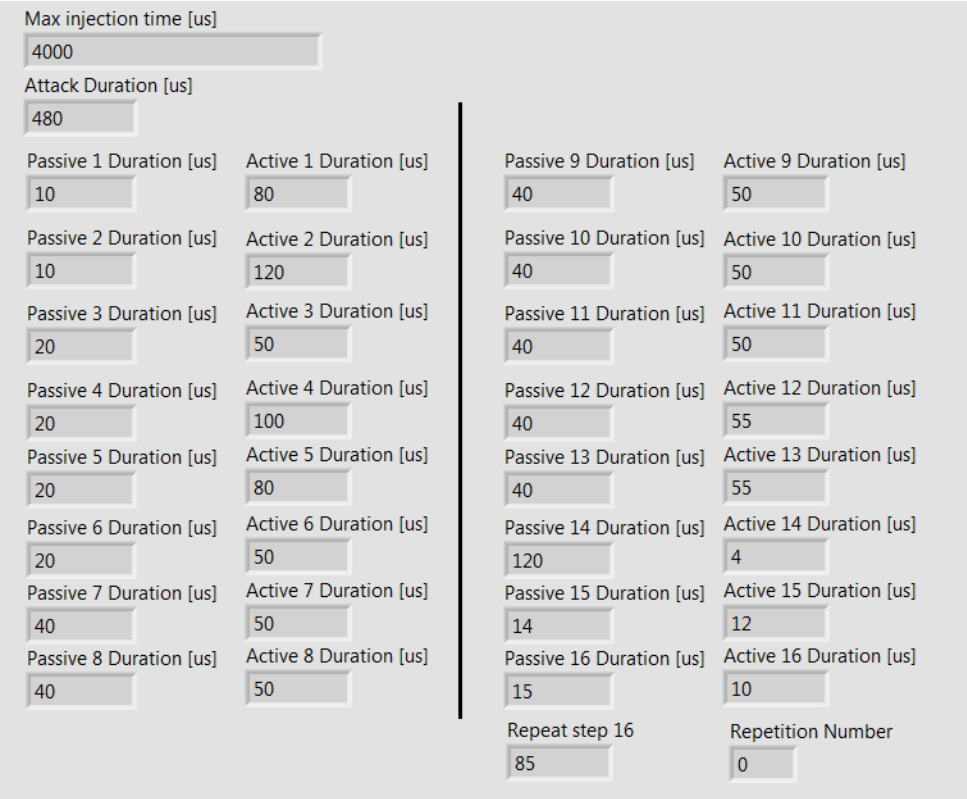

Figure 6.16: Injector PWM generator values.

6.3.5 Rail Valve PWM Generator

The PWM generator is a square wave generator and it receives a duty cycle value from the rail pressure controller in section 6.2.7. It has a base frequency of 100Hz and this high frequency requires it to be part of the FPGA SW due to the required processing frequency. The base frequency was not known from the engine test performed with the original ECU and the only reason for selecting this value is from previous experience at NTNU with common rail engines. The PWM output signal which is a pulse train with varying duty cycle is then sent to the i/o card where it is transformed into a digital signal with a high period of 5V and a low period with 0V. This signal is sent to the Injector Driver Unit, see section Injector Driver Unit, before it is sent to the rail valve on the engine. The Labview logic for the PWM generator is located in subVI "RailValvePWM_FPGA.vi".

6.3.6 Shutdown FPGA

The logic for generating a shutdown in the FPGA controller is shown in figure 6.17 and is an OR gate with multiple inputs. This is the main shutdown controller that controls the shutdown relay K1 in the relay logic, see 6.4.1. It also controls overspeed shutdown and SW shutdown of the injectors. When one of the inputs are true, the shutdown output of the OR gate is set true and the output from the RS latch is set true. The RS latch output is connected to an invert block that inverts the digital value so that the digital output is true in no shutdown condition and false in shutdown condition. The invert block is connected to a dedicated i/o channel which drives relay K1. This is a fail safe design where de-energizing is the safe condition. The Shutdown FPGA output is forwarded to RT controller for display purpose. When all shutdown are cleared, the shutdown logic must be reset by activating the reset button in the main RT VI to reset the RS latch.

The Labview logic for the shutdown FPGA is located in subVI "Shutdown_FPGA.vi".

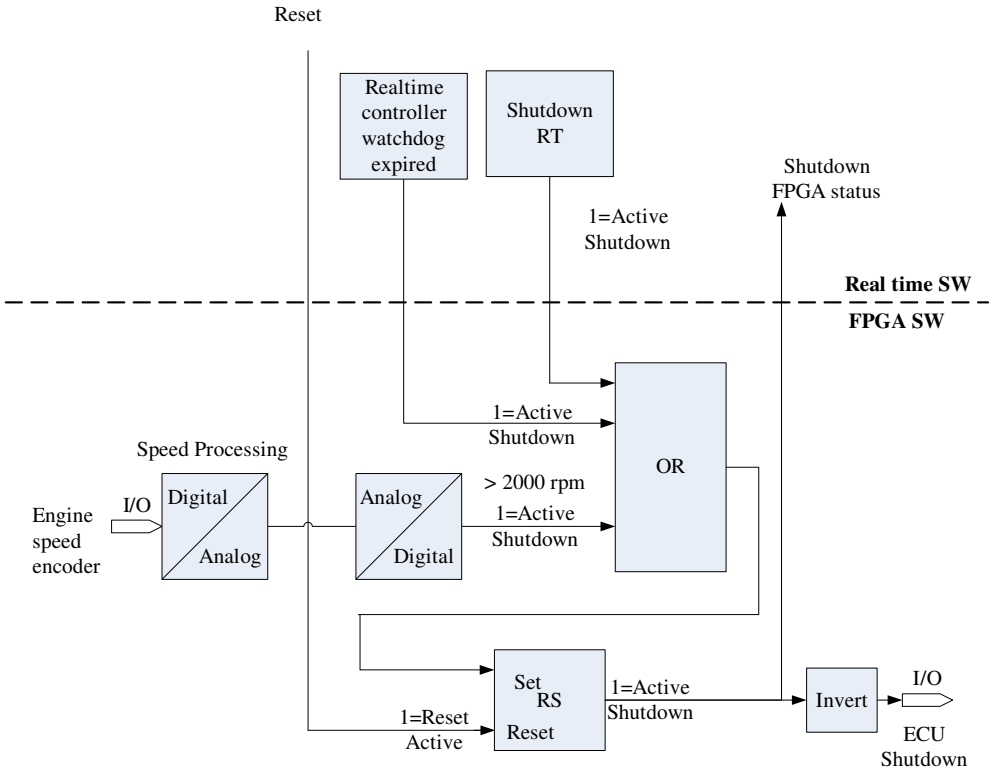

Figure 6.17: Shutdown FPGA logic.

6.4 Hardware

This section presents the hardware developed for the project.

6.4.1 ECU Relay Logic

The hardware shutdown is a relay logic independent of the controller software logic. It has a link to the software shutdown logic through relay K1, see section 6.3.6 but it still is independent.

Note: It is of great importance that any fault in the software shall not block a manual shutdown of the engine.

Figure 6.18 shows the layout of the relay logic. Relay K4 is the main shutdown relay. When it is de-energized both the +24V power supply to the starter motor relay and the +12V power supply to the injector driver unit are cut. This will block/stop the starter motor and the injector driver unit will not have the +12V voltage required for driving the output circuit for the injectors, thus no fuel is injected and the engine stops. The main shutdown relay is de-energized if there is no +24V power supply or one of the two emergency push buttons are activated or the ECU software shutdown, section 6.3.6, is de-energizing relay K1.

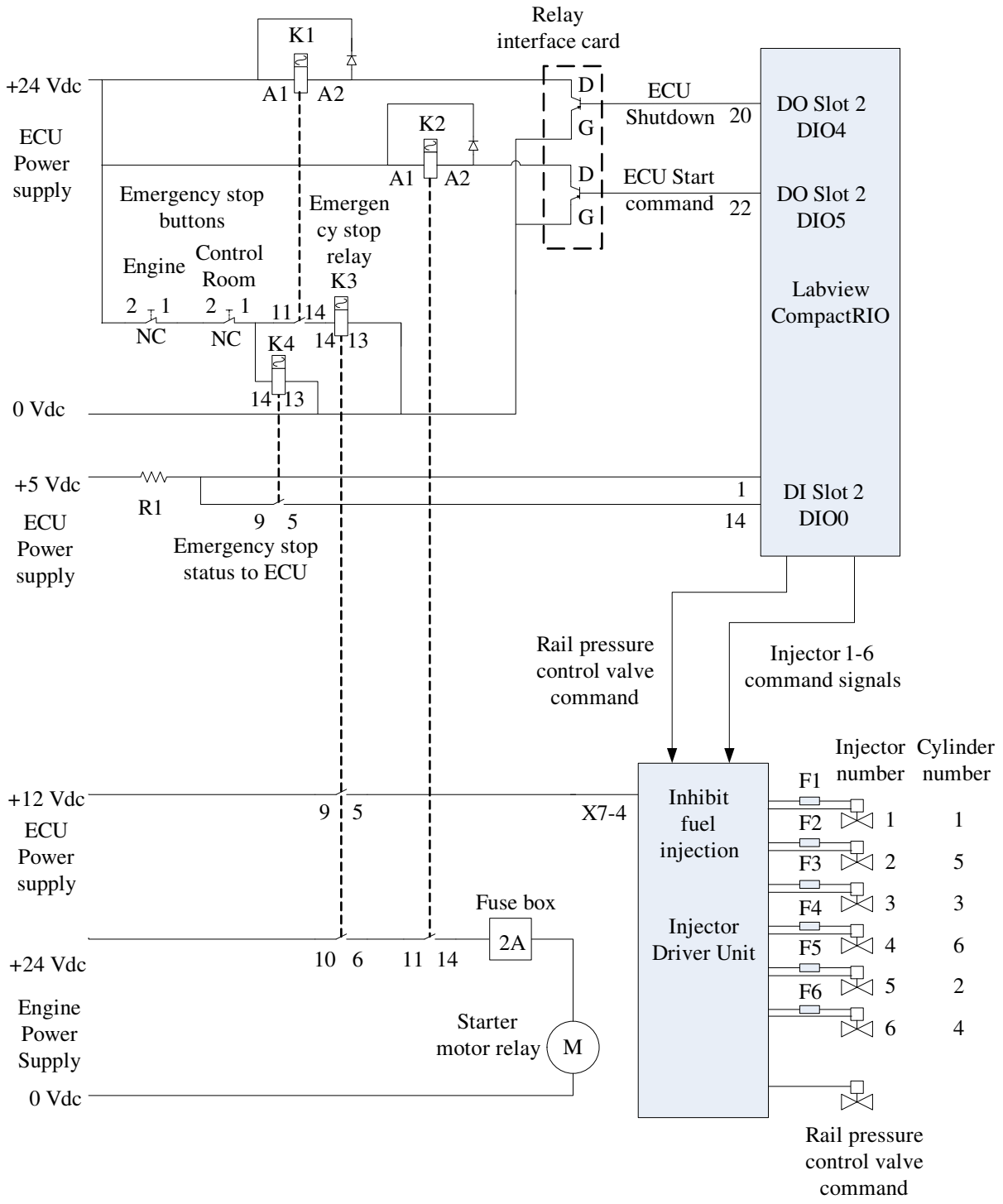

Figure 6.18: Hardware shutdown relay logic.

6.4.2 Injector Driver Unit

The injector driver unit is a hardware interface card used for creating the required electrical power to drive the injector coils and also an interface to the rail pressure control valve. With a required voltage level of 110V and a maximum current of 6.7A for the injectors it was not possible to find an off the shelf product. Therefore an NTNU in-house driver unit is used. It is designed and built by the NTNU Marintek Lab staff. See appendix A for card interfaces, component lay-out and circuit schematics.

Rail Pressure Control Valve

For the rail pressure control valve the 0-5V PWM signal from the CompactRIO is converted into a 0-12V PWM signal which is sent to the valve, see figure 6.19. When the CompactRIO sends a 5V signal, transistor T1 starts to lead current and the current flows through the valve coil between +12V and ground (Gnd). When the CompactRIO sends 0V, T1 breaks the current and the coil will start to induce current to counteract the change. This is not desirable since the current through the coil shall be zero. Therefore a resistor R1 in series with a diode is used so that the energy created by the induced current is removed by heat dissipation in R1.

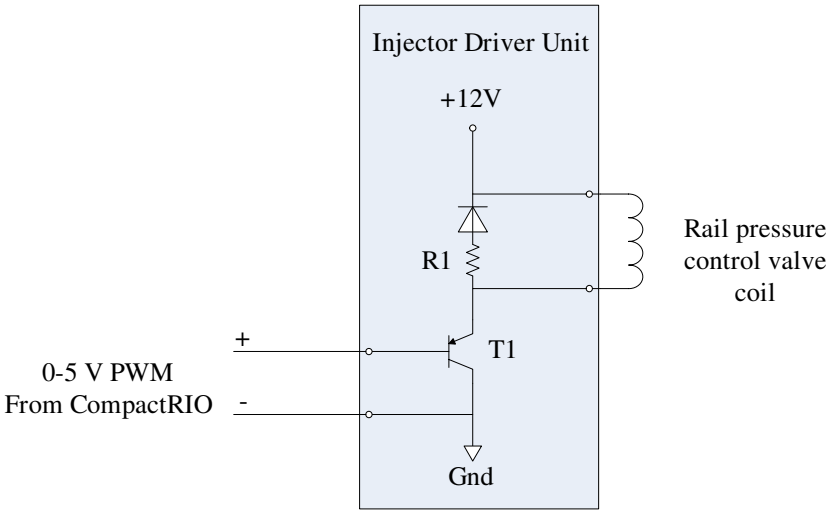

Figure 6.19: Rail valve PWM signal simplified circuit schematic.

Injectors

For the injectors two command signals are used for controlling the current flow in the injector coil, see figure 6.20. The high command controls the voltage level seen by the coil terminals while the inject command controls the current flow through the coil. When the high command sends 5V, transistor T3 leads current and the coil sees 110V and when 0V is sent, T3 breaks the current, it sees 50V at its terminals. The high command is only active during the attack phase to provide an extra voltage boost to the injector. The current flow through the injector coil is controlled by the inject command. When the inject command sends a 5V signal to T2, it start to lead and a current starts to flow through the injector. And when inject command goes to 0V, T2 breaks the current and the coil will induce a current. To remove the energy from this current a resistor R2 and a diode are used, as for the rail pressure control valve. Note that high command signal is used for a group of three injectors while inject command is a single signal for each injector.

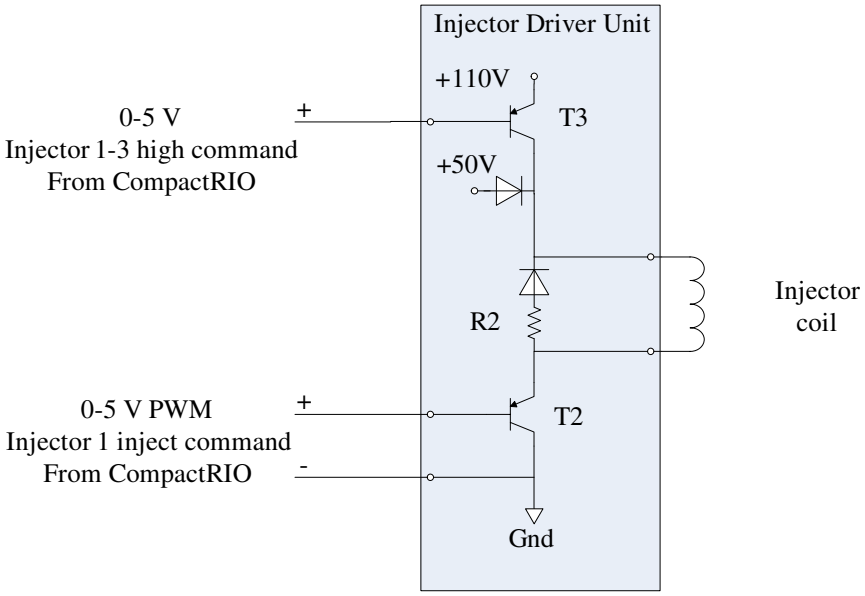

Figure 6.20: Injector PWM signal simplified circuit schematic.

6.4.3 Hardware Layout of ECU Cabinet

The layout of the ECU cabinet and its components are shown in figure 6.21. Cabinet dimensions are H x W x D = 400 x 300 x 150mm.

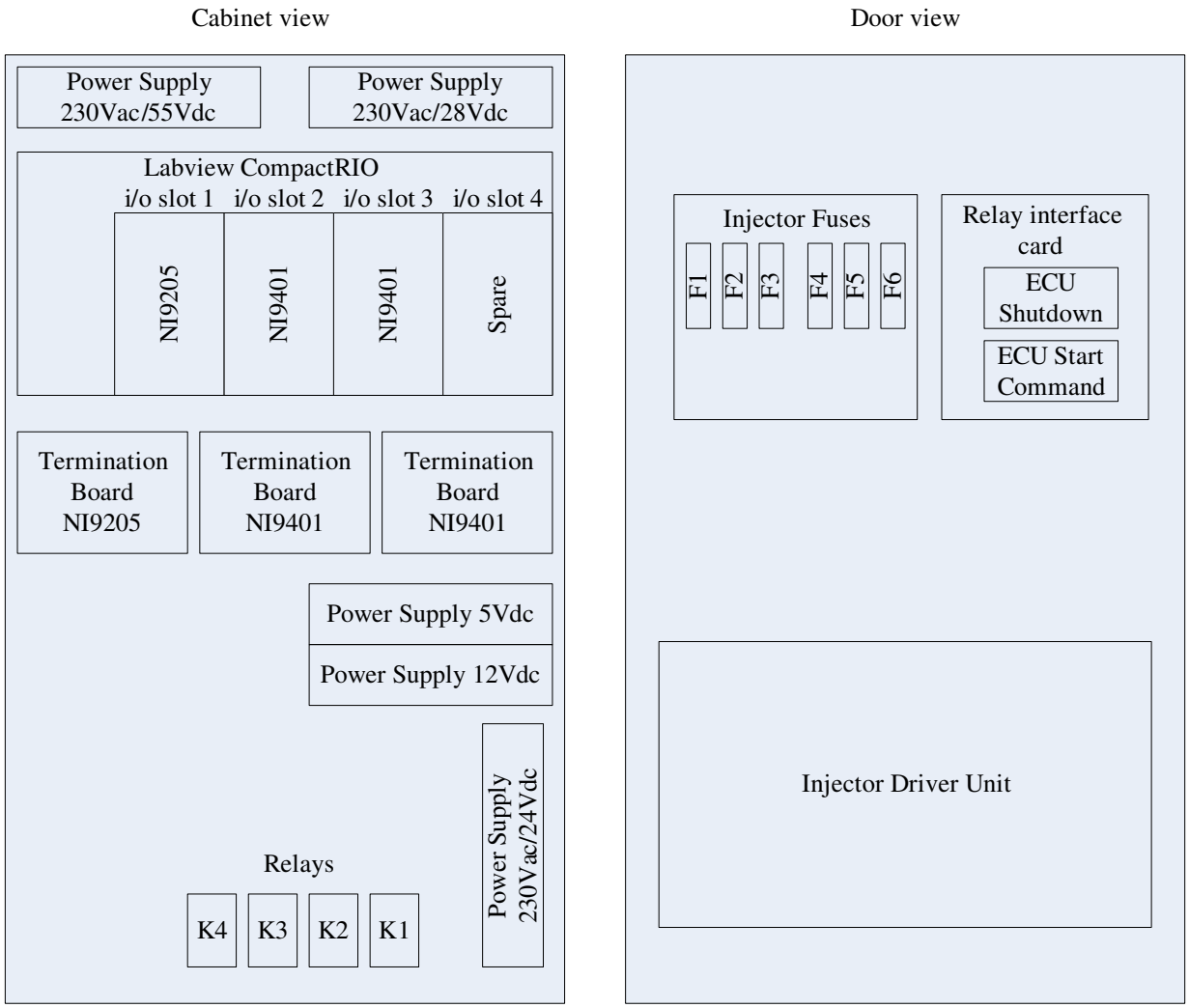

Figure 6.21: ECU cabinet layout.

6.5 Engine Interface

6.5.1 Engine Sensor Interface

Engine sensor interfaces prepared are shown in table 6.6. Currently only rail pressure, camshaft encoder and crankshaft top dead center are connected. Oil temperature, oil pressure and coolant water temperature sensors are not connected since the scaling of these sensors are not known. Because the engine has a duplicate set of sensors connected to a separate monitoring computer, these are used to visually monitor the values. Note that the camshaft encoder requires a pull up resistor of 4.7kOhm and a 5V supply for creating a voltage over 2V for I/O high detection.

Table 6.6: Sensor interfaces.

Description	Type	Signal
Rail Pressure	Analog Input	0-5V
Oil Temperature	Analog Input	0-5V
Oil Pressure	Analog Input	1-5V
Coolant Water Temperature	Analog Input	1-5V
Camshaft Encoder	Digital Input	0-5V
Crankshaft Top Dead Center	Digital Input	0-5V

6.5.2 Engine Actuators

Engine actuator interfaces are shown in table 6.7. All actuators are needed for running the engine.

Table 6.7: Actuator interfaces.

Description	Type	Signal
Starter motor	Digital Output	0-5V
Rail pressure control valve	Digital Output	0-5V PWM
Injector 1-3 high command	Digital Output	0-5V
Injector 1 inject command	Digital Output	0-5V PWM
Injector 2 inject command	Digital Output	0-5V PWM
Injector 3 inject command	Digital Output	0-5V PWM
Injector 4-6 high command	Digital Output	0-5V
Injector 4 inject command	Digital Output	0-5V PWM
Injector 5 inject command	Digital Output	0-5V PWM
Injector 6 inject command	Digital Output	0-5V PWM

Chapter 7

Test Results

This chapter presents the different tests, with the developed ECU connected to the engine, see figure 7.1, and their results. The ECU cabinet is shown to the top right in the picture, while the yellow engine is to the left. Tests are done with a stopped and running engine and the acquisition equipment used for reverse engineering, see chapter 5, are used for data gathering. For the first engine start, run parameters from section 5.4.4 are used as inputs to the ECU. Note that the data from reverse engineering is used as reference data and not data that must be used. Therefore the final tuning data might differ from the reference data.

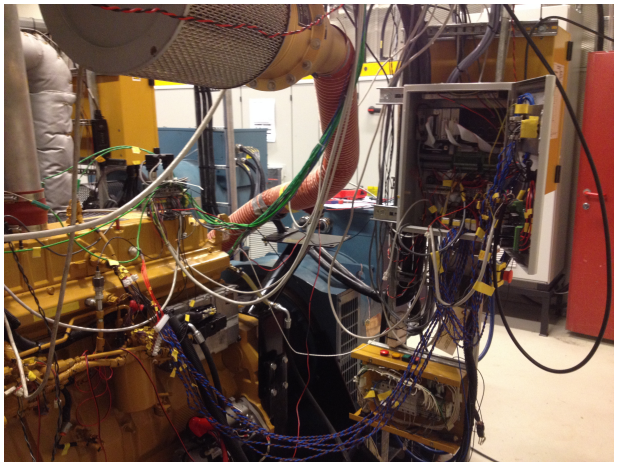

Figure 7.1: Engine test setup.

First, safety is of great concern with rotating machinery since a failure can cause great damage to both personnel and equipment. Therefore this has a high priority during engine testing,

see section 7.1. A test is done to verify the engine speed algorithm since this is important for determining the camshaft angular position, see section 7.2. Two tests with a stopped engine are done to tune the rail oil pressure control valve, see section 7.3, and tuning of HEUI (injectors), see section 7.4. Before starting the engine with fuel admission a cranking test was done, see section 7.5.1. Engine start test is discussed in section 7.5.2, engine stop test in section 7.5.3 and finally running tests in section 7.5.4. A discussion of the results is done at the end of each section.

7.1 Shutdown Function

All shutdown function are tested and found to work as designed in chapter 6. Shutdowns tested are emergency stop buttons in engine- and control-room and over-speed shutdown at 1900rpm. The shutdowns not tested are oil temperature, oil pressure and coolant water temperature since these sensors are not connected and are visually monitored on a separate computer, see also 6.5.1.

7.2 Engine Speed Algorithm Verification

The engine angular position algorithm are essential for determining start of injection and engine speed. Therefore a dedicated test with the engine stopped is performed to see the algorithm assessed angular position versus a simulated camshaft signal. The input to the simulator was engine speed and the output was the teeth pulse signals found during reverse engineering and a TDC signal. The assessed angular position was then connected to channel one on an analog output module. This module, Labview NI9263, was added to spare I/O slot 4 of the CompactRIO. The analog output was then logged on an oscilloscope together with the simulated tooth duration and TDC signals, see figure 7.2. TDC signal is used for triggering. In the figure magenta line is the assessed camshaft angular position changing between a minimum and a maximum value of 0 and 720deg. Yellow line is the simulated tooth signal for the camshaft while the cyan line is the TDC signal. Note that 0 to 720deg equals one rotation of the camshaft and two for the crankshaft.

Discussion

Figure 7.2a displays seven full rotations 0-720deg of the camshaft. Each rotation has duration of 1.2s and equal a camshaft speed of 72rpm. The camshaft angular position creates a sawtooth pattern as it rotates since 0 and 720deg position are in the same position in the circle. Figure 7.2b is a zoomed in view and displays one rotation of the camshaft and the TDC signal is seen for 0, 360 and 720deg. The assessed position incremental steps for each half tooth duration are clearly shown in figure 7.2c and 7.2d. Note also the short top tooth high duration at left in figure 7.2d. Figure 7.2e and 7.2f display the two highest camshaft speeds tested. The highest is a camshaft speed of 1500rpm which equals 3000rpm for the crankshaft. This is within the expected maximum operational speed limit for the crankshaft of 2100rpm.

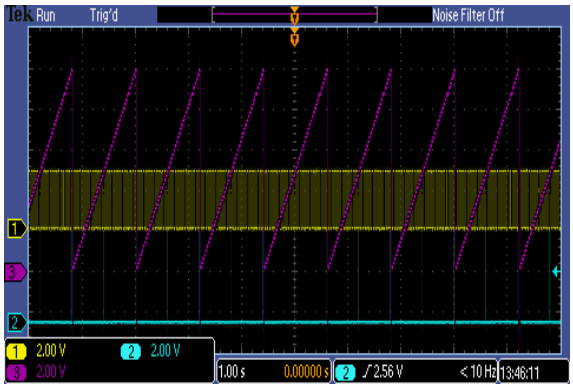

(a) Simulated camshaft speed of 72rpm.

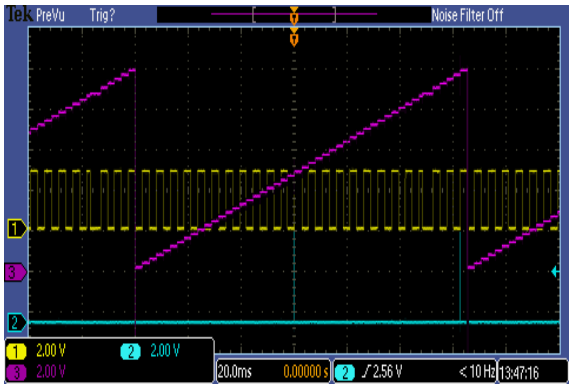

(b) Simulated camshaft speed of 72rpm.

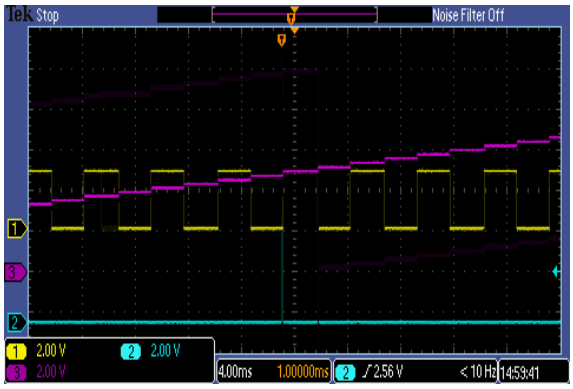

(c) Simulated camshaft speed of 72rpm and TDC at 360deg.

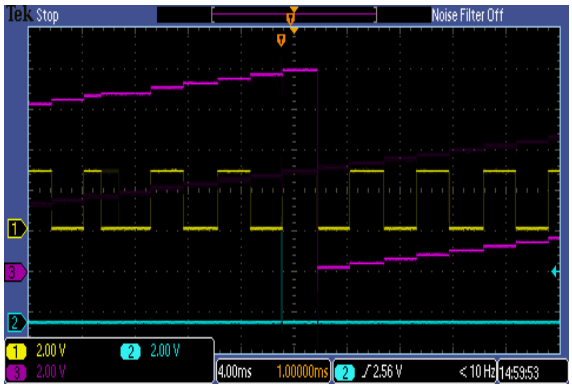

(d) Simulated camshaft speed of 72rpm and TDC at 720deg.

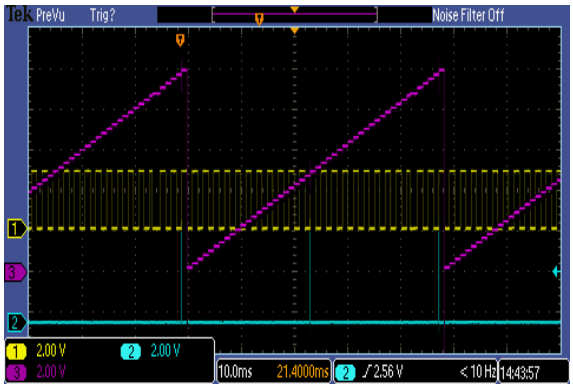

(e) Simulated speed of camshaft 1250rpm.

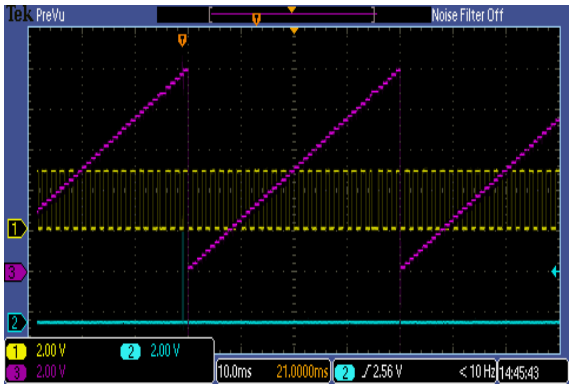

(f) Simulated speed of camshaft 1500rpm.

Figure 7.2: Verification of angular position algorithm.

7.3 Rail Pressure Control Valve

A mapping is created between the duty cycle and the measured voltage applied to the valve, see table 7.1. It is assumed that the voltage value measured is the same as found during reverse

engineering.

Discussion

It is not possible to verify the functionality of the rail valve since there are no position feedback. When the engie is running, a change in the rail oil pressure shall be observed so then this can be used as a feedback. Thus the only way to have any feedback when the engine is stopped is an audible sound from the valve. This was verified by listening to a clicking sound from the valve for different duty cycle values. The clicking sound is assumed to be the piston strokes.

Table 7.1: Rail valve duty cycle map.

Duty cycle [%]	**HydrPressCtrl [V]**	**Duty cycle [%]**	**HydrPressCtrl [V]**
0	0	37	0.18
5	0.01	37	0.18
10	0.02	38	0.19
15	0.04	45	0.25
21	0.07	46	0.26
22	0.08	47	0.27
26	0.1	51	0.31
29	0.12	51.5	0.32
35	0.16	56	0.37
36	0.17	56.5	0.38

7.4 HEUI Tuning

Tuning of the HEUI injector is done by using a dedicated tuning display for the injector by activating the inject command and changing the PWM values, see figure 7.3. The values shown in the figure are the end result of the tuning. An oscilloscope is used to display the current characteristic and the PWM signal (Inject command) from the CompactRIO output. The high voltage command is used for triggering. Current level is provided by an analog output on the IDU (Current sense 1..6) that measures the current through the injector as a voltage output, with a scaling

of 200mV/A. After tuning the same parameters are used on all six injectors and a verification test is done, see figure 7.4. Yellow line is the injector current presented as voltage with 200mV/A. Thus 6.7A = 1.34V and 4.3A = 0.86V. The cyan line is the PWM command from the CompactRIO. Note that the current sense output has an offset of 0.49V when current is 0A.

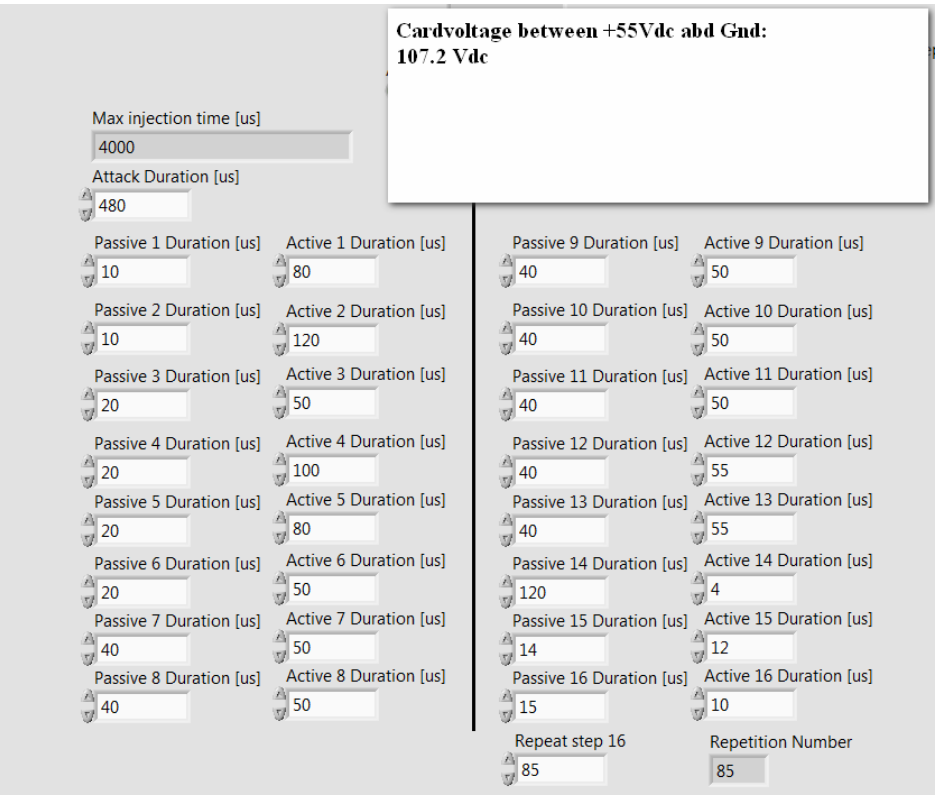

Figure 7.3: Injector tuning parameters.

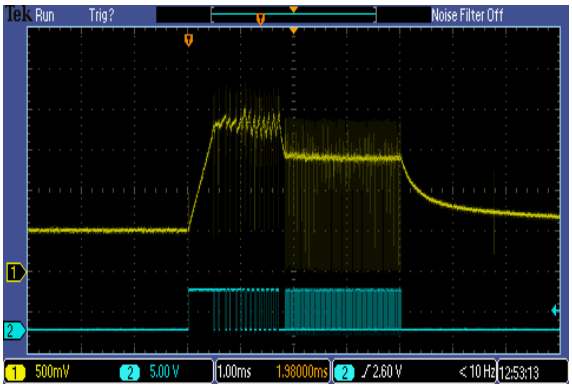

(a) HEUI cylinder 1.

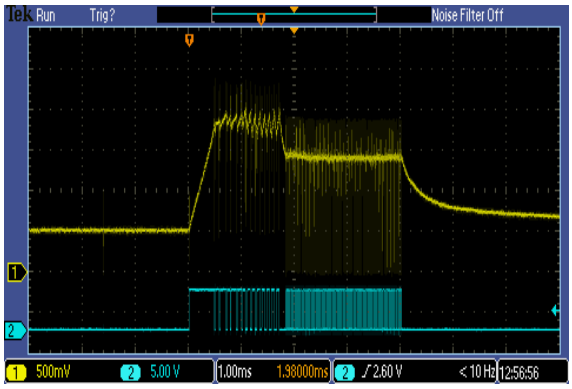

(b) HEUI cylinder 2.

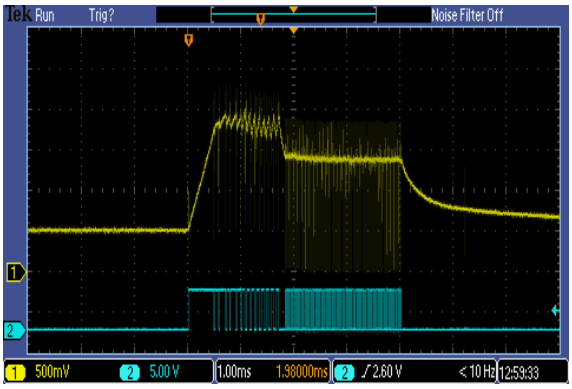

(c) HEUI cylinder 3.

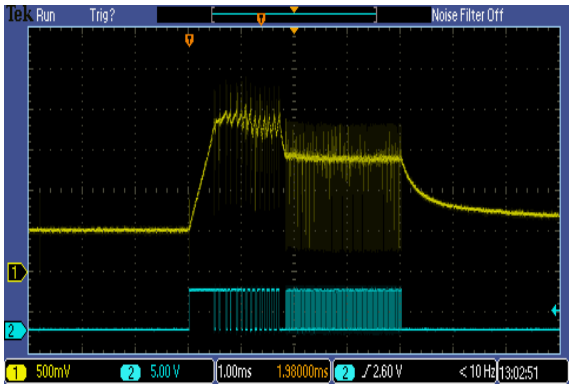

(d) HEUI cylinder 4.

(e) HEUI cylinder 5.

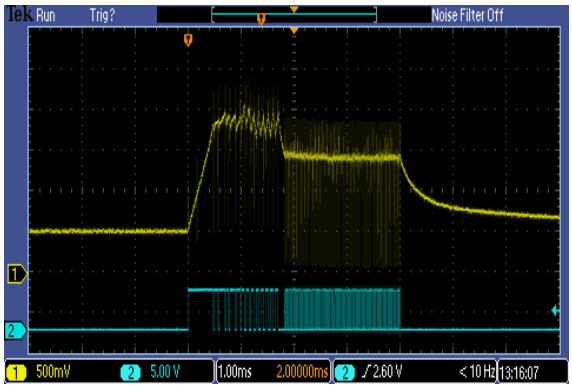

(f) HEUI cylinder 6.

Figure 7.4: HEUI current characteristic.

Discussion

For the attack phase the requirement from reverse engineering is an attack duration of 0.48ms from 0 to 6.7A. This was accomplished by defining the attack duration and adjusting the voltage supplies so that the IDU had a voltage between terminal X7:56V+ and X7:5V/Gnd of 107.2V. The withstand phase is tuned for a current level of approximately 6.7A by adjusting passive and

active duration 1-13 so that the total duration of the withstand is 1.22ms, as required. The requirement for the holding phase is a current 4.3A and switching to the holding phase is done by the "Passive period 14" of 120us. To ensure that the injection time is not to short at higher engine loads the longest duration for the injectors are set to 4.0ms (the longest observed from reverse engineering was approximately 3.0ms). This is also seen as max injection time in figure 7.3. Thus the passive and active duration 16 is repeated 85 times.There is no position feedback available for the injector, so it is not possible to say at what time the oil valve opens. However, an audible click can be heard from the injector and this is assumed to be the stroking of the oil inlet valve. This sound is heard with an injection duration down to 0.15 [ms] when the engine is not running. Since there is no rail oil pressure in the system it is not possible to say how the pressure influences the opening time when the engine is running. The current characteristic corresponds well with what was found during reverse engineering but there are current spikes during the withstand phase. The reason is a different filtering time for the clamp measuring tool used for reverse engineering.

7.5 Engine Run Test

The engine is tuned to run in the speed range 900 to 1600rpm and 1000rpm is regarded as idle speed. To verify the ECU calculated speed, an external speed sensor is connected to an analog input on the ECU CompactRIO. The sensor is of type RS2261 (PR-Electronics, 2016) and uses teeth on the crankshaft flywheel as encoder input. All tests are done with an engine coolant temperature of approximately 85°C, i.e. a "warm engine".

7.5.1 Engine Cranking

A cranking test of the engine is performed by disabling the injection and only rotating the engine by the starter motor, see figure 7.5. The top graph displays the in cylinder pressure for cylinder 6, middle graph the camshaft angular position and the bottom graph crankshaft speed. Middle and bottom graphs are calculated by the diagnostic program from the camshaft encoder input.

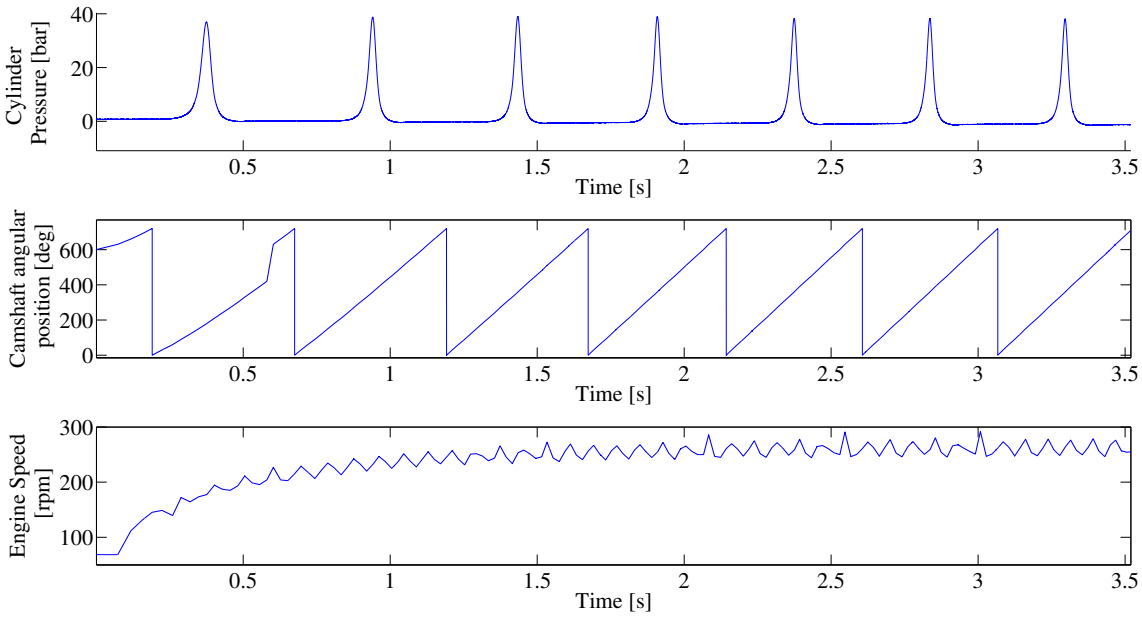

Figure 7.5: Cranking of engine.

Discussion

It was not possible to only do a crank test during reverse engineering without blocking the fuel supply. However, with the developed ECU it is possible to disable the injectors. Then it was possible to crank the engine and verify the maximum cranking speed. From the top graph it is seen that the cranking pressure is approximately 38bar at a cranking speed of approximately 250rpm. This also matches what was found during reverse engineering and is obvious since the engine is only rotated by the starter motor. It was also verified that the calculated speed by the ECU was approximately 250rpm as expected from reverse engineering.

7.5.2 Engine Start

For the engine start, values was entered into the start maps for the ECU. The values are rail valve duty cycle, see table B.1, SOI, see table B.2 and ID, see table B.3.

Discussion

As seen from table table B.1 and B.2 the final values corresponds with the reverse engineering data. For the ID, table B.3, shows that the ECU map is also dependent on the rail pressure. This dependency was not found during reverse engineering, and was implemented to prevent over fueling the engine during start, in case of a high rail pressure and a long ID. For a speed of 1286rpm the ID is reduced to 1.67ms which is lower than the value from reverse engineering. This was done to reduce speed overshoot at 1286rpm.

Rail Pressure During Start

Figure 7.6 shows how the rail pressure develops during start. The top graph is the rail pressure, middle graph is the current supplied to the valve coil and the bottom graph is the crankshaft speed calculated by the diagnostic program from the camshaft encoder input.

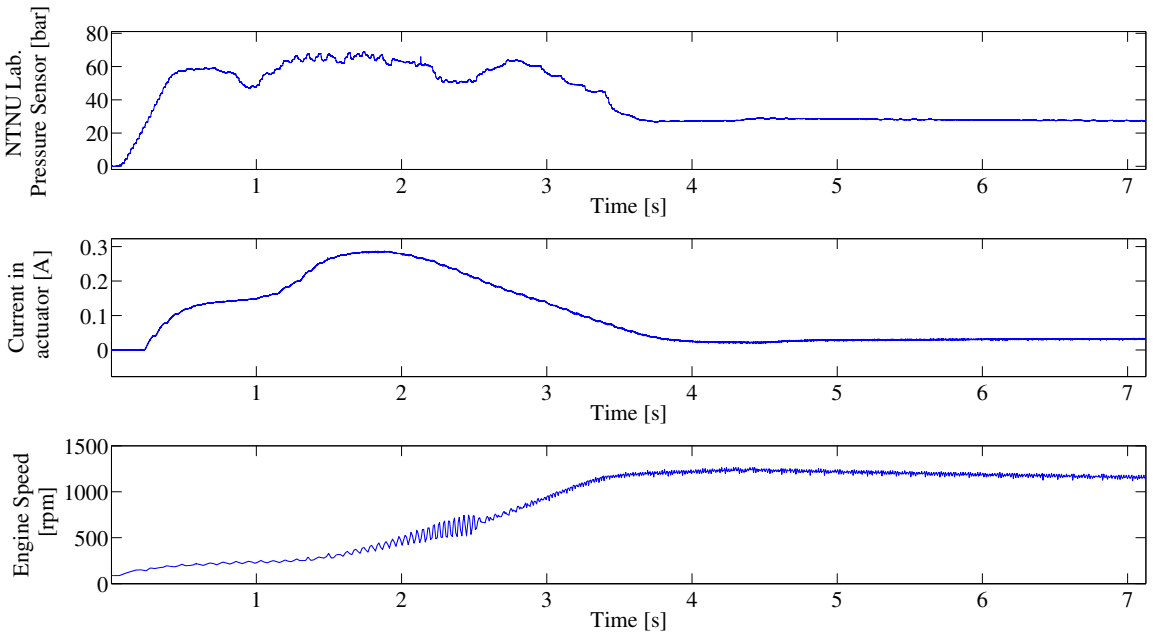

Figure 7.6: Rail pressure during start.

Discussion

The rail valve duty cycle is controlled by the values in table B.1 until 1200rpm is reached. At 1200rpm PID controllers for speed and rail pressure is enabled. Thus the pressure is controlled by the rail pressure PID. This happens approximately at 3.67s. This is the start time of the engine and is close to what was found during reverse engineering, see figure 5.3. As seen from the figure the maximum pressure is lower than what was seen during reverse engineering. This is due to a lower duty cycle value sent to the rail valve. However, the engine has no problem to start with this lower rail pressure. Since a lower pressure implies that the engine will use less fuel, this was found to be acceptable. Note also that the test is done with an engine coolant temperature of 85°C. A coolant temperature of 20°C will give a higher viscosity and a higher pressure for the rail oil. This implies that the duty cycle is dependent of the engine coolant temperature. This is not taken into account in this thesis.

Cylinder Pressure and Injection During Start

In figure 7.7 an engine start from 0 to 1200rpm is shown. The top graph is the in cylinder pressure for cylinder 6, blue line, TDC at 360deg is black dotted line and the injector current in red. The injector current is only for information so the left axis does not represent the current level. The middle graph show the camshaft angular position and the bottom graph the crankshaft speed, both of these are calculated by the diagnostic program from the camshaft encoder input. In figure 7.8 the correlation between the camshaft teeth are shown. The vertical black dotted line is TDC for cylinder 6. Figure 7.9 displays the pressure development during start. Pressure peaks in figure 7.7 are numbered left to right and the first peak is number 1.

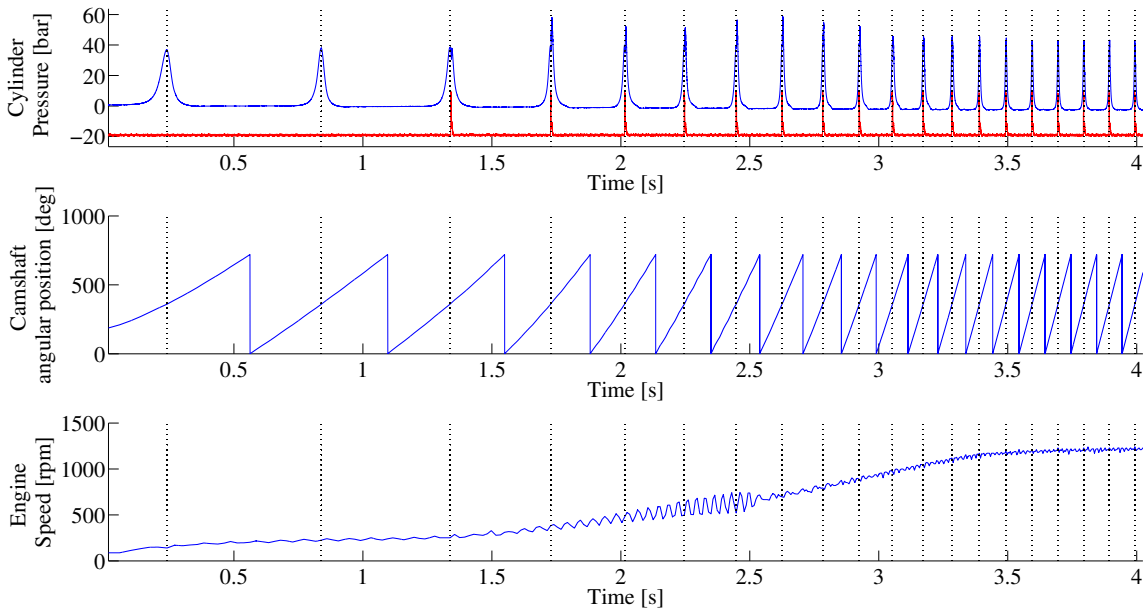

Figure 7.7: Start of engine.

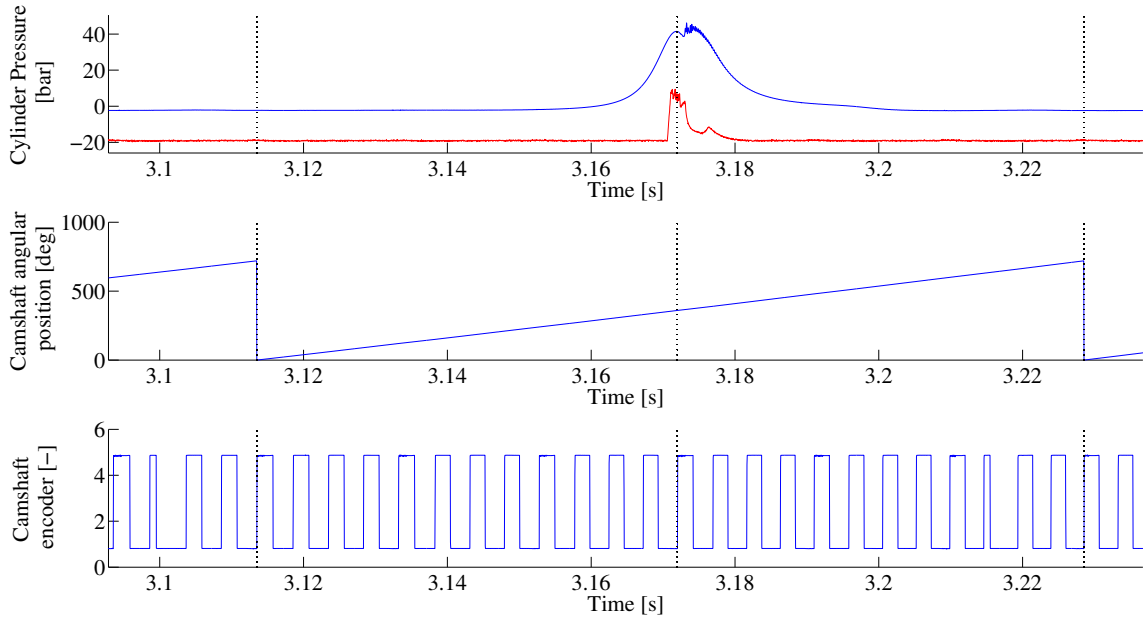

Figure 7.8: Start of engine with camshaft encoder.

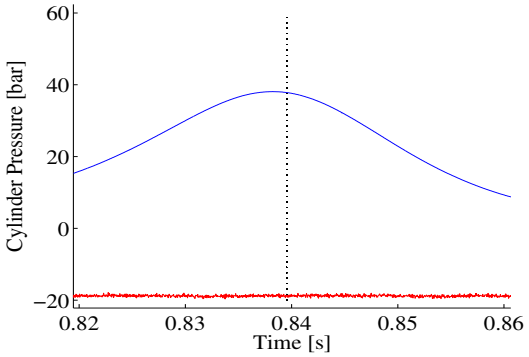

(a) Pressure peak 2.

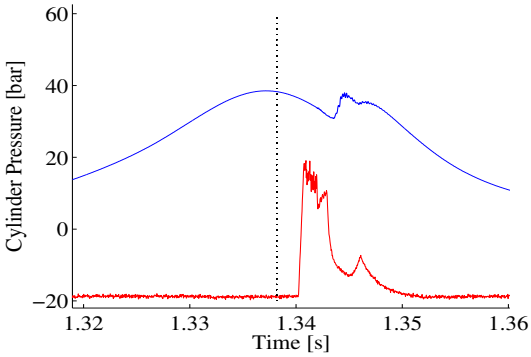

(b) Pressure peak 3.

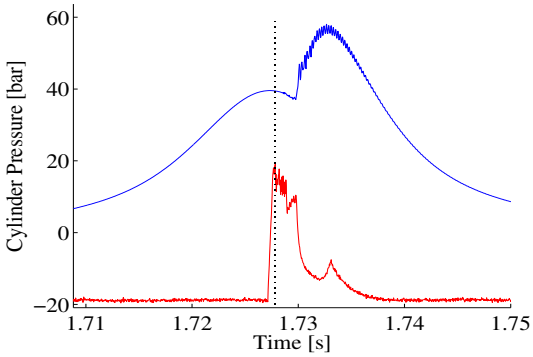

(c) Pressure peak 4.

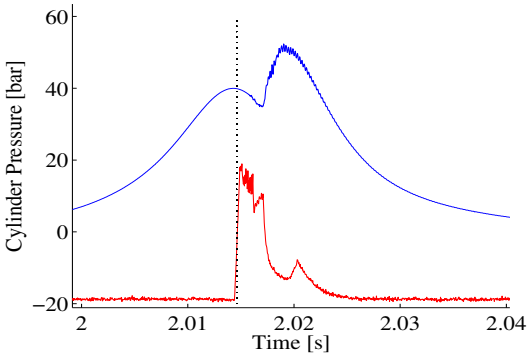

(d) Pressure peak 5.

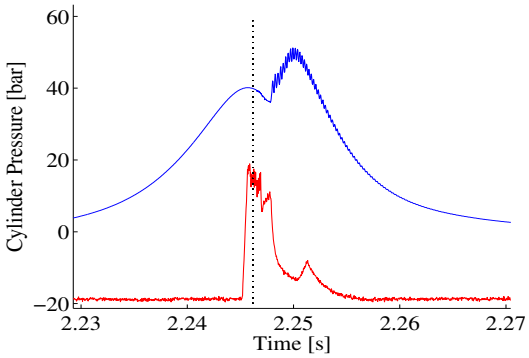

(e) Pressure peak 6.

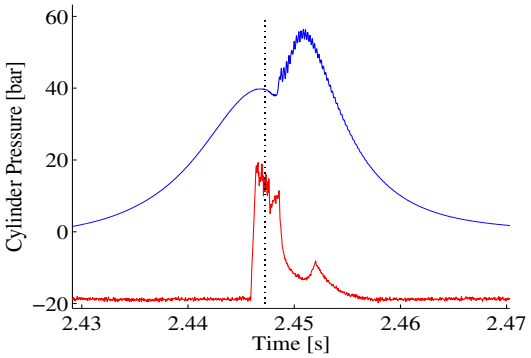

(f) Pressure peak 7.

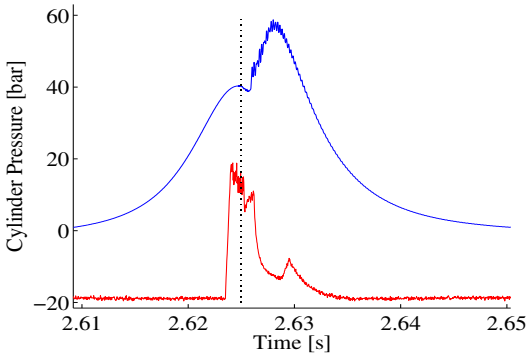

(g) Pressure peak 8.

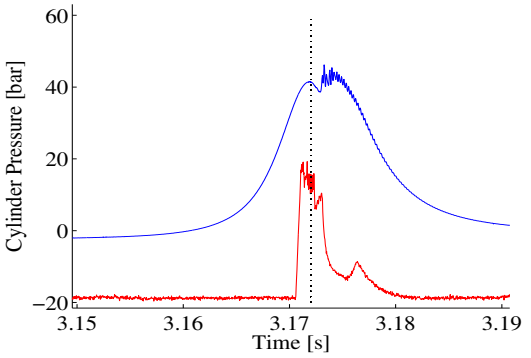

(h) Pressure peak 15.

Figure 7.9: Cylinder pressure during start.

Discussion

From the top graph in figure 7.7, it is seen that from the 3rd compression peak injection is active, since an injector current peak occurs. From this point on, the angular position rate and the engine speed increases, thus fuel injected is ignited. A peak cylinder pressure is reached for injections 2-7 before it drops as the engine reaches it target speed of 1200rpm. Fluctuations of the speed is seen between 400 and 800rpm, which was also seen during reverse engineering. This suggest unstable combustion or critical speed of the shaft in this region. Since all cylinder pressures in this region is showing ignition and no large pressure fluctuation, it is assumed that the cause is critical speed.

In figure 7.8, bottom graph, the camshaft top tooth is clearly seen to the left and to the right as a short pulse. From one top tooth to the other 24 pulses are observed, one for each of the 24 teeth. The vertical black dotted line to the left is the TDC at 0 or 720deg. It is offset with 90deg from the top tooth as mentioned in section 6.3.2. The vertical black dotted line in the middle is the TDC at 360deg and the right for 720 or 0deg. Between the black dotted line to the left and in the middle each tooth period is 30deg. Thus each half period is 15deg. When looking at the top graph it is seen that SOI is before TDC at approximately -7deg which is close to a half half tooth. Note that the camshaft position is only exactly known when transition between low and high occurs. Between the transition the position is an assessed position, see section 6.3.2.

Figure 7.9a is the pressure at cranking speed and figure 7.9b is pressure peak from the first injection. It is seen that this injection has a retarded SOI. Thus a delayed increase in pressure after TDC. It would be desirable to have this pressure increase as an extension of the highest compression pressure, which is at TDC, see also reverse engineering section 5.3.2. As speed increases the SOI is advanced. SOI was not tuned any further since the engine started without any problems. In figure 7.9b to 7.9h the injector current are shown. The current characteristic are clearly seen for the three phases; attack, withstand and holding. The current peak to the right is the induced current from the coil when the injector command is switched off. This is not desirable and is due to a too small resistor on the IDU, see 6.4.2. This means that the induced current increases quicker than the the resistor can handle. To remove the peak a modification to the resistors on the IDU card must be made.

PID Controller During Start

PID controller responses are shown in figure 7.10. To the left speed controller and to the right the rail oil pressure controller. Time-axis in seconds.

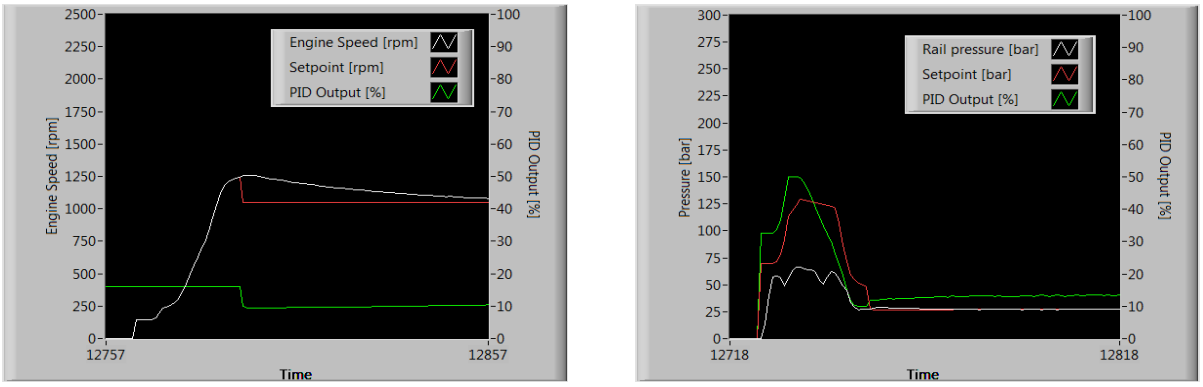

(a) PID speed controller.

(b) PID rail pressure controller.

Figure 7.10: Start of engine, 0-1200rpm, PID controllers.

Discussion

Figure 7.10 show the PID controller response during start and the transition to speed control. The speed controller on the left is in a tracking mode from 0-1200rpm therefore the speed set point and engine speed are overlapped in this range. At 1200rpm the speed controller is released at a speed set point of 1050rpm and therefore the PID output (throttle) is reduced to reduce engine speed. The rail pressure PID controller is not controlling the duty cycle value during start. This is done by a table, see table B.1. It starts to control at the same time as the speed controller. This is seen in the graph when the pressure drops to approximately 30bar.

Engine Data During Start

Engine start response in figure 7.11 displays the essential parameters for the engine. See legend on the right in the figure. Time-axis in seconds.

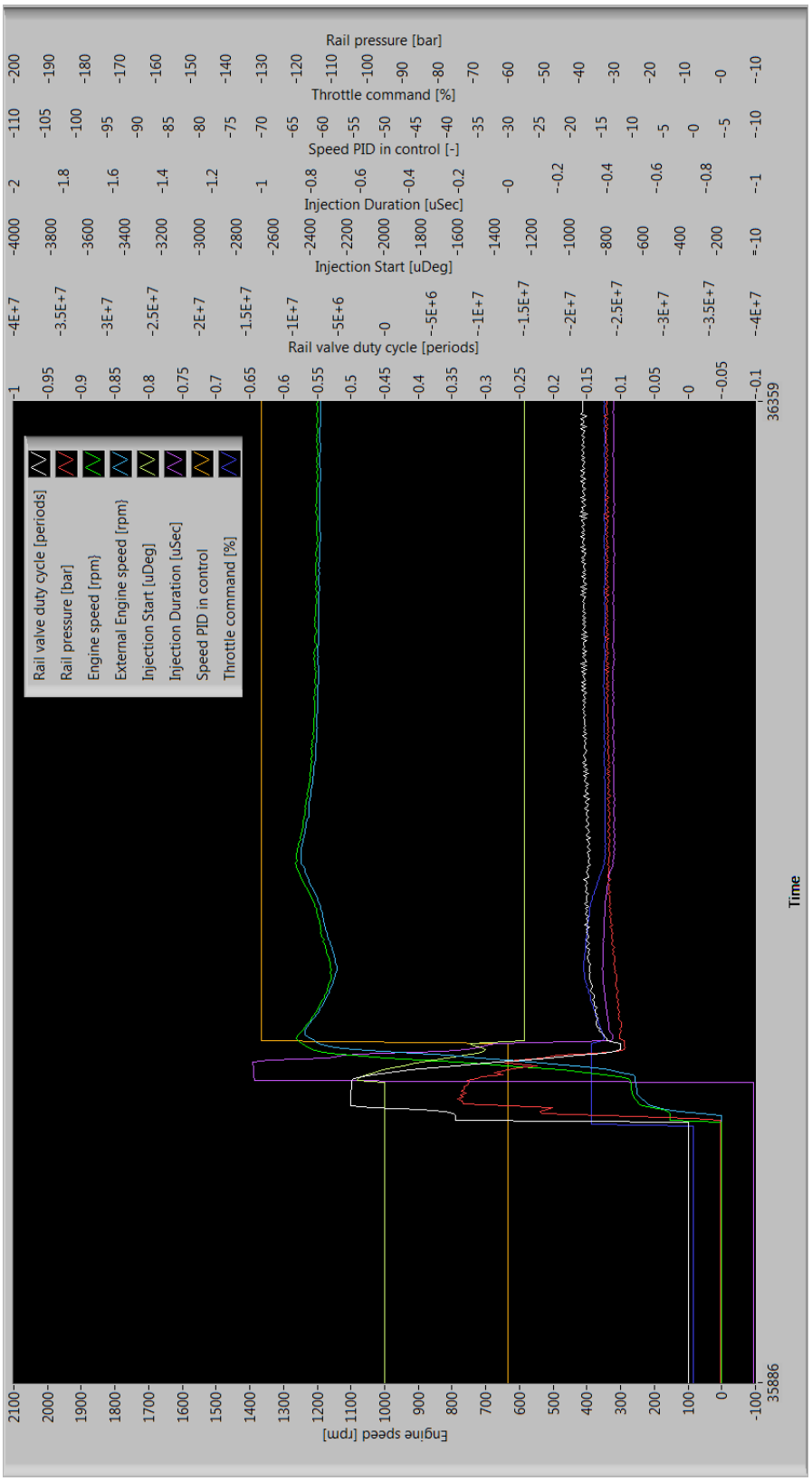

Figure 7.11: Start of engine, 0-1200rpm.

Discussion

A high rail oil pressure, red line, is required for the initial injections. This is accomplished by a closed rail valve. Therefore a high duty cycle value, white line. SOI, yellow line, is retarded for the initial injections as well as long ID, purple line. The orange line in the figure indicates when the speed controller becomes active, this is at 1200rpm. Speed controller output is the throttle, dark blue line. When the speed controller is active, the rail pressure is reduced, SOI is advanced to -15deg before TDC and the ID is reduced to approximately 0.78ms. This is to keep the speed at 1200rpm. The figure also show that the calculated speed, green line, and the external speed sensor, cyan line, are almost equal. The difference is smaller than 50rpm. Thus the ECU calculated speed algorithm works as assumed.

7.5.3 Engine Stopping

An engine stop test is shown in figure 7.12. Time-axis in seconds.

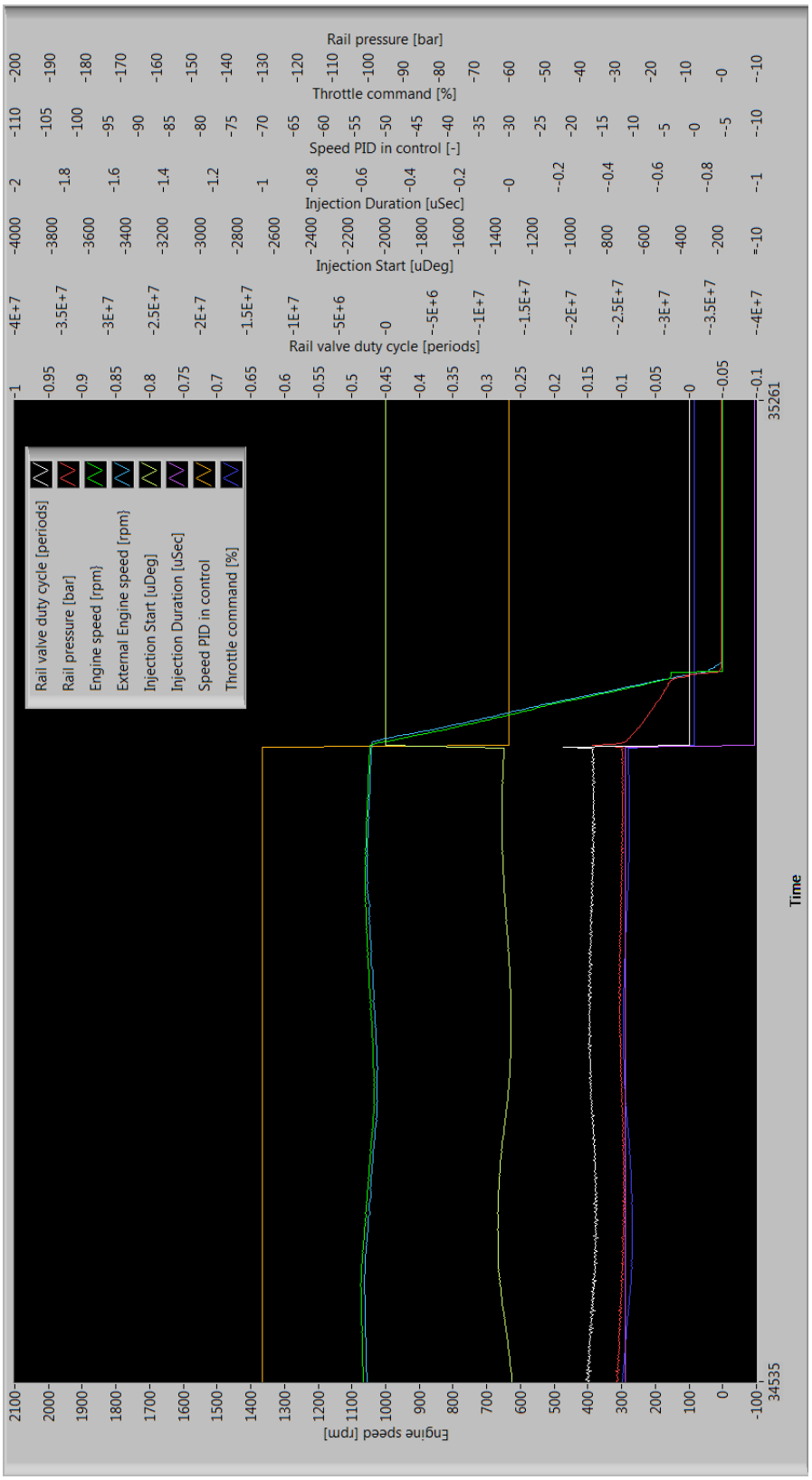

Figure 7.12: Engine stopping 1050-0rpm.

Discussion

As seen from figure 7.12 the speed is below 1100rpm and thus no ramp-down before fuel is cut. When the fuel is cut, the engine speed drops rapidly before it comes to a halt. During fuel cut both throttle and rail valve duty cycle is forced to 0% to stop fuel injection.

7.5.4 Engine Running

With the engine in running state, a step response test was done from 1200 to 1400rpm, then constant speed at 1400rpm and then a step from 1400 to 1200rpm, see figure 7.15. PID controller responses are shown in figure 7.13 and 7.14. In figure 7.16 and 7.17 a detailed view of the rail pressure during the tests are shown.

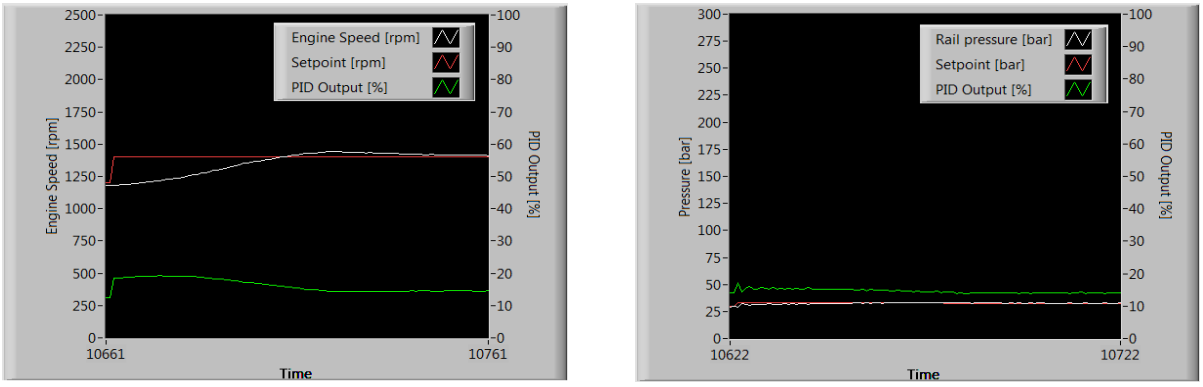

(a) PID speed controller.

(b) PID rail pressure controller.

Figure 7.13: Step 1200-1400rpm, PID controllers.

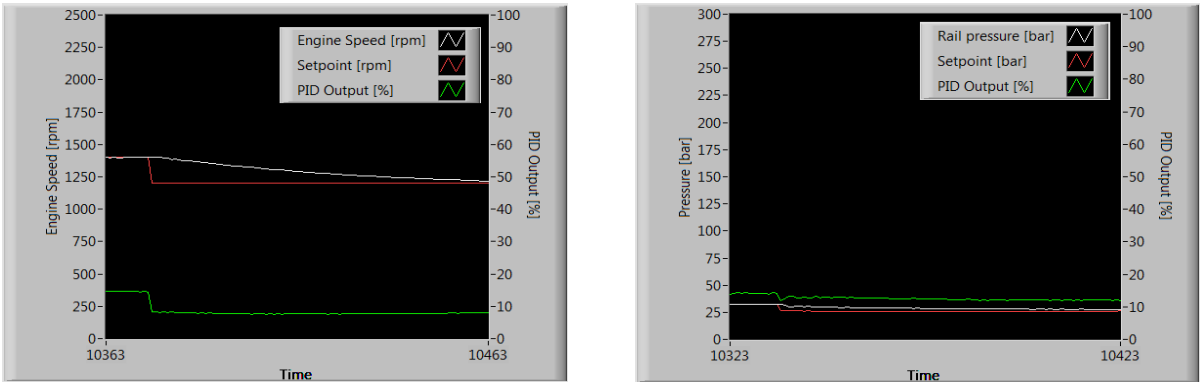

(a) PID speed controller.

(b) PID rail pressure controller.

Figure 7.14: Step 1400-1200rpm, PID controllers.

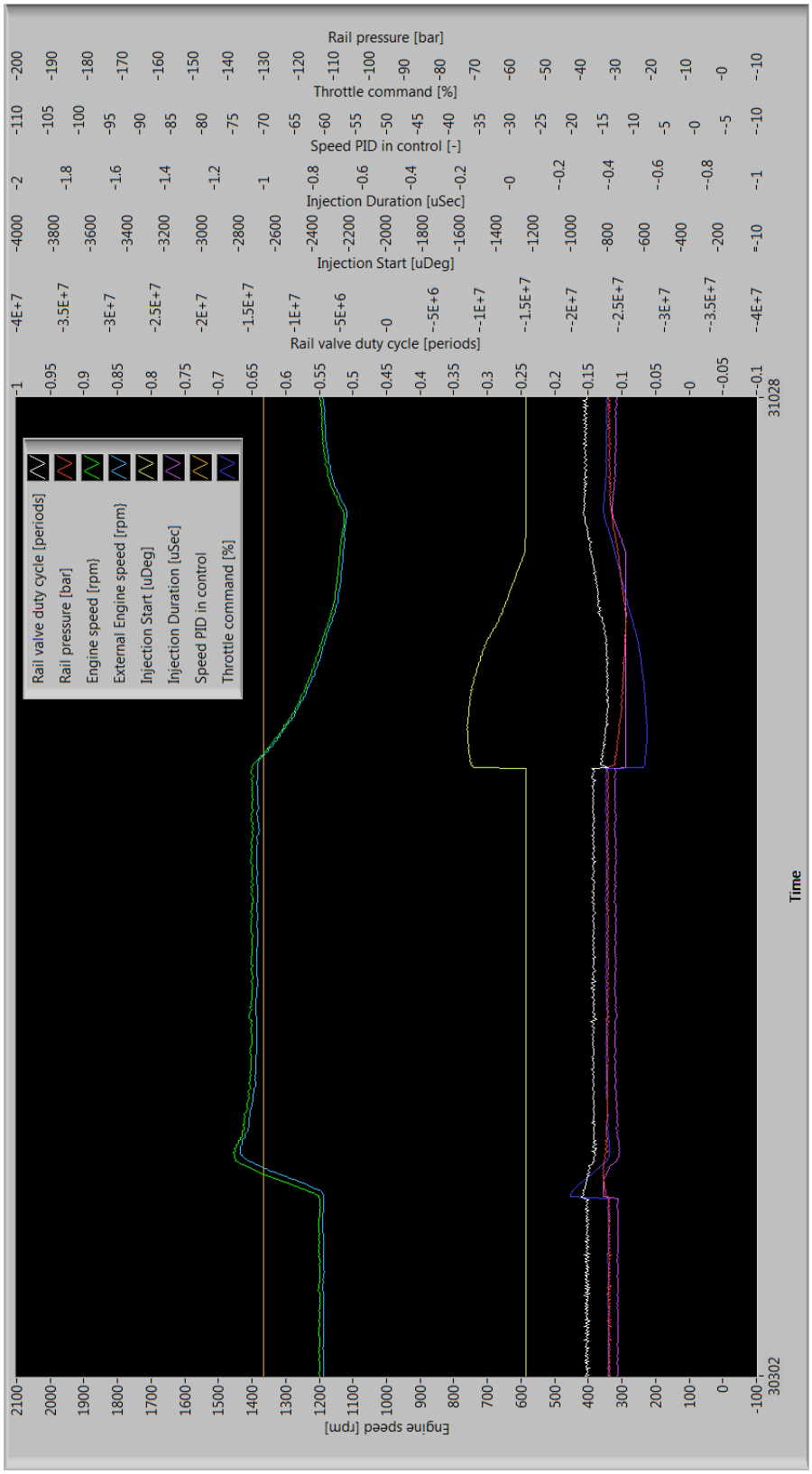

Figure 7.15: Engine response 1200-1400-1200rpm.

Discussion

Figure 7.15 shows speed transitions from 1200 to 1400 1200rpm without any instability of the system. The PID controllers in figure 7.13 and 7.14 also show stable operation. In figure 7.15 it is seen that the external speed sensor and the calculated speed are following each other closely indicating that the speed algorithm works as assumed.

Rail Pressure When Engine Running

Rail pressure for a speed change from 1200 to 1400rpm are shown in figure 7.16 and from 1400 to 1200rpm in figure 7.17. Top graph is rail pressure, middle is rail control valve current and the bottom graph is engine speed.

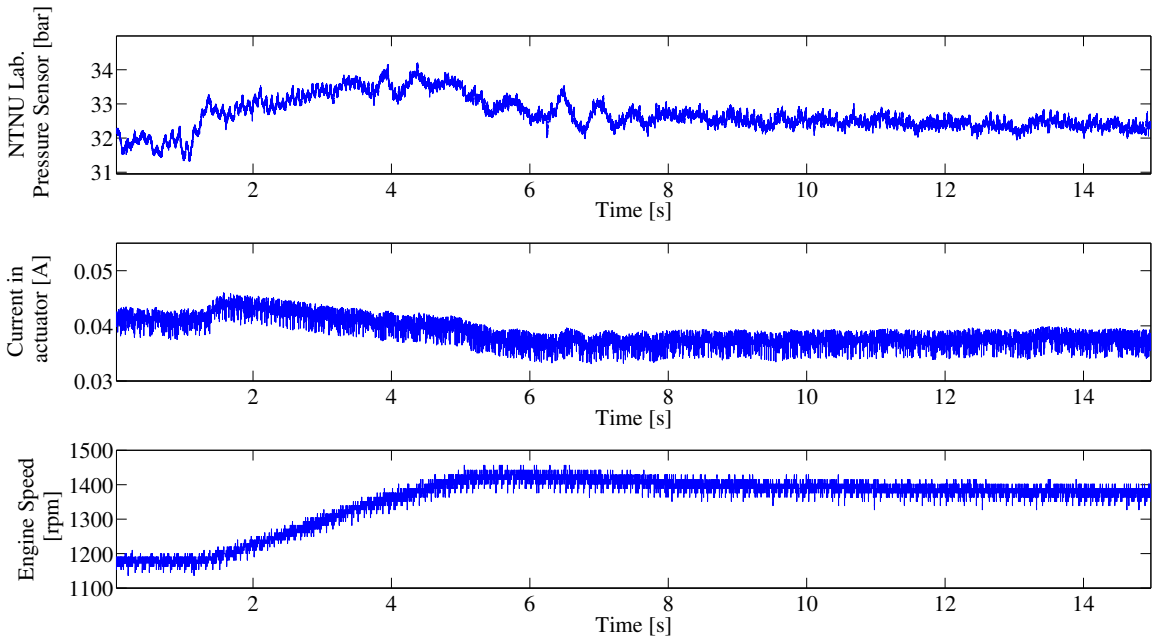

Figure 7.16: Engine speed step 1200-1400rpm.

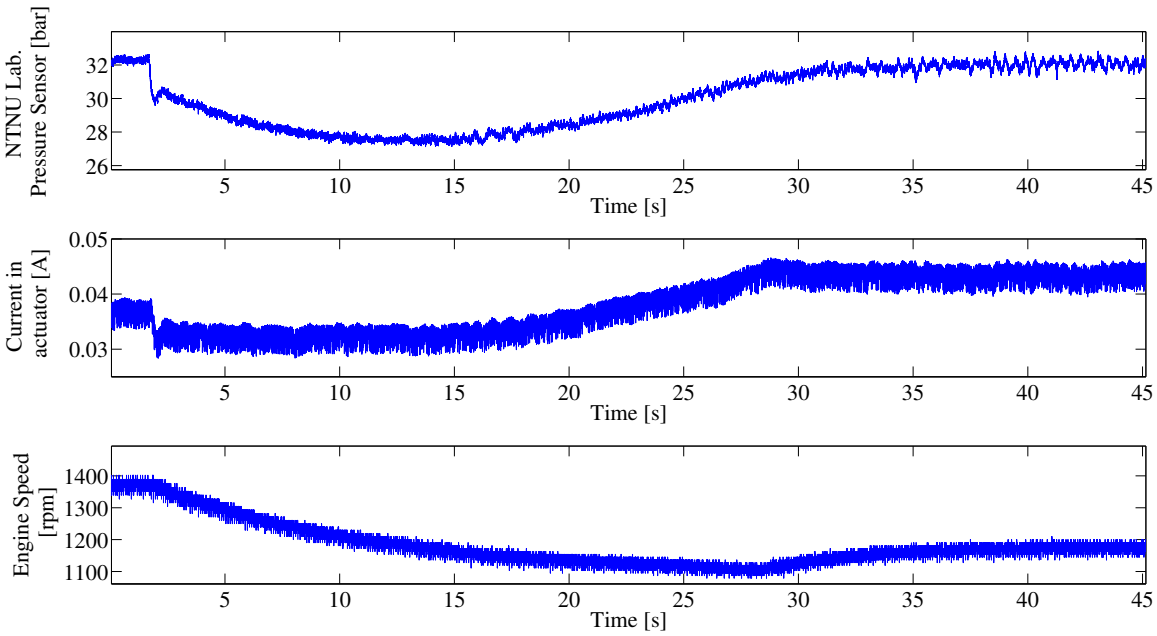

Figure 7.17: Engine speed step 1400-1200rpm.

Discussion

From figure 7.16 it is seen that a small increase in the rail pressure, from 32bar to 33bar changes the speed from 1200 to 1400rpm. This is accomplished by a increase in the current to the rail valve from 0.042 to 0.045A. When 1400rpm is reached the pressure settles at 31.5bar. Note that as the engine speed increases the rail valve current decreases. This is because the rail pressure increases with increasing speed due to the constant displacement rail oil pump. By reducing the current the rail valve increases its opening time to bypass more oil, thus a pressure reduction. This is also seen for a constant engine speed of 1400rpm where the valve current is lower than for 1200rpm but the rail pressure is higher. The same pattern is seen in figure 7.17 for a speed change from 1400 to 1200rpm. Figure 7.16 and 7.17 shows that engine speed is sensitive to rail pressure. A rail pressure change of approximately 1bar results in a speed change of 200rpm.

Cylinder Pressure and Injection when Running

In cylinder pressure for cylinder 6 are shown in figure 7.18 for an engine speed of 1400rpm. Figure 7.19 gives a detailed view of two injection for 1200rpm and 1400rpm. The vertical black dotted line is the TDC for cylinder 6. As mentioned earlier the current in red is not scaled to the left axis.

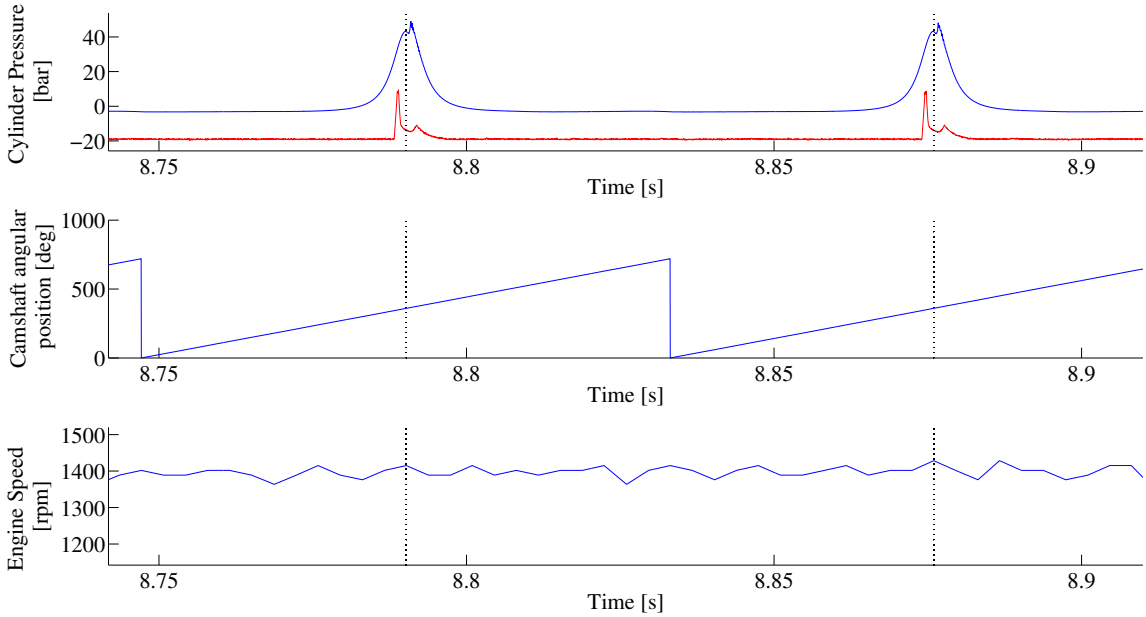

Figure 7.18: Engine steady state at 1400rpm.

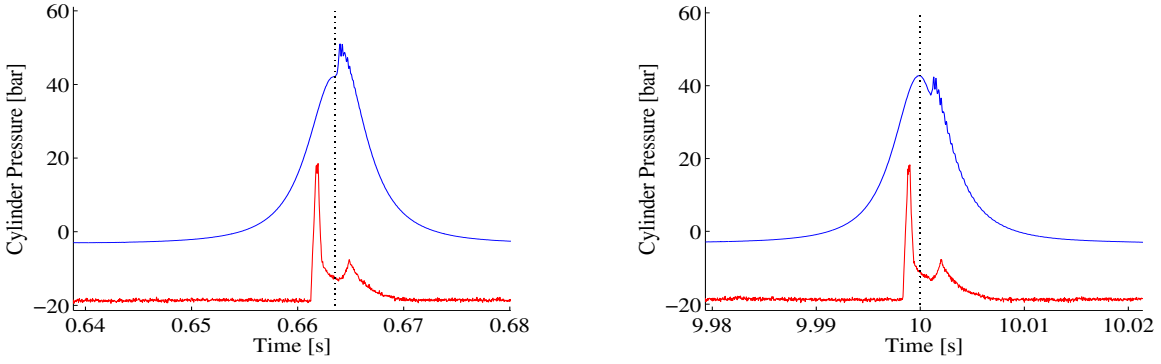

(a) 1200rpm, SOI -15deg, ID 0.77ms.

(b) 1400rpm, SOI -15deg, ID 0.70ms.

Figure 7.19: Cylinder pressure, detailed view.

Discussion

When the engine speed is 1400rpm the cylinder pressure is stable at approximately 48bar with a SOI of -15deg and an ID of 0.67ms. In figure 7.19a it is seen that the pressure increase from combustion continues from the maximum compression pressure. This will give a high efficiency. Figure 7.19b shows that the pressure increase from combustion occurs after passing TDC. This gives a less efficient engine but since the pressure peak is lower it can be assumed that the NOx formation is reduced.

7.5.5 Tuning of Injection Parameters

With the engine in running state different combinations of injection parameters was tested, see figure 7.21. A too retarded timing created a large amount of white smoke escaping the exhaust stack, see figure 7.20, and after 15 minutes of running a strong smell of unburnt fuel was smelled. The black dotted vertical line in figure 7.21 is the TDC position. Injector current (red) is included in the cylinder pressure graph to see the correlation with the pressure (blue) and scaled to fit inside the pressure curve. Thus the left axis is only valid for the pressure. Final values for SOI and ID are shown in tables B.4 and B.5.

Figure 7.20: White smoke due to retarded start of injection.

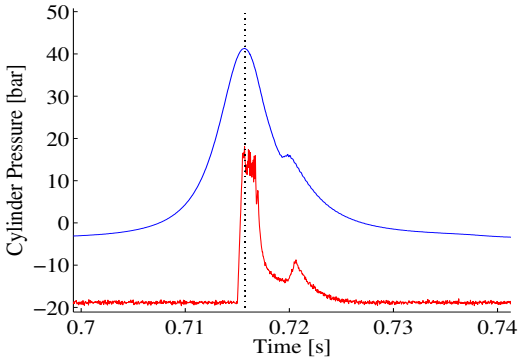

(a) 1220rpm, SOI -2.0deg, ID 1.93ms, rail pressure 33.6bar.

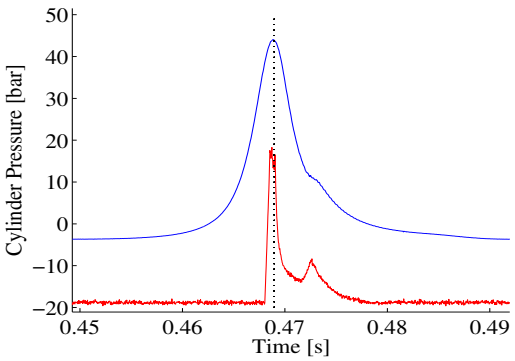

(b) 1560rpm, SOI -6.2deg, ID 1.00ms, rail pressure 35.3bar.

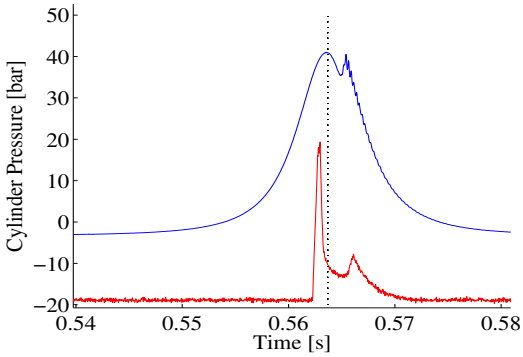

(c) 1050rpm, SOI -6.2deg, ID 0.70ms, rail pressure 29.4bar.

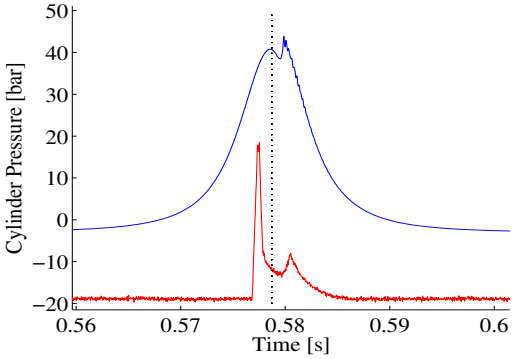

(d) 1000rpm, SOI -9deg, ID 0.70ms, rail pressure 27.0bar.

Figure 7.21: Cylinder pressure for changing speed, SOI, ID and rail pressure.

Discussion

In figure 7.21a and 7.21b cylinder pressure during with smoke condition is shown. From both graphs, the pressure increase from combustion is seen when the cylinder pressure is approximately 15bar after TDC. The reason is a to retarded SOI, long ID and a high rail pressure. This resulted in too much fuel injected into the cylinder too late and a late partial ignition of the injected fuel, due to low cylinder pressure and combustion temperature. Thus not all the fuel is burnt and the assumption is that it enters a vaporized stage before it condenses in the atmosphere, seen as white smoke. Therefore it is clear that SOI, ID and rail pressure have an influence on start of combustion. By reducing ID and rail pressure in figure 7.21b to the parameters shown in figure 7.21c, the white smoke disappeared. This also resulted in reduced engine speed since less fuel is injected. A further advance of SOI and reduction in rail pressure resulted in a speed

drop of 50rpm and the pressure rise peak moved towards TDC, figure 7.21d. As mentioned earlier, ideally the pressure rise from combustion shall be a continuation of maximum compression pressure at TDC.

Chapter 8

Conclusion and Recommendations for Further Work

This chapter presents the conclusions and recommendations for further work.

8.1 Conclusions

A literature review shows how engine performance can be determined by using mathematical equations. It also shows that engine fuel consumption and emissions are influenced by injection parameters like start of injection and injection duration. To determine these injection parameters, engine characteristic at different operation points can be stored in maps or tables in the engine controller. Inputs to the maps can be throttle position and engine speed and the outputs are start of injection and injection duration. Thus an accurate control of engine speed is possible. But this requires an accurate amount of fuel injected into the combustion chamber. With engine speeds over 1000rpm this requires fast acting injector actuators with a response time in the range 1.25ms. To provide this fast response the injector opening is divided into three phases; attack, withstand and holding. The attack phase is a high power phase where the voltage supplied to the coil is higher than in the two other phases. This is to overcome the initial induced current in the coil. In phases withstand and holding the current in the coil are controlled by PWM. The PWM signal has a fixed base frequency where duration of the on period is changed. The duration of this on period is referred to as the duty cycle. An important aspect with PWM

and coils is the induced current when the PWM cuts the current through the coil. This is also referred to as inductor kickback. To protect the circuit from this induced current a diode can be connected in parallel with the coil.

Smoke and torque limitations for the engine have been identified from performance data in the engine manual and engine test run results with the original Perkins Engine Control Unit (PECU). The data in the manual shows that the maximum torque curve is higher than what the Hybrid Power Lab engine can deliver with the installed PECU. It is assumed that this is because the engine is configured as a prime unit which has a lower maximum torque level than if it was configured as a standby unit. Also the generator rated power is 182kW. This is lower than the engine maximum power in both prime and standby configuration. With the assumption of minimum engine speed of 1000rpm and maximum speed of 2100rpm a maximum torque curve was developed. During load test of the generator the maximum power level reached was 150 kW. This is lower than the maximum power of 182kW if the generator is configured as a prime unit. At lower speeds the engine stopped when a certain load level was reached for each speed tested. This is assumed to be the smoke limit for the engine since it is lower than the maximum power and torque limit.

Development and installation of a new ECU that controls the engine speed for the Perkins engine has been done. Since no data was available for the existing ECU reverse engineering was used to determine important control parameters at different operating points. These parameters are engine speed and angular position, in cylinder pressure, start of injection, injection duration, injector current characteristics, rail pressure and rail pressure control valve characteristics. The ECU is designed on a Labview CompactRIO platform and provides a platform for testing of different controller concepts by modifying the Labview logic. A controller for controlling the engine speed was developed. It controls the engine rail pressure, start of injection and injection duration to regulate the engine speed to the desired set point.

The control parameters gathered from the reverse engineering was used as input values for the first test runs with the developed ECU. After this the data was modified as required to provide stable running of the engine between 900 and 1600rpm at zero generator load. Engine speed controller steps changes are tested to verify that the system is stable. A test with a too retarded or late injection resulted in an incomplete combustion. Cylinder pressure increase from

combustion was observed at approximately 15bar after top dead center. This could be seen as white smoke escaping into the atmosphere and unburnt hydrocarbons could be smelled. It is assumed this was unburnt fuel that condensed in contact with the atmosphere.

8.2 Recommendations for Further Work

This section gives recommendation for further work with an objective and a suggested approach. Items are prioritized with an increasing number where the lowest number has the highest priority.

1. **Objective:** Engine safety protection.

   Approach: Connect lube oil temperature and pressure and cooling water temperature sensors to ECU so that these values can be used for shutdown and monitoring. ECU SW is already prepared for these inputs. It is recommended to use the NTNU sensor since the scaling of these are known. Scaling is not known for the original engine sensors.

2. **Objective:** Improved logging of engine data. Today when studying sampled engine data, angular position and speed of the crankshaft have been calculated by the diagnostic program itself, based on the encoder input. This is because the corresponding ECU values are not available. It would be of great interest to use ECU calculated values instead. This will provide the possibility to see the correlation between ECU calculated values and encoder signal, in-cylinder pressure and injector current.

   Approach: Add an analog output module to Labview CompactRIO. Connect the ECU calculated assessed angular position and crankshaft speed and the external speed sensor to the diagnostic computer.

3. **Objective:** Currently a current peak occurs after the injector is switched off. This is due to the induced current from the injector coil. To solve this the resistor size must be changed.

   Approach: Determine size of resistor and modify injector driver unit card.

4. **Objective:** Mapping of engine with current controller.

   Approach: Map engine parameters for start of injection, injection duration and rail pressure for 0-100% load and speed and measure fuel consumption and emissions.

5. **Objective:** Gather engine reference data with original Perkins ECU for zero load condition and variable speed. Test points should be the same as for reverse engineering.
   Approach: Run the engine with the Perkins ECU and gather data for zero load conditions at varying speed. Use the same speed intervals as for reverse engineering so that data overlap.

6. **Objective:** The engine is designed for 100% load at an engine speed of 1500rpm. It is therefore of interest to see the engine behaviour at this point. Collect engine reference data with original Perkins ECU for load condition at a speed of 1500rpm.
   Approach: Run the engine with the Perkins ECU and collect data for 0-100% load conditions at 1500rpm.

7. **Objective:** Improved engine control at different engine coolant temperatures.
   Approach: Develop a control algorithm that compensates engine control parameters with changing engine coolant temperature, i.e cold or warm engine. It require that the coolant temperature sensor is connected to the ECU.

8. **Objective:** Improved injector current control. Reduce injector current peak values, especially during high current phase (withstand phase), and simplify control logic. By reducing the electrical power consumed by the injectors the engine fuel specific fuel consumption is improved.
   Approach: The injector driver unit card has a current sensor that measures the current through each injector. This signal can be used to control the pulse width modulation signal to the injector driver unit, in a closed loop control. The controller can be e.g a PID controller or a threshold controller that controls the current between limit values.

9. **Objective:** Test of injector to find relationship between rail pressure, injection duration and the mass of fuel injected i.e. the injected fuel mass rate as a function of rail pressure for a given injection time. It is also important to determine the time from injector current is applied and until fuel is sprayed, i.e injector opening time or opening delay.
   Approach: Test the injector in a purpose built test bench. The test bench must include a fuel supply pump, rail oil pump, a rail pressure control valve and an interface to a control

system, preferably Labview CompactRIO..

10. **Objective:** Calculate amount of fuel to be injected into the cylinder as mass e.g. grams. Use this value to determine injection duration and start of injection based on measured rail pressure value.

    Approach: When injector fuel mass rate function is known, the injector command is a function of the mass rate or rail pressure and injection duration. Since the crankshaft angular speed in degrees per second for the engine is known, the duration of the injection can be presented in degrees. When the angular injection duration is known, start of injection angular position can be determined.

11. **Objective:** ECU calculated fuel consumption versus an external fuel consumption sensor.

    Approach: Create an algorithm for calculating fuel consumption in the ECU based on rail pressure and injection duration. Verify the algorithm with an external sensor. When injector mass rate is known the fuel consumption is a function of mass rate and injection duration. This can be used to calculate actual fuel consumption and accumulated consumption over time.

Bibliography

Barnes, T. E. (1994). *Electronic Control System and Method For a Hydraulically-Actuated Fuel Injection System.* Number US005357912, Unlted States Patent.

Barnes, T. E. (1995). *Method for Controlling a Hydraulically-Actuated Fuel Injection System to Start an Engine.* Number US005447138, Unlted States Patent.

Baukal, C. E. (2004). *Industrial combustion pollution and control.* Marcel Dekker.

Bishop, R. H., editor (2008). *The Mechatronics Handbook.* CRC Press, 2nd edition.

Bosch, R. (2006). *Diesel-Engine Management.* Robert Bosch GmbH, 4th edition.

Caterpillar (1999). *HEUI Fuel Systems,.* Caterpillar, pehp9526 edition.

Caterpillar (2007). *System Operation Testing and Adjusting 3126B and 3126E Truck Engine.* Caterpillar.

Heywood, J. B. (1988). *Internal Comustion Engine Fundamentals.* McGraw-Hill.

Hillier, V. and Coombes, P. (2004). *Hillier´s fundamentals of motor vehicle technology.* Nelson Thornes, 5th edition.

Lieuwen, T. C. and Yang, V. (2016). *Gas Turbine Emissions.* Cambridge Books Online.

National-Instrument (2009). *CompactRIO Developers Guide.*

National-Instrument (2015). *Device Specifications, NI USB-6210, M Series Data Acquisition: 16 AI, 4 DI, 4 DO Bus-Powered USB.* National-Instrument, 375194b-01 edition.

Perkins-Engines (2001). *Perkins, Peregrine EDi and 1300 Series EDi, WORKSHOP MANUAL, TPD1353E*. Perkins Engines Company Limited, issue 3 edition.

Pon-Cat (2012). *Olympian GEP 250 – 259 kVA Generatorsett NTNU*. Pon Power AS, document number 52820/31155 edition.

PR-Electronics (2016). *2261 mv transmitter*, doc. 2261v101-uk edition.

Sybele (2009). *Use of inductive injectors Driver IMS06*. Sybele by Skynam, v.100 edition.

Sørensen, A. J. (2013). *Marine Control Systems, Propulsion and Motion Control of Ships and Ocean Structures, Lecture Notes*. NTNU.

Total (2010). *MARKETING SPECIFICATIONS GAS OIL – Sulphur-free BS 2869:2010 - Class A2* . Total.

Appendix A

Injector Driver Unit Card

Design details for the injector driver unit card are shown in this chapter. The card is designed and built by NTNU Marintek Lab staff. Section A.1 shows card i/o interfaces, layout of components in section A.2 and section A.3 shows the electrical circuit schematics for the card. Printed circuit board layout is shown is section A.4 and a component list is found in section A.5. Card size is W x H = 100 x 160mm.

A.1 Card Interfaces

Card inputs are shown in table A.1 and outputs in table A.2. Out 1-6 are the high power outputs used for driving the injector coils. These outputs have a dedicated current measuring component that measures the current flow through each of the six outputs. The measured current level is available as a voltage level at the current sense X6 terminal. The output is a scaled value where 200mV corresponds to 1A , i.e. 200mV/A.

Table A.1: Card inputs.

Card input	**Signal**	**Terminals**	**Description**
Power supply	5 [V]	X7:5V/Gnd	Power supply
Power supply	12 [V]	X7:12V/Gnd	Power supply
Power supply	26 [V]	X7:26V+/Gnd	Power supply
Power supply	26 [V]	X7:26V_2+/26V_2-	Power supply
Power supply	56 [V]	X7:56V+/56V-	Power supply
PWM In 1	0-5 [V]	X2:1/5	PWM signal for PWM Out 1
PWM In 2	0-5 [V]	X2:2/5	PWM signal for PWM Out 2
HV1	0-5 [V]	X2:3/6	High voltage command for Inj command 1-3
HV2	0-5 [V]	X2:4/6	High voltage command for Inj command 4-6
Inj Command 1	0-5[V]	X1:1/8	Injection command 1
Inj Command 2	0-5[V]	X1:2/8	Injection command 2
Inj Command 3	0-5[V]	X1:3/8	Injection command 3
Inj Command 4	0-5[V]	X1:4/8	Injection command 4
Inj Command 5	0-5[V]	X1:5/8	Injection command 5
Inj Command 6	0-5[V]	X1:6/8	Injection command 6

Table A.2: Card outputs.

Card output	Signal	Terminals	Description
PWM1 Out	0-12 [V]	X5:PWM1 Out+/PWM1 Out-	PWM output 1
PWM2 Out	0-12 [V]	X5:PWM2 Out+/PWM2 Out-	PWM output 2
Out 1	0-110 [V]	X3:Out1+/Out1-	PWM output Injector 1
Out 2	0-110 [V]	X3:Out2+/Out2-	PWM output Injector 2
Out 3	0-110 [V]	X3:Out3+/Out2-	PWM output Injector 3
Out 4	0-110 [V]	X4:Out4+/Out4-	PWM output Injector 4
Out 5	0-110 [V]	X4:Out5+/Out5-	PWM output Injector 5
Out 6	0-110 [V]	X4:Out6+/Out6-	PWM output Injector 6
Current sense 1	0-5 [V]	X6:1/Gnd	Current measurement for Out 1
Current sense 2	0-5 [V]	X6:2/Gnd	Current measurement for Out 2
Current sense 3	0-5 [V]	X6:3/Gnd	Current measurement for Out 3
Current sense 4	0-5 [V]	X6:4/Gnd	Current measurement for Out 4
Current sense 5	0-5 [V]	X6:5/Gnd	Current measurement for Out 5
Current sense 6	0-5 [V]	X6:6/Gnd	Current measurement for Out 6

Note: Current sens 1-6 output are offset with 0.49V, thus 0.49V= 0A.

A.2 Card Component Layout

Card component layout is shown in figure A.1.

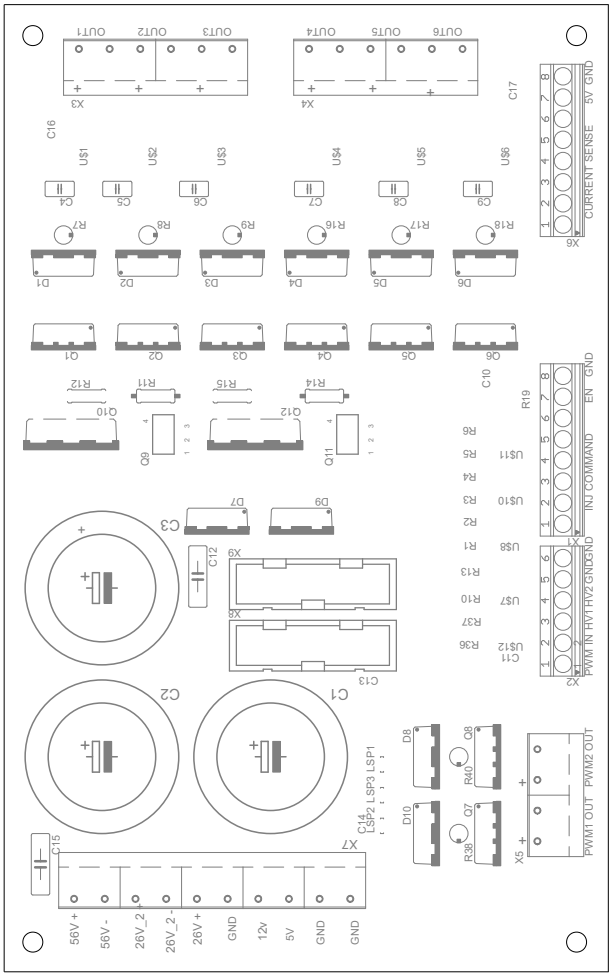

Figure A.1: Card component layout.

A.3 Card Circuit Schematic

Circuit schematics for the card are shown in figure A.2 and A.3.

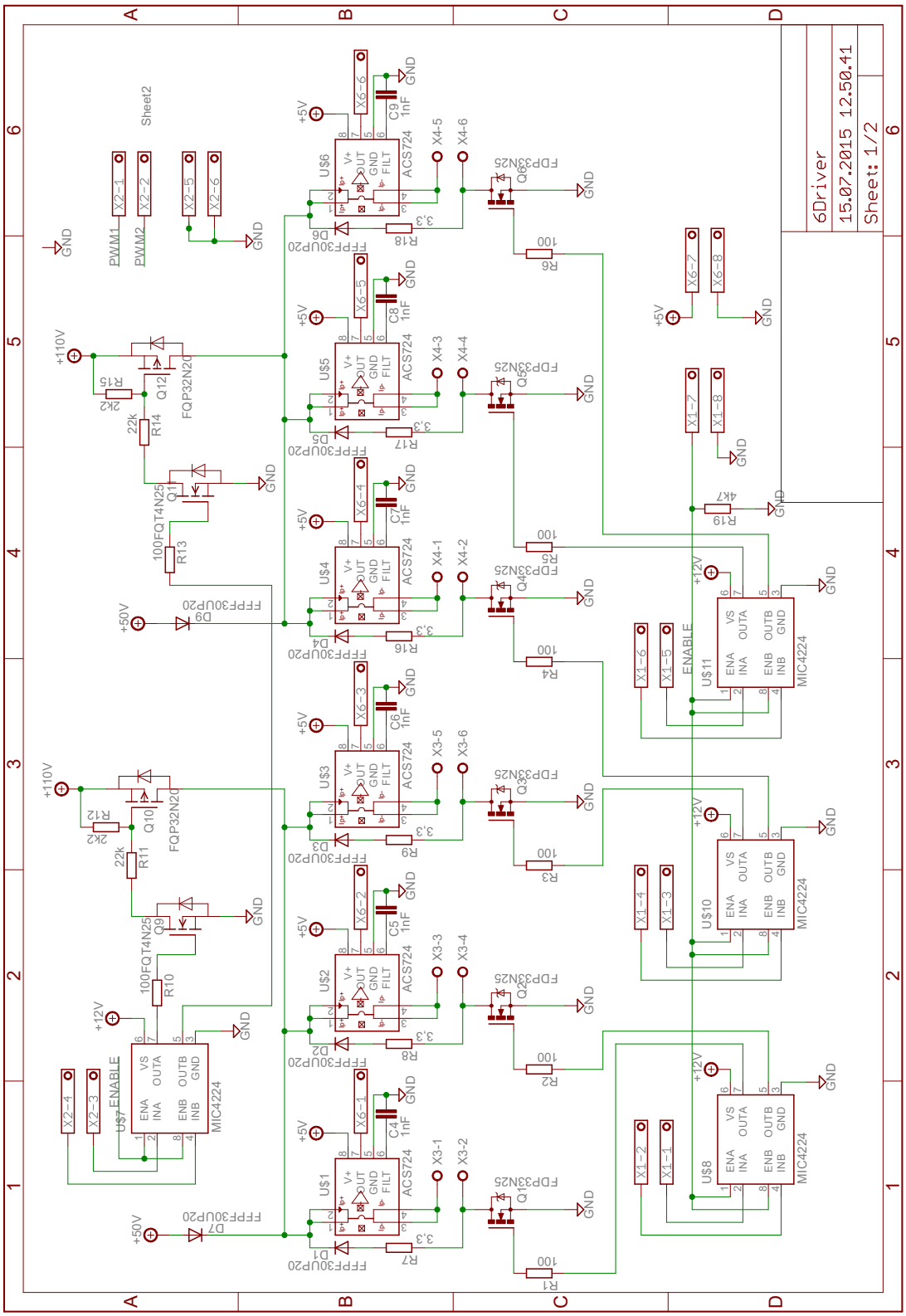

Figure A.2: Card circuit schematic page 1/2.

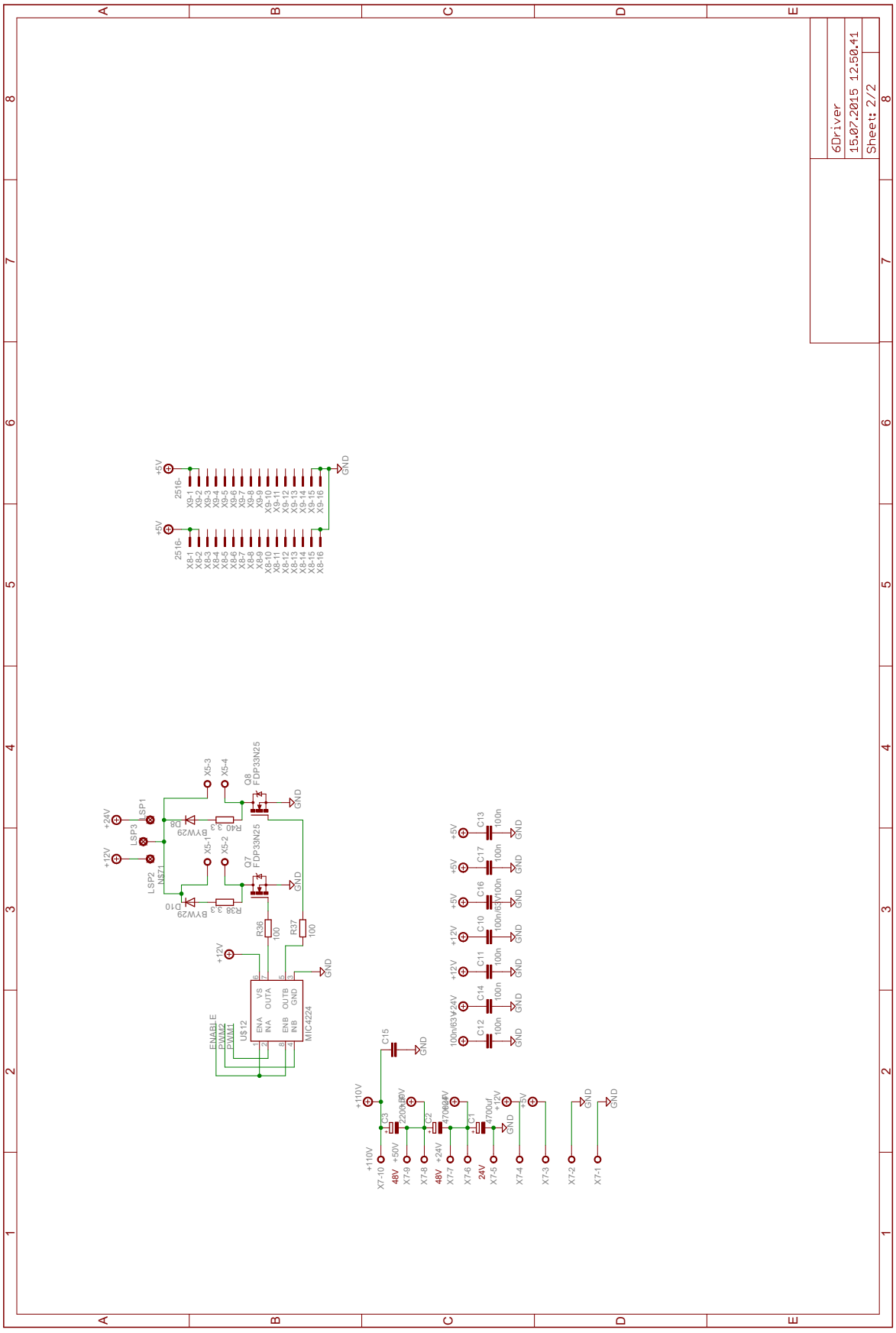

Figure A.3: Card circuit schematic page 2/2.

A.4 Card Printed Circuit Board Layout

Card printed circuit board layout is shown in figure A.4 and A.5.

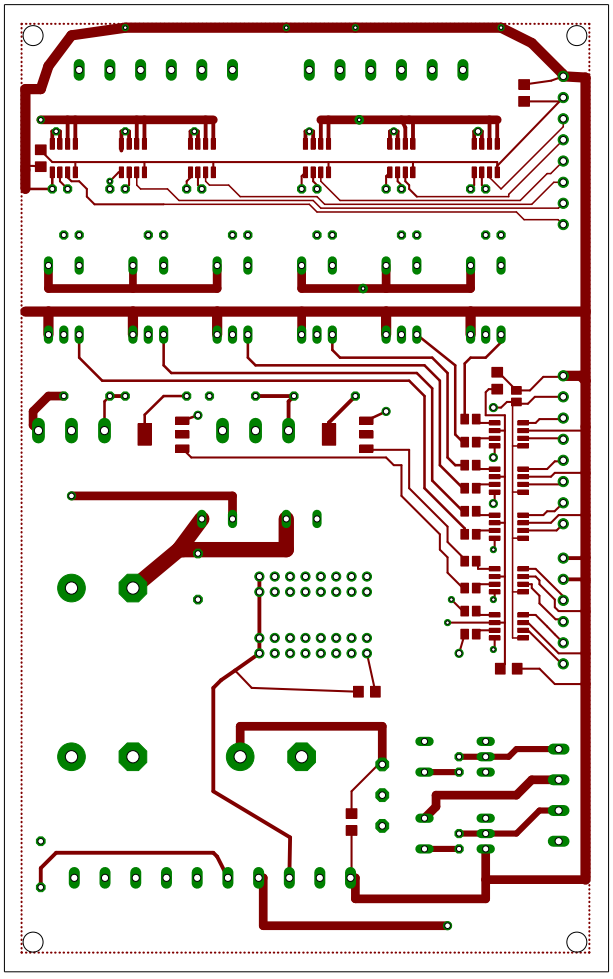

18.05.2016 08.58.19 C:\Users\frogra\Get Sky\Jobb\6CylDriver_2\6Driver.brd

Figure A.4: Card circuit top layer.

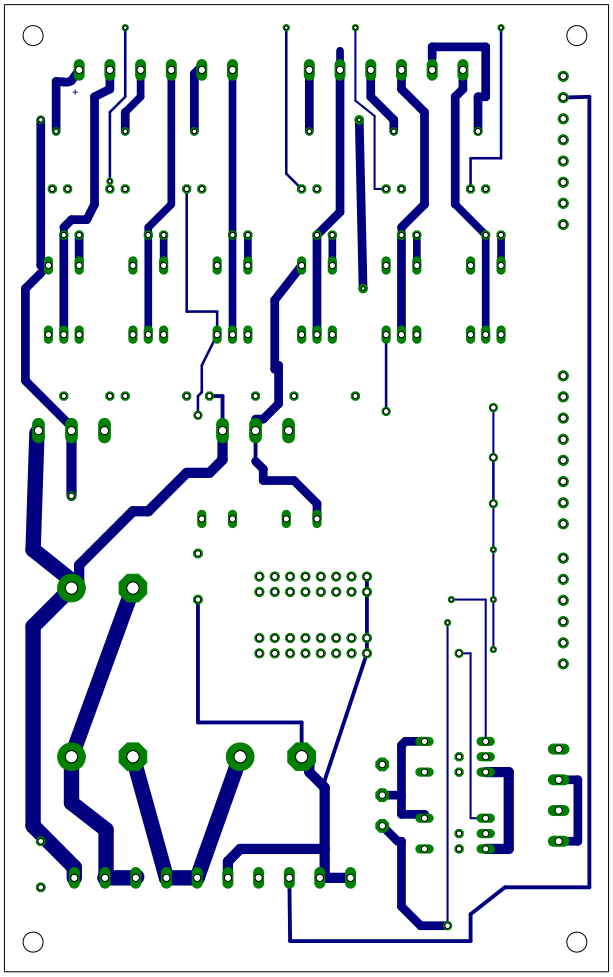

18.05.2016 08.59.02 C:\Users\frogra\Get Sky\Jobb\6CylDriver_2\6Driver.brd

Figure A.5: Card circuit bottom layer.

A.5 Card Component List

Card component lists are shown in tables A.3, A.4, A.5 and A.6.

Table A.3: Card Component List.

Part	Value	Device	Package	Description
C1	4700uf	CPOL-EUE10-25	EB25D	POLARIZED
C2	4700uf	CPOL-EUE10-25	EB25D	POLARIZED
C3	2200uf	CPOL-EUE10-25	EB25D	POLARIZED
C4	1nF	C-EU025-025X050	C025-025X050	"CAPACITOR,"
C5	1nF	C-EU025-025X050	C025-025X050	"CAPACITOR,"
C6	1nF	C-EU025-025X050	C025-025X050	"CAPACITOR,"
C7	1nF	C-EU025-025X050	C025-025X050	"CAPACITOR,"
C8	1nF	C-EU025-025X050	C025-025X050	"CAPACITOR,"
C9	1nF	C-EU025-025X050	C025-025X050	"CAPACITOR,"
C10	100n/63V	C-EUC1206	C1206	"CAPACITOR,"
C11	100n	C-EUC1206	C1206	"CAPACITOR,"
C12	100n	C-EU075-032X103	C075-032X103	"CAPACITOR,"
C13	100n	C-EUC1206	C1206	"CAPACITOR,"
C14	100n	C-EUC1206	C1206	"CAPACITOR,"
C15	100n	C-EU075-032X103	C075-032X103	"CAPACITOR,"
C16	100n	C-EUC1206	C1206	"CAPACITOR,"
C17	100n	C-EUC1206	C1206	"CAPACITOR,"
D1	BYC20DX	BYW29	DO220S	DIODE
D2	BYC20DX	BYW29	DO220S	DIODE
D3	BYC20DX	BYW29	DO220S	DIODE
D4	BYC20DX	BYW29	DO220S	DIODE
D5	BYC20DX	BYW29	DO220S	DIODE
D6	BYC20DX	BYW29	DO220S	DIODE
D7	BYC20DX	BYW29	DO220S	DIODE
D8	BYC20DX	BYW29	DO220S	DIODE

Table A.4: Card Component List.

Part	Value	Device	Package	Description
D9	BYC20DX	BYW29	DO220S	DIODE
D10	BYC20DX	BYW29	DO220S	DIODE
LSP1	LSP11	LSP11	LSP11	SOLDER PAD
LSP2	LSP11	LSP11	LSP11	SOLDER PAD
LSP3	LSP11	LSP11	LSP11	SOLDER PAD
Q1	FQPF32N20C	IRF740	TO220BV	N-CHANNEL MOS FET
Q2	FQPF32N20C	IRF740	TO220BV	N-CHANNEL MOS FET
Q3	FQPF32N20C	IRF740	TO220BV	N-CHANNEL MOS FET
Q4	FQPF32N20C	IRF740	TO220BV	N-CHANNEL MOS FET
Q5	FQPF32N20C	IRF740	TO220BV	N-CHANNEL MOS FET
Q6	FQPF32N20C	IRF740	TO220BV	N-CHANNEL MOS FET
Q7	IRF540	IRF540	TO220BV	HEXFET Power MOSFET
Q8	IRF540	IRF540	TO220BV	HEXFET Power MOSFET
Q9	FQT4N25	N-CHANMOS-SOT223	SOT223	
Q10	FQP32N20	P-CHANPOWERFFET TOP3V	TOP3V	P-chan MOSFET Transistor
Q11	FQT4N25	N-CHANMOS-SOT223	SOT223	
Q12	FQP32N20	P-CHANPOWERFFET TOP3V	TOP3V	P-chan MOSFET Transistor

Table A.5: Card Component List.

Part	**Value**	**Device**	**Package**	**Description**
R1	100	R-EU_M0805	M0805	"RESISTOR,"
R2	100	R-EU_M0805	M0805	"RESISTOR,"
R3	100	R-EU_M0805	M0805	"RESISTOR,"
R4	100	R-EU_M0805	M0805	"RESISTOR,"
R5	100	R-EU_M0805	M0805	"RESISTOR,"
R6	100	R-EU_M0805	M0805	"RESISTOR,"
R7	"3,3"	R-EU_0309/V	0309V	"RESISTOR,"
R8	"3,3"	R-EU_0309/V	0309V	"RESISTOR,"
R9	"3,3"	R-EU_0309/V	0309V	"RESISTOR,"
R10	100	R-EU_M0805	M0805	"RESISTOR,"
R11	22k	R-EU_0207/10	0207/10	"RESISTOR,"
R12	2k2	R-EU_0207/7	0207/7	"RESISTOR,"
R13	100	R-EU_M0805	M0805	"RESISTOR,"
R14	22k	R-EU_0207/10	0207/10	"RESISTOR,"
R15	2k2	R-EU_0207/7	0207/7	"RESISTOR,"
R16	"3,3"	R-EU_0309/V	0309V	"RESISTOR,"
R17	"3,3"	R-EU_0309/V	0309V	"RESISTOR,"
R18	"3,3"	R-EU_0309/V	0309V	"RESISTOR,"
R19	4k7	R-EU_M0805	M0805	"RESISTOR,"
R36	100	R-EU_M0805	M0805	"RESISTOR,"
R37	100	R-EU_M0805	M0805	"RESISTOR,"
R38	"3,3"	R-EU_0309/V	0309V	"RESISTOR,"
R40	"3,3"	R-EU_0309/V	0309V	"RESISTOR,"
U$1	ACS724	ACS724	SO08	
U$2	ACS724	ACS724	SO08	
U$3	ACS724	ACS724	SO08	
U$4	ACS724	ACS724	SO08	
U$5	ACS724	ACS724	SO08	
U$6	ACS724	ACS724	SO08	
U$7	MIC4224	MIC4224	SO08	

Table A.6: Card Component List.

Part	**Value**	**Device**	**Package**	**Description**
U$8	MIC4224	MIC4224	SO08	
U$10	MIC4224	MIC4224	SO08	
U$11	MIC4224	MIC4224	SO08	
U$12	MIC4224	MIC4224	SO08	
X1	1751303	1751303	MKDS	1/ "8-3,5" Printk-lemme
X2	1751280	1751280	MKDS	1/ "6-3,5" Printk-lemme
X3	W237-06P	W237-6P	WAGO	SREW CLAMP
X4	W237-06P	W237-6P	WAGO	SREW CLAMP
X5	W237-04P	W237-4P	WAGO	SREW CLAMP
X6	1751303	1751303	MKDS	1/ "8-3,5" Printk-lemme
X7	W237-10P	W237-10P	WAGO	SREW CLAMP
X8	-2516	-2516	PAK100/2500-16	3M (TM) Pak
X9	-2516	-2516	PAK100/2500-16	3M (TM) Pak

Appendix B

Engine Control Unit Mapping Tables

This chapter shows the final ECU mapping tables from the engine run tests. Start maps are shown in B.1, running maps in B.2 and limitation map in B.3.

B.1 Start Maps

The displayed map values are the final values used by the ECU and the corresponding values found during reverse engineering. The values are rail valve duty cycle, table B.1, SOI, table B.2 and ID, table B.3.

Table B.1: ECU start 2D-LUT for rail valve duty cycle vs. reverse engineering start data.

ECU start 2D-LUT for duty cycle [%]			**Rail valve map, see table 7.1**	**Rev. Eng. Data**	
n	-		**Rail Press**	**n**	**Rail Press**
[rpm]	0	0	**Ctrl [V]**	**[rpm]**	**Ctrl [V]**
0	0	0	0	0	0.31
220	50	50	0.30	220	0.29
267	50	50	0.30	261	0.28
861	25	25	0.095	861	0.16
1019	20	20	0.065	1019	0.09
1213	10	10	0.02	1213	0.1
1286	10	10	0.02	1286	0.05

Table B.2: ECU start 2D-LUT for SOI vs. reverse engineering start data.

ECU start 2D-LUT forSOI [deg]			**Rev. Eng. Data**	
n	-		**n**	**SOI**
[rpm]	0	0	**[rpm]**	**[deg]**
220	3	3	220	0
267	3	3	261	3.1
861	-5	-5	861	-5
1019	-7	-7	1019	-7.2
1213	-11	-11	1213	-11.2
1286	-7	-7	1286	-7.2

Table B.3: ECU start 2D-LUT for ID vs. reverse engineering start data.

ECU start 2D-LUT for ID [ms]									**Rev. Eng. Data**	
n	**Rail oil pressure [bar]**								**n**	**ID**
[rpm]	0	38	39	54	89	121	129	160	**[rpm]**	**[ms]**
0	0	0	0	0	0	0	0	0	0	0
220	0	2.7	2.7	2.7	2.7	2.7	2.7	2.5	220	0
267	0	2.7	2.7	2.7	2.7	2.7	2.7	2.5	261	2.7
861	0	2.71	2.71	2.71	2.71	2.71	2.2	2.5	861	2.7
1019	0	2.23	2.23	2.23	2.23	1.6	0	0	1019	2.23
1213	0	2.2	2.2	2.2	1.6	0	0	0	1213	2.2
1286	0	1.67	1.2	0	0	0	0	0	1286	2.089

B.2 Running Maps

This section show the final maps for engine in running state. Start of injection is shown in table B.4 and injection duration in table B.5.

Table B.4: ECU running 2D-LUT for SOI.

ECU running 2D-LUT for SOI [deg]								
n	**Throttle [%]**							
[rpm]	0	6	8	10	13	15	18	20
0	0	0	0	0	0	0	0	0
240	0	0	0	0	0	0	0	0
900	0	-7	-9	-12	-15	-15.09	-15.09	-15.09
950	0	-7	-9	-12	-15	-15.09	-15.09	-15.09
1000	0	-7	-9	-12	-15	-15.09	-15.09	-15.09
1200	0	-7	-9	-12	-15	-15.09	-15.09	-15.09
1400	0	-7	-9	-12	-15	-15.09	-15.09	-15.09
1600	0	-7	-9	-12	-15	-15.09	-15.09	-15.09
1800	0	-7	-9	-12	-15	-15.09	-15.09	-15.09

Table B.5: ECU running 2D-LUT for ID.

ECU running 2D-LUT for ID [ms]								
n	**Throttle [%]**							
[rpm]	0	6	8	10	13	15	18	20
0	0	0	0	0	0	0	0	0
240	0	0	0	0	0	0	0	0
900	0	0.7	0.7	0.7	0.7	0.78	0.82	0.82
950	0	0.7	0.7	0.7	0.7	0.78	0.82	0.82
1000	0	0.7	0.7	0.7	0.7	0.78	0.82	0.82
1200	0	0.7	0.7	0.7	0.7	0.78	0.82	0.82
1400	0	0.7	0.7	0.7	0.7	0.78	0.82	0.82
1600	0	0.7	0.7	0.7	0.7	0.78	0.82	0.82
1800	0	0.7	0.7	0.7	0.7	0.78	0.82	0.82

B.3 Limitation Map

This section shows the final injecton duration limitation map to prevent over fueling of engine in start, stop and running state, see table B.6.

Table B.6: ECU running 2D-LUT for ID limit.

ECU running 2D-LUT for ID limit [ms]									
n	**Rail oil pressure [bar]**								
[rpm]	0	29	31.41	37	63.16	86	89	121	129
0	0	0	0	0	0	0	0	0	0
240	0	3	3	3	3	3	3	3	3
900	0	3.4	3.4	2.9	2.9	2.9	2.9	2.9	2.5
1000	0	3.2	3.2	2.7	2.7	2.6	2.6	1.9	0
1200	0	3.2	3.2	2.5	2.5	2.5	1.9	0	0
1400	0	2.3	2.3	2.3	2.3	2.3	0	0	0
1600	0	2	2	2	2	2	0	0	0
1800	0	1.8	1.8	1.8	1.8	1.8	0	0	0